

*Electronic Supplementary Information for*

**New phenyl-nickel complexes of bulky 2-iminopyrrolyl chelates:  
synthesis, characterisation, and application as aluminium-free  
catalysts for the production of hyperbranched polyethylene**

Cláudia A. Figueira,<sup>a</sup> Patrícia S. Lopes,<sup>a</sup> Clara S. B. Gomes,<sup>a</sup> Joselaine S. Gomes,<sup>a</sup>  
Francisco Lemos,<sup>b</sup> and Pedro T. Gomes\*<sup>a</sup>

<sup>a</sup> *Centro de Química Estrutural, Departamento de Engenharia Química, Instituto Superior Técnico, Universidade de Lisboa, Av. Rovisco Pais, 1, 1049-001 Lisboa, Portugal;*

<sup>b</sup> *CERENA, Departamento de Engenharia Química, Instituto Superior Técnico, Universidade de Lisboa, Av. Rovisco Pais, 1, 1049-001 Lisboa, Portugal*

\* Corresponding Author; e-mail: [pedro.t.gomes@tecnico.ulisboa.pt](mailto:pedro.t.gomes@tecnico.ulisboa.pt)

## *Table of Contents*

	<b>Page</b>
Details of the experimental procedures and product characterisation of the 5-aryl-2-( <i>N</i> -arylformimino)pyrrole ligand precursors <b>I-VII</b> .	S3
Details of the experimental procedures and product characterisation of the 5-aryl-2-( <i>N</i> -arylformimino)pyrrolyl sodium salts <b>I<sub>Na</sub>-VII<sub>Na</sub></b> .	S7
Single-crystal X-ray diffraction data of ligand precursors and complexes	S11
NMR spectra of complexes <b>1-7</b>	S27
Catalytic kinetic profiles for the polymerisation of ethylene	S36
GC chromatograms	S37
Polyethylene characterisation by <sup>1</sup> H NMR: Determination of M <sub>n</sub> and branching degree	S38
Polyethylene characterisation by <sup>13</sup> C{ <sup>1</sup> H} NMR: Microstructure analysis	S51
GPC/SEC chromatograms	S60

## Detailed synthetic procedures and characterisation of ligand precursors I-VII and sodium salts I<sub>Na</sub>-VII<sub>Na</sub>

### A. 5-Aryl-2-(*N*-arylformimino)pyrrole ligand precursors I-VII

**5-Phenyl-2-[*N*-(2,6-dimethylphenyl)formimino]pyrrole (I):** The 5-phenyl-2-formyl-1*H*-pyrrole (5.98 mmol, 1.02 g), the 2,6-dimethylaniline (5.50 mmol, 0.70 ml) and a catalytic amount of *p*-toluenesulfonic acid (0.30 mmol, 0.058 g) were suspended in toluene (20 ml). The light orange suspension turned overnight into an orange brown solution. After 24 h, the heating was stopped and the solution worked-up. The light red *n*-hexane solution was stored at -20 °C and a first crop containing unreacted formyl reagent was separated by filtration. Concentration of the *n*-hexane filtrate solution yielded **I** (1.06 g, 70%) as an old pink solid. Recrystallisation of a portion in *n*-hexane at room temperature gave colourless crystals. <sup>1</sup>H NMR (300 MHz, CDCl<sub>3</sub>): δ *NH* resonance absent, 7.95 (s, 1H, N=CH), 7.66 (d, <sup>3</sup>*J*<sub>HH</sub> = 7.2 Hz, 2H, 5-Ph-H<sub>ortho</sub>), 7.43 (t, <sup>3</sup>*J*<sub>HH</sub> = 7.9 Hz, 2H, 5-Ph-H<sub>meta</sub>), 7.31 (t, <sup>3</sup>*J*<sub>HH</sub> = 7.5 Hz, 1H, 5-Ph-H<sub>para</sub>), 7.09 (d, <sup>3</sup>*J*<sub>HH</sub> = 7.3 Hz, 2H, N-Ph-H<sub>meta</sub>), 6.99-6.94 (m, 1H, N-Ph-H<sub>para</sub>), 6.70 (d, <sup>3</sup>*J*<sub>HH</sub> = 3.7 Hz, 1H, H3 pyr), 6.64 (d, <sup>3</sup>*J*<sub>HH</sub> = 3.8 Hz, 1H, H4 pyr), 2.19 (s, 6H, CH<sub>3</sub>). <sup>13</sup>C{<sup>1</sup>H} NMR (75 MHz, CDCl<sub>3</sub>): δ 152.4 (N=CH), 151.0 (N-Ph-C<sub>ipso</sub>), 136.8 (C5 pyr), 131.7 (5-Ph-C<sub>ipso</sub>), 131.1 (C2 pyr), 129.1 (5-Ph-C<sub>meta</sub>), 128.2 (N-Ph-C<sub>meta</sub>), 128.0 (N-Ph-C<sub>ortho</sub>), 127.7 (5-Ph-C<sub>para</sub>), 124.8 (5-Ph-C<sub>ortho</sub>), 123.7 (N-Ph-C<sub>para</sub>), 117.8 (C3 pyr), 108.0 (C4 pyr), 18.5 (CH<sub>3</sub>). **Anal. Calcd.** for C<sub>19</sub>H<sub>18</sub>N<sub>2</sub>·(Si(CH<sub>3</sub>)<sub>2</sub>O)<sub>0.04</sub>: C 82.62, H 6.63, N 10.11; **Found:** C 82.18, H 6.70, N 10.13. *Trace amounts of chemically inert silicon grease [Si(CH<sub>3</sub>)<sub>2</sub>O] (soluble in *n*-hexane) were found, as confirmed by <sup>1</sup>H NMR spectroscopy.*

**5-Phenyl-2-[*N*-(2,6-diisopropylphenyl)formimino]pyrrole (II):** This compound was already described,<sup>1</sup> but a new purification method was followed and crystals suitable for x-ray diffraction were also obtained. The 5-phenyl-2-formyl-1*H*-pyrrole (5.00 mmol, 0.856 g), the 2,6-diisopropylaniline (6.00 mmol, 1.10 ml) and a catalytic amount of *p*-

<sup>1</sup> T. F. C. Cruz, C. A. Figueira, J. C. Waerenborgh, L. C. J. Pereira, Y. Li, R. Lescouëzec, P. T. Gomes, *Polyhedron*, 2018, **152**, 179.

toluenesulfonic acid (0.28 mmol, 0.048 g) were suspended in toluene (20 ml) and refluxed for 60 h. Purification of the crude by column chromatography with *n*-hexane:ethyl acetate (2:1) was made, yielding **II** as a yellow solid (1.02 g, 62%). Recrystallisation in *n*-hexane and slow evaporation at room temperature afforded colourless crystals.

**5-Phenyl-2-[N-(pentafluorophenyl)formimino]pyrrole (III):** The 5-phenyl-2-formyl-1*H*-pyrrole (5.97 mmol, 1.02 g), the pentafluoroaniline (7.16 mmol, 1.30 g) and a catalytic amount of *p*-toluenesulfonic acid (0.30 mmol, 0.057 g) were suspended in xylene (25 ml). After 72 h, the reaction was allowed to cool and the solvent evaporated to dryness, giving a brown solid. A pure fraction was achieved by column chromatography, with a mixture of *n*-hexane:ethyl acetate (4:1) as eluent. The elution was monitored by TLC, and the combined purified fractions were evaporated to dryness. The product was dissolved in *n*-hexane and stored at -20 °C, yielding **III** (0.958 g, 48%) as yellow fluorescent cotton-like solid. Concentration of the mother liquor and storage at -20 °C yielded suitable crystals for X-ray diffraction. **<sup>1</sup>H NMR** (400 MHz, CDCl<sub>3</sub>): δ 9.83 (br, 1H, NH), 8.34 (s, 1H, N=CH), 7.62 (d, <sup>3</sup>J<sub>HH</sub> = 7.4 Hz, 2H, 5-Ph-H<sub>ortho</sub>), 7.43 (t, <sup>3</sup>J<sub>HH</sub> = 7.3 Hz, 2H, 5-Ph-H<sub>meta</sub>), 7.33 (t, <sup>3</sup>J<sub>HH</sub> = 7.0 Hz, 1H, 5-Ph-H<sub>para</sub>), 6.84 (d, <sup>3</sup>J<sub>HH</sub> = 2.8 Hz, 1H, H3 pyrr), 6.65 (d, <sup>3</sup>J<sub>HH</sub> = 2.8 Hz, 1H, H4 pyrr). **<sup>13</sup>C{<sup>1</sup>H} NMR** (101 MHz, CDCl<sub>3</sub>): δ 156.1 (dd, <sup>4</sup>J<sub>CF</sub> = 3.8, <sup>5</sup>J<sub>CF</sub> = 2.6 Hz, N=CH), 142.1 (m, N-Ph-C<sub>para</sub>), 139.5 (m, N-Ph-C<sub>ortho</sub>), 139.1 (C5 pyrr), 136.9 (m, N-Ph-C<sub>meta</sub>), 131.1 (5-Ph-C<sub>ipso</sub>), 130.9 (C2 pyrr), 129.2 (5-Ph-C<sub>meta</sub>), 128.4 (5-Ph-C<sub>para</sub>), 126.96-126.67 (m, N-Ph-C<sub>ipso</sub>), 125.1 (5-Ph-C<sub>ortho</sub>), 121.2 (C3 pyrr), 109.1 (C4 pyrr). **<sup>19</sup>F{<sup>1</sup>H} NMR** (376 MHz, CDCl<sub>3</sub>): δ -153.61 to -153.68 (m, 2F, N-Ph-F<sub>ortho</sub>), -161.73 (t, <sup>3</sup>J<sub>FF</sub> = 21.2 Hz, 1F, N-Ph-F<sub>para</sub>), -163.43 to -163.56 (m, 2F, N-Ph-F<sub>meta</sub>). **Anal. Calcd.** for C<sub>17</sub>H<sub>9</sub>F<sub>5</sub>N<sub>2</sub>: C 60.72, H 2.70, N 8.33; **Found:** C 60.63, H 2.45, N 8.30.

**5-(3,5-Dimethylphenyl)-2-[N-(2,6-dimethylphenyl)formimino]pyrrole (IV):** The 5-(3,5-dimethylphenyl)-2-formyl-1*H*-pyrrole (4.47 mmol, 0.890 g), the 2,6-dimethylaniline (5.36 mmol, 0.66 ml) and a catalytic amount of *p*-toluenesulfonic acid (0.22 mmol, 0.043 g) were suspended in toluene (20 ml). The reaction was performed overnight and, after removing the solvent, the components of the initially brown oil

were separated through column chromatography. The mixture *n*-hexane:ethyl acetate (4:1) was used as eluent and the combined pure fractions were evaporated to dryness and further recrystallised in *n*-hexane. Storage at -20 °C afforded **IV** (0.835 g, 62%) as yellow crystals. <sup>1</sup>H NMR (300 MHz, CDCl<sub>3</sub>): δ NH resonance absent, 7.95 (s, 1H, N=CH), 7.26 (s, 2H, 5-Ph-H<sub>ortho</sub>), 7.08 (d, <sup>3</sup>J<sub>HH</sub> = 7.5 Hz, 2H, N-Ph-H<sub>meta</sub>), 6.98-6.93 (m, 2H, 5-Ph-H<sub>para</sub> and N-Ph-H<sub>para</sub>), 6.67 (d, <sup>3</sup>J<sub>HH</sub> = 3.8 Hz, 1H, H3 pyrr), 6.60 (d, <sup>3</sup>J<sub>HH</sub> = 3.8 Hz, 1H, H4 pyrr), 2.38 (s, 6H, 5-Ph-CH<sub>3</sub>), 2.19 (s, 6H, N-Ph-CH<sub>3</sub>). <sup>13</sup>C{<sup>1</sup>H} NMR (75 MHz, CDCl<sub>3</sub>): δ 152.3 (N=CH), 151.0 (N-Ph-C<sub>ipso</sub>), 138.7 (5-Ph-C<sub>meta</sub>), 137.0 (C5 pyrr), 131.5 (5-Ph-C<sub>ipso</sub>), 130.9 (C2 pyrr), 129.5 (5-Ph-C<sub>para</sub>), 128.2 (N-Ph-C<sub>meta</sub>), 128.0 (N-Ph-C<sub>ortho</sub>), 123.7 (N-Ph-C<sub>para</sub>), 122.7 (5-Ph-C<sub>ortho</sub>), 117.7 (C3 pyrr), 107.9 (C4 pyrr), 21.5 (5-Ph-CH<sub>3</sub>), 18.6 (N-Ph-CH<sub>3</sub>). **Anal. Calcd.** for C<sub>21</sub>H<sub>22</sub>N<sub>2</sub>: C 83.40, H 7.33, N 9.26; **Found:** C 83.14, H 7.61, N 9.28.

**5-(3,5-Dimethylphenyl)-2-[N-(2,6-diisopropylphenyl)formimino]pyrrole (V):** The 5-(3,5-dimethylphenyl)-2-formylpyrrole (2.79 mmol, 0.555 g), the 2,6-diisopropylaniline (2.65 mmol, 0.50 ml) and a catalytic amount of *p*-toluenesulfonic acid (0.14 mmol, 0.027 g) were suspended in toluene (20 ml). The initial yellow suspension became dark green overnight. After 24 h reaction, the solvent was removed under vacuum and the product extracted with *n*-hexane. The purification was achieved by column chromatography, using *n*-hexane:ethyl acetate (4:1) as eluent. The elution was followed by TLC, being the pure product the first to be eluted. After removal of all the volatiles, recrystallisation in *n*-hexane and storage at -80 °C yielded **V** (0.543 g, 57%) as a light yellow solid. <sup>1</sup>H NMR (400 MHz, CDCl<sub>3</sub>): δ NH resonance absent, 7.92 (s, 1H, N=CH), 7.27 (s, 2H, 5-Ph-H<sub>ortho</sub>), 7.18-7.12 (m, 3H, N-Ph-H<sub>meta</sub> and N-Ph-H<sub>para</sub>), 6.96 (s, 1H, 5-Ph-H<sub>para</sub>), 6.68 (d, <sup>3</sup>J<sub>HH</sub> = 2.9 Hz, 1H, H3 pyrr), 6.61 (d, <sup>3</sup>J<sub>HH</sub> = 3.5 Hz, 1H, H4 pyrr), 3.13-3.02 (m, 2H, CH(CH<sub>3</sub>)<sub>2</sub>), 2.38 (s, 6H, CH<sub>3</sub>), 1.19 (d, <sup>3</sup>J<sub>HH</sub> = 6.9 Hz, 12H, CH(CH<sub>3</sub>)<sub>2</sub>). <sup>13</sup>C{<sup>1</sup>H} NMR (101 MHz, CDCl<sub>3</sub>): δ 152.0 (N=CH), 148.9 (N-Ph-C<sub>ipso</sub>), 138.7 (5-Ph-C<sub>meta</sub> and N-Ph-C<sub>ortho</sub>), 137.3 (C5 pyrr), 131.5 (5-Ph-C<sub>ipso</sub>), 130.8 (C2 pyrr), 129.5 (5-Ph-C<sub>para</sub>), 124.3 (N-Ph-C<sub>para</sub>), 123.2 (N-Ph-C<sub>meta</sub>), 122.7 (5-Ph-C<sub>ortho</sub>), 117.9 (C3 pyrr), 107.8 (C4 pyrr), 27.9 (CH(CH<sub>3</sub>)<sub>2</sub>), 23.8 (CH(CH<sub>3</sub>)<sub>2</sub>), 21.5 (CH<sub>3</sub>). **Anal. Calcd.** for C<sub>25</sub>H<sub>30</sub>N<sub>2</sub>·(Si(CH<sub>3</sub>)<sub>2</sub>O)<sub>0.09</sub>: C 82.81, H 8.44, N 7.67; **Found:** C 82.58, H 9.00,

N 7.76. Trace amounts of chemically inert silicon grease  $\{Si(CH_3)_2O\}$  (soluble in *n*-hexane) were found, as confirmed by  $^1H$  NMR spectroscopy.

**5-(3,5-Di(trifluoro)methylphenyl)-2-[N-(2,6-diisopropylphenyl)formimino]pyrrole**

**(VI):** The 5-[(3,5-bis(trifluoromethyl)phenyl)-2-formyl]-1*H*-pyrrole (3.7 mmol, 1.15 g), the 2,6-diisopropylaniline (3.5 mmol, 0.66 mL) and a catalytic amount of *p*-toluenesulfonic acid (0.20 mmol, 0.035 g) were suspended in toluene (30 mL). The reaction mixture was refluxed for 39 h and, after solvent removal under vacuum, an orange solid was obtained. The compound was purified by column chromatography, using as eluent a mixture of *n*-hexane:ethyl acetate (10:1). Evaporation of the combined pure fractions yielded **VI** (1.10 g, 68%) as a beige solid.  $^1H$  NMR (300 MHz,  $CDCl_3$ ):  $\delta$  8.49 (br, 1H, NH), 8.06 (s, 2H, 5-Ph- $H_{ortho}$ ), 7.96 (s, 1H, N=CH), 7.78 (s, 1H, 5-Ph- $H_{para}$ ), 7.21-7.13 (m, 3H, N-Ph- $H_{meta}$  and N-Ph- $H_{para}$ ), 6.79-6.77 (m, 2H, H3 pyr and H4 pyr), 3.04 (h,  $^3J_{HH} = 6.8$  Hz, 2H,  $CH(CH_3)_2$ ), 1.19 (d,  $^3J_{HH} = 6.9$  Hz, 12H,  $CH(CH_3)_2$ ).  $^{13}C\{^1H\}$  NMR (75 MHz,  $CDCl_3$ ):  $\delta$  152.7 (N=CH), 148.1 (N-Ph- $C_{ipso}$ ), 138.8 (N-Ph- $C_{ortho}$ ), 134.0 (5-Ph- $C_{ipso}$ ), 133.9 (C5 pyr), 132.1 (C2 pyr), 132.6 (q,  $^2J_{CF} = 33.25$  Hz, 5-Ph- $C_{meta}$ ), 124.9 (N-Ph- $C_{para}$ ), 124.6 (d,  $^3J_{CF} = 2.6$  Hz, 5-Ph- $C_{ortho}$ ), 123.4 (q,  $^1J_{CF} = 271.2$  Hz,  $CF_3$ ), 123.4 (N-Ph- $C_{meta}$ ), 120.8 (quint,  $^3J_{CF} = 3.8$  Hz, 5-Ph- $C_{para}$ ), 118.8 (C3 pyr), 110.1 (C4 pyr), 28.0 ( $CH(CH_3)_2$ ), 24.0 ( $CH(CH_3)_2$ ).  $^{19}F\{^1H\}$  NMR (376 MHz,  $CDCl_3$ ):  $\delta$  -63.04 ( $CF_3$ ). **Anal. Calcd.** for  $C_{25}H_{24}N_2F_6$ : C 64.37, H 5.19, N 6.01; **Found:** C 64.07, H 5.00, N 5.99.

**5-(2,4,6-Triisopropylphenyl)-2-[N-(2,6-diisopropylphenyl)formimino]pyrrole**

**(VII):**

This compound was already described in a recent work of our group.<sup>2</sup> In the present work, after obtaining **VII** as a brown powder precipitated from a *n*-hexane solution at -20 °C, the mother liquor was concentrated and stored at -20 °C, and crystals suitable for X-ray diffraction were obtained.

<sup>2</sup> T. F. C. Cruz, P. S. Lopes, L. C. J. Pereira, L. F. Veiros, P. T. Gomes, *Inorg. Chem.*, 2018, **57**, 8146.

## B. Sodium 5-Aryl-2-(N-arylformimino)pyrrolyl salts $I_{Na}$ -VII $_{Na}$

### 5-Phenyl-2-[N-(2,6-dimethylphenyl)formimino]pyrrolyl sodium salt ( $I_{Na}$ ):

Deprotonation of ligand precursor **I** (0.558 g, 2.04 mmol) with NaH (0.064 g, 2.67 mmol) yielded  $I_{Na}$  as a salmon solid (0.815 g, > 99%), which revealed to be a THF adduct (1:0.7).  $^1\text{H NMR}$  (300 MHz,  $\text{CD}_3\text{CN}$ ):  $\delta$  7.79 (dd,  $^3J_{\text{HH}} = 8.4$  Hz,  $^4J_{\text{HH}} = 1.2$  Hz, 2H, 5-Ph- $\text{H}_{ortho}$ ), 7.73 (s, 1H, N=CH), 7.29-7.23 (m, 2H, 5-Ph- $\text{H}_{meta}$ ), 7.07 (dt,  $^3J_{\text{HH}} = 7.7$  Hz,  $^4J_{\text{HH}} = 1.4$  Hz, 1H, 5-Ph- $\text{H}_{para}$ ), 7.02 (d,  $^3J_{\text{HH}} = 7.9$  Hz, 2H, N-Ph- $\text{H}_{meta}$ ), 6.86-6.81 (m, 1H, N-Ph- $\text{H}_{para}$ ), 6.63 (d,  $^3J_{\text{HH}} = 3.4$  Hz, 1H, H3 pyr), 6.53 (d,  $^3J_{\text{HH}} = 3.4$  Hz, 1H, H4 pyr), 3.67-3.62 (m, 2.8H, (2,5)- $\text{CH}_2$  THF), 2.12 (s, 6H,  $\text{CH}_3$ ), 1.83-1.78 (m, 2.8H, (3,4)- $\text{CH}_2$  THF).  $^{13}\text{C}\{^1\text{H}\}$  NMR (101 MHz,  $\text{CD}_3\text{CN}$ ):  $\delta$  160.0 (N=CH), 154.5 (N-Ph- $\text{C}_{ipso}$ ), 148.0 (C5 pyr), 141.0 (5-Ph- $\text{C}_{ipso}$ ), 140.8 (C2 pyr), 130.1 (N-Ph- $\text{C}_{ortho}$ ), 129.0 (5-Ph- $\text{C}_{meta}$ ), 128.8 (N-Ph- $\text{C}_{meta}$ ), 125.8 (5-Ph- $\text{C}_{ortho}$ ), 125.1 (5-Ph- $\text{C}_{para}$ ), 123.2 (N-Ph- $\text{C}_{para}$ ), 121.7 (C3 pyr), 108.5 (C4 pyr), 68.4 ((2,5)- $\text{CH}_2$  THF), 26.3 ((3,4)- $\text{CH}_2$  THF), 19.0 ( $\text{CH}_3$ ).  $^{23}\text{Na NMR}$  (106 MHz,  $\text{CD}_3\text{CN}$ ):  $\delta$  4.24 (s,  $\Delta\nu_{1/2} = 381$  Hz).

### 5-Phenyl-2-[N-(2,6-diisopropylphenyl)formimino]pyrrolyl sodium salt ( $II_{Na}$ ):

Deprotonation of ligand precursor **II** (0.672 g, 2.04 mmol) with NaH (0.062 g, 2.59 mmol) gave an oily product that became a foam upon drying under vacuum for several hours. The foam was grounded to a fine dark pink powder of  $II_{Na}$  (0.832 g, 98%), which revealed to be a THF adduct (1:0.88).  $^1\text{H NMR}$  (300 MHz,  $\text{CD}_3\text{CN}$ ):  $\delta$  7.82 (s, 1H, N=CH), 7.77 (dd,  $^3J_{\text{HH}} = 8.4$  Hz,  $^4J_{\text{HH}} = 1.1$  Hz, 2H, 5-Ph- $\text{H}_{ortho}$ ), 7.34 (t,  $^3J_{\text{HH}} = 7.5$  Hz, 2H, 5-Ph- $\text{H}_{meta}$ ), 7.19-7.13 (m, 3H, 5-Ph- $\text{H}_{para}$  and N-Ph- $\text{H}_{meta}$ ), 7.05-7.01 (m, 1H, N-Ph- $\text{H}_{para}$ ), 6.64 (d,  $^3J_{\text{HH}} = 3.6$  Hz, 1H, H3 pyr), 6.59 (d,  $^3J_{\text{HH}} = 3.6$  Hz, 1H, H4 pyr), 3.67-3.63 (m, 3.5H, (2,5)- $\text{CH}_2$  THF), 3.17-3.07 (m, 2H,  $\text{CH}(\text{CH}_3)_2$ ), 1.83-1.78 (m, 3.5H, (3,4)- $\text{CH}_2$  THF), 1.13 (d,  $^3J_{\text{HH}} = 6.9$  Hz, 12H,  $\text{CH}(\text{CH}_3)_2$ ).  $^{13}\text{C}\{^1\text{H}\}$  NMR (75 MHz,  $\text{CD}_3\text{CN}$ ):  $\delta$  156.6 (N=CH), 151.5 (N-Ph- $\text{C}_{ipso}$ ), 140.2 (N-Ph- $\text{C}_{ortho}$ ), resonances absent (C5 pyr, 5-Ph- $\text{C}_{ipso}$ , C2 pyr), 129.4 (5-Ph- $\text{C}_{meta}$ ), 126.5 (5-Ph- $\text{C}_{para}$ ), 125.9 (5-Ph- $\text{C}_{ortho}$ ), 124.3 (N-Ph- $\text{C}_{para}$ ), 123.8 (N-Ph- $\text{C}_{meta}$ ), 119.9 (C3 pyr), 108.7 (C4 pyr), 68.3 ((2,5)- $\text{CH}_2$  THF), 28.6 ( $\text{CH}(\text{CH}_3)_2$ ), 26.3 ((3,4)- $\text{CH}_2$  THF), 24.0 ( $\text{CH}(\text{CH}_3)_2$ ).  $^{23}\text{Na NMR}$  (79 MHz,  $\text{CD}_3\text{CN}$ ):  $\delta$  3.85 (s,  $\Delta\nu_{1/2} = 476$  Hz).

**5-Phenyl-2-[N-(pentafluorophenyl)formimino]pyrrolyl sodium salt (III<sub>Na</sub>):**

Deprotonation of ligand precursor **III** (0.673 g, 2.00 mmol) with NaH (0.067 g, 2.70 mmol) yielded **III<sub>Na</sub>** (0.724 g, > 99%) as a yellow solid. <sup>1</sup>H NMR (400 MHz, CD<sub>3</sub>CN): δ 8.21 (t, <sup>5</sup>J<sub>HF</sub> = 1.5 Hz, 1H, N=CH), 7.81 (d, <sup>3</sup>J<sub>HH</sub> = 7.9 Hz, 2H, 5-Ph-H<sub>ortho</sub>), 7.24 (t, <sup>3</sup>J<sub>HH</sub> = 7.7 Hz, 2H, 5-Ph-H<sub>meta</sub>), 7.10 (t, <sup>3</sup>J<sub>HH</sub> = 7.3 Hz, 1H, 5-Ph-H<sub>para</sub>), 6.81 (d, <sup>3</sup>J<sub>HH</sub> = 3.5 Hz, 1H, H3 pyrr), 6.63 (d, <sup>3</sup>J<sub>HH</sub> = 3.6 Hz, 1H, H4 pyrr). <sup>13</sup>C{<sup>1</sup>H} NMR (75 MHz, CD<sub>3</sub>CN): δ 160.8 (t, <sup>4</sup>J<sub>CF</sub> = 3.6 Hz, N=CH), 152.2 (C5 pyrr), 144.0 (m, N-Ph-C<sub>para</sub>), 141.3 (5-Ph-C<sub>ipso</sub>), 140.7 (m, N-Ph-C<sub>ortho</sub>), 139.8 (C2 pyrr), 137.3 (m, N-Ph-C<sub>meta</sub>), 130.3 (m, N-Ph-C<sub>ipso</sub>), 129.0 (5-Ph-C<sub>meta</sub>), 126.3 (C3 pyrr), 126.2 (5-Ph-C<sub>para</sub>), 126.1 (5-Ph-C<sub>ortho</sub>), 111.0 (C4 pyrr). <sup>19</sup>F NMR (376 MHz, CD<sub>3</sub>CN): δ -157.09 to -157.18 (m, 2F, N-Ph-F<sub>ortho</sub>), -167.51 to -167.65 (m, 2F, N-Ph-F<sub>meta</sub>), -169.73 (t, <sup>3</sup>J<sub>FF</sub> = 21.0 Hz, 1F, N-Ph-F<sub>para</sub>). <sup>23</sup>Na NMR (106 MHz, CD<sub>3</sub>CN): δ 2.09 (s, Δν<sub>1/2</sub> = 339 Hz).

**5-(3,5-Dimethylphenyl)-2-[N-(2,6-dimethylphenyl)formimino]pyrrolyl sodium salt (IV<sub>Na</sub>):**

Deprotonation of ligand precursor **IV** (0.835 g, 2.76 mmol) with NaH (0.074 g, 3.09 mmol) gave a foam that was grounded after drying, yielding **IV<sub>Na</sub>** as a crystalline brown powder (1.12 g, > 99%) and a THF adduct (1:0.9). <sup>1</sup>H NMR (300 MHz, CD<sub>3</sub>CN): δ 7.74 (s, 1H, N=CH), 7.44 (s, 2H, 5-Ph-H<sub>ortho</sub>), 7.03 (d, <sup>3</sup>J<sub>HH</sub> = 7.5 Hz, 2H, N-Ph-H<sub>meta</sub>), 6.88-6.82 (m, 1H, N-Ph-H<sub>para</sub>), 6.74 (s, 1H, 5-Ph-H<sub>para</sub>), 6.56 (d, <sup>3</sup>J<sub>HH</sub> = 3.4 Hz, 1H, H3 pyrr), 6.52 (d, <sup>3</sup>J<sub>HH</sub> = 3.3 Hz, 1H, H4 pyrr), 3.67-3.63 (m, 3.6H, (2,5)-CH<sub>2</sub> THF), 2.28 (s, 6H, 5-Ph-CH<sub>3</sub>), 2.12 (s, 6H, N-Ph-CH<sub>3</sub>), 1.83-1.79 (m, 3.6H, (3,4)-CH<sub>2</sub> THF). <sup>13</sup>C{<sup>1</sup>H} NMR (75 MHz, CD<sub>3</sub>CN): δ 159.3 (N=CH), 154.3 (N-Ph-C<sub>ipso</sub>), 147.2 (C5 pyrr), 140.1 (5-Ph-C<sub>ipso</sub>), 139.8 (C2 pyrr), 138.3 (5-Ph-C<sub>meta</sub>), 129.9 (N-Ph-C<sub>ortho</sub>), 128.7 (N-Ph-C<sub>meta</sub>), 127.0 (5-Ph-C<sub>para</sub>), 123.6 (5-Ph-C<sub>ortho</sub>), 123.2 (N-Ph-C<sub>para</sub>), 121.2 (C3 pyrr), 108.5 (C4 pyrr), 68.3 ((2,5)-CH<sub>2</sub> THF), 26.3 ((3,4)-CH<sub>2</sub> THF), 21.5 (5-Ph-CH<sub>3</sub>), 18.9 (N-Ph-CH<sub>3</sub>). <sup>23</sup>Na NMR (106 MHz, CD<sub>3</sub>CN): δ 4.31 (s, Δν<sub>1/2</sub> = 434 Hz).

**5-(3,5-Dimethylphenyl)-2-[N-(2,6-diisopropylphenyl)formimino]pyrrolyl sodium salt (V<sub>Na</sub>):**

Deprotonation of ligand precursor **V** (0.430 g, 1.20 mmol) with NaH (0.038 g, 1.57 mmol) yielded **V<sub>Na</sub>** as a light yellow solid (0.409 g, 70%), which revealed to be a THF adduct (1:1.5). <sup>1</sup>H NMR (300 MHz, CD<sub>3</sub>CN): δ 7.72 (s, 1H, N=CH), 7.43 (s, 2H, 5-Ph-H<sub>ortho</sub>), 7.12 (d, <sup>3</sup>J<sub>HH</sub> = 7.6 Hz, 2H, N-Ph-H<sub>meta</sub>), 7.03-6.98 (m, 1H, N-Ph-H<sub>para</sub>),

6.75 (s, 1H, 5-Ph-H<sub>para</sub>), 6.56 (d, <sup>3</sup>J<sub>HH</sub> = 3.1 Hz, 1H, H3 pyrr), 6.50 (d, <sup>3</sup>J<sub>HH</sub> = 3.1 Hz, 1H, H4 pyrr), 3.67-3.63 (m, 6H, (2,5)-CH<sub>2</sub> THF), 3.23-3.09 (m, 2H, CH(CH<sub>3</sub>)<sub>2</sub>), 2.29 (s, 6H, CH<sub>3</sub>), 1.83-1.78 (m, 6H, (3,4)-CH<sub>2</sub> THF), 1.13 (d, <sup>3</sup>J<sub>HH</sub> = 6.8 Hz, 12H, CH(CH<sub>3</sub>)<sub>2</sub>). <sup>13</sup>C{<sup>1</sup>H} NMR (75 MHz, CD<sub>3</sub>CN): δ 159.5 (N=CH), 152.3 (N-Ph-C<sub>ipso</sub>), 140.8 (5-Ph-C<sub>meta</sub>), 138.3 (N-Ph-C<sub>ortho</sub>), resonances absent (C5 pyrr, 5-Ph-C<sub>ipso</sub> and C2 pyrr), 127.0 (5-Ph-C<sub>para</sub>), 124.0 (N-Ph-C<sub>para</sub>), 123.7 (5-Ph-C<sub>ortho</sub> and N-Ph-C<sub>meta</sub>), 121.2 (C3 pyrr), 108.5 (C4 pyrr), 68.3 ((2,5)-CH<sub>2</sub> THF), 28.6 (CH(CH<sub>3</sub>)<sub>2</sub>), 26.3 ((3,4)-CH<sub>2</sub> THF), 24.0 (CH(CH<sub>3</sub>)<sub>2</sub>), 21.5 (CH<sub>3</sub>). <sup>23</sup>Na NMR (106 MHz, CD<sub>3</sub>CN): δ 3.77 (s, Δv<sub>1/2</sub> = 381 Hz).

**5-(3,5-Di(trifluoro)methylphenyl)-2-[N-(2,6-diisopropylphenyl)formimino]pyrrolyl**

**sodium salt (VI<sub>Na</sub>):** Deprotonation of ligand precursor **VI** (1.10 g, 2.4 mmol) with NaH (0.07 g, 2.8 mmol) yielded a beige powder of **VI<sub>Na</sub>** (1.49 g, 99%) as a THF adduct (1:1).

<sup>1</sup>H NMR (300 MHz, CD<sub>3</sub>CN): δ 8.29 (s, 2H, 5-Ph-H<sub>ortho</sub>), 7.79 (s, 1H, N=CH), 7.59 (s, 1H, 5-Ph-H<sub>para</sub>), 7.15 (d, <sup>3</sup>J<sub>HH</sub> = 7.8 Hz, 2H, N-Ph-H<sub>meta</sub>), 7.04 (t, <sup>3</sup>J<sub>HH</sub> = 7.6 Hz, 1H, N-Ph-H<sub>para</sub>), 6.72 (d, <sup>3</sup>J<sub>HH</sub> = 3.4 Hz, 1H, H3 pyrr), 6.60 (d, <sup>3</sup>J<sub>HH</sub> = 3.4 Hz, 1H, H4 pyrr), 3.74-3.55 (m, 4H, (2,5)-CH<sub>2</sub> THF), 3.13 (h, <sup>3</sup>J<sub>HH</sub> = 6.9 Hz, 2H, CH(CH<sub>3</sub>)<sub>2</sub>), 1.84-1.77 (m, 4H, (3,4)-CH<sub>2</sub> THF), 1.16 (d, <sup>3</sup>J<sub>HH</sub> = 6.9 Hz, 12H, CH(CH<sub>3</sub>)<sub>2</sub>). <sup>13</sup>C{<sup>1</sup>H} NMR (75 MHz, CD<sub>3</sub>CN): δ 160.6 (N=CH), 151.9 (N-Ph-C<sub>ipso</sub>), 144.7 (5-Ph-C<sub>ipso</sub>), 143.1 (C5 pyrr), 142.2 (C2 pyrr), 140.7 (N-Ph-C<sub>ortho</sub>), 131.7 (q, <sup>2</sup>J<sub>CF</sub> = 32.25 Hz, 5-Ph-C<sub>meta</sub>), 125.2 (q, <sup>1</sup>J<sub>CF</sub> = 270.0 Hz, CF<sub>3</sub>), 125.1 (d, <sup>3</sup>J<sub>CF</sub> = 2.8 Hz, 5-Ph-C<sub>ortho</sub>), 124.3 (N-Ph-C<sub>para</sub>), 123.7 (N-Ph-C<sub>meta</sub>), 121.6 (C3 pyrr), 117.3 (quint, <sup>3</sup>J<sub>CF</sub> = 3.9 Hz, 5-Ph-C<sub>para</sub>), 110.1 (C4 pyrr), 68.3 ((2,5)-CH<sub>2</sub> THF), 28.6 (CH(CH<sub>3</sub>)<sub>2</sub>), 26.3 ((3,4)-CH<sub>2</sub> THF), 23.9 (CH(CH<sub>3</sub>)<sub>2</sub>). <sup>19</sup>F{<sup>1</sup>H} NMR (282 MHz, CDCl<sub>3</sub>): δ -63.24 (CF<sub>3</sub>). <sup>23</sup>Na NMR (79 MHz, CD<sub>3</sub>CN): δ 3.30 (s, Δv<sub>1/2</sub> = 371 Hz).

**5-(2,4,6-Triisopropylphenyl)-2-[N-(2,6-diisopropylphenyl)formimino]pyrrolyl**

**sodium salt (VII<sub>Na</sub>):** Deprotonation of ligand precursor **VII** (0.91 g, 2.0 mmol) with NaH (0.06 g, 2.5 mmol) yielded a brown powder of **VII<sub>Na</sub>** (1.12 g, 99%) as a THF adduct (1:1.2).

<sup>1</sup>H NMR (400 MHz, CD<sub>3</sub>CN): δ 7.68 (s, 1H, N=CH), 7.12 (d, <sup>3</sup>J<sub>HH</sub> = 7.6 Hz, 2H, N-Ph-H<sub>meta</sub>), 7.04-6.98 (m, 3H, 5-Ph-H<sub>meta</sub> and N-Ph-H<sub>para</sub>), 6.56 (s br, 1H, H3 pyrr), 5.87 (s br, 1H, H4 pyrr), 3.66-3.63 (m, 5H, (2,5)-CH<sub>2</sub> THF), 3.23 (h, <sup>3</sup>J<sub>HH</sub> = 6.7 Hz, 2H, N-Ph<sub>ortho</sub>(CH(CH<sub>3</sub>)<sub>2</sub>)), 3.04 (h, <sup>3</sup>J<sub>HH</sub> = 6.7 Hz, 2H, 5-Ph<sub>ortho</sub>(CH(CH<sub>3</sub>)<sub>2</sub>)), 2.91

(h,  $^3J_{\text{HH}} = 6.7$  Hz, 1H, 5-Ph<sub>para</sub>(CH(CH<sub>3</sub>)<sub>2</sub>), 1.82-1.79 (m, 5H, (3,4)-CH<sub>2</sub> THF), 1.27 (d,  $^3J_{\text{HH}} = 6.9$  Hz, 6H, N-Ph<sub>ortho</sub>(CH(CH<sub>3</sub>)<sub>2</sub>)), 1.17-1.07 (m, 24H, N-Ph<sub>ortho</sub>(CH(CH<sub>3</sub>)<sub>2</sub>), 5-Ph<sub>ortho</sub>(CH(CH<sub>3</sub>)<sub>2</sub>) and 5-Ph<sub>para</sub>(CH(CH<sub>3</sub>)<sub>2</sub>)).

## Single-crystal X-ray diffraction data of ligand precursors and complexes

As referred in the manuscript, crystals suitable for single-crystal X-ray diffraction analysis were obtained for the iminopyrrole ligand precursors **I-IV** and **VII**, from *n*-hexane solutions, at room temperature or -20 °C. A (1:1) co-crystal of **I** with 2,6-dimethylaniline (**I<sub>A</sub>**) and a polymorph of **II** (**II<sub>A</sub>**) are also reported. In Figure S1 are represented the perspective views of the compounds **I-IV** and **VII**.

The structural features of these compounds are relatively comparable to analogous unsubstituted 2-(*N*-arylformimino)pyrrole molecules,<sup>3</sup> being the essential difference the dihedral angles formed between the pyrrole and the aryl ring planes, due to the presence of the new 5-aryl substituents. The driving force for the crystallisation of unsubstituted 2-iminopyrrole molecules is the ability to form coplanar dimers across two complementary hydrogen-bond interactions of type N-H...N(Ar)=C. In our case, the dimerisation is observed for compounds **I** and **IV**, but the dimer fragments are sterically constrained and deviate from the coplanarity (see Figure S2a). The presence of the 5-aryl substituents led to dihedral angles of 59.93° (**I**) and 62.59° (**IV**) between dimer fragments, in contrast with 0.00° for the analogous dimer of the 5-unsubstituted 2-(2,4,6-trimethylphenyl)acetiminopyrrole. In fact, **I** and **IV** can be considered as limiting cases of the formation of complementary hydrogen-bond interactions in these compounds. The higher steric hindrance of the *N*-2,6-diisopropylphenylimino group blocks the approach between molecules and, consequently, the typical dimerization.

---

<sup>3</sup> Bellabarba, R. M.; Gomes, P. T.; Pascu, S. I. *Dalton Trans.* 2003, 4431.

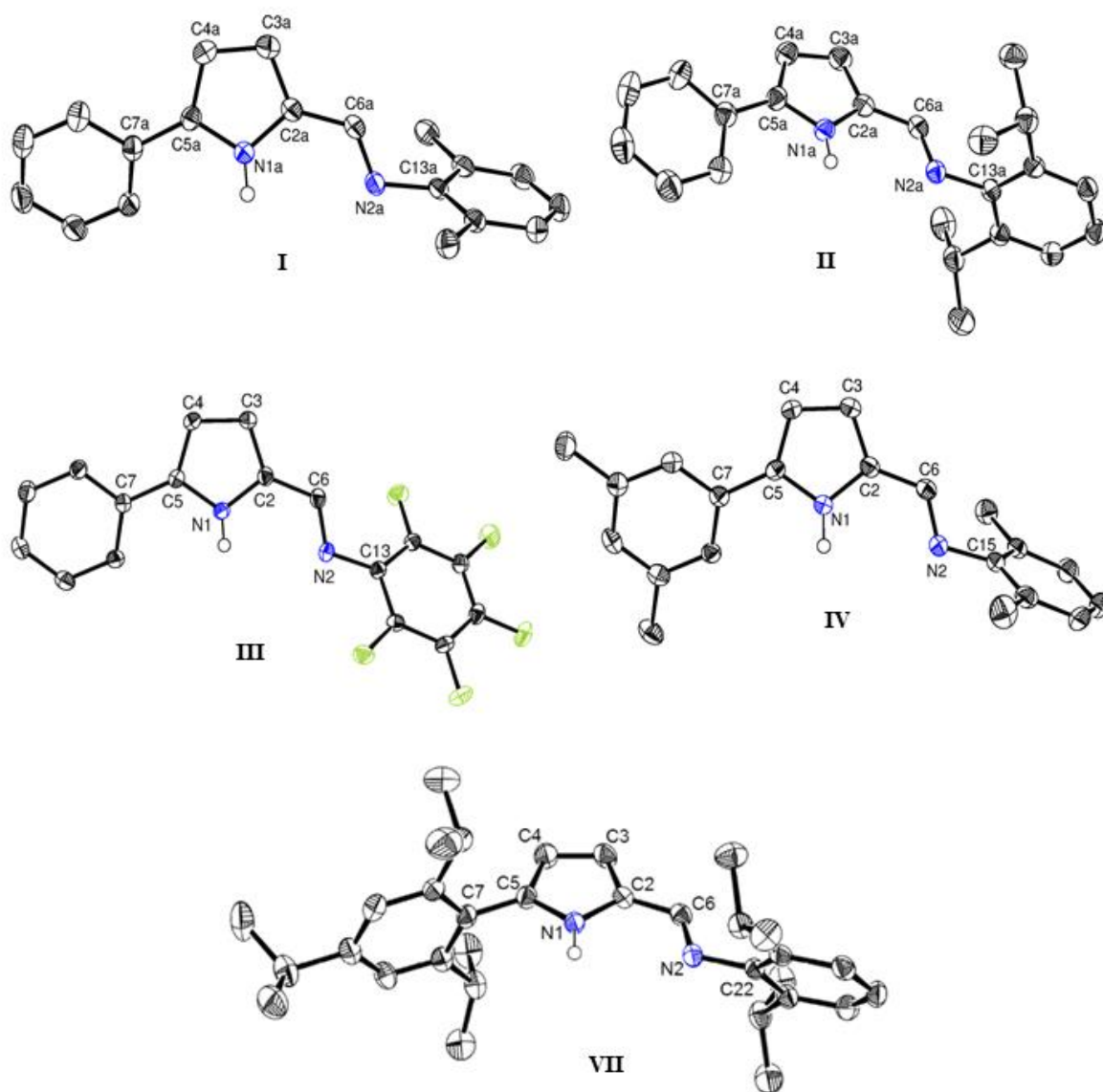


**Figure S1** ORTEP-3 diagrams of 5-aryl-2-(*N*-arylformimino)-1*H*-pyrroles **I-IV** and **VII**, using 50% probability level ellipsoids. Hydrogen atoms have been omitted for clarity, except the *NH* protons that were located in the electron density map. The asymmetric units of compounds **I** and **II** include two independent molecules (A and B), and those of compounds **III**, **IV** and **VII** a single one.

In the case of **VII**, to overcome the hindrance problems, the molecules organised in pseudo-dimers through  $N-H \cdots \pi C$  intermolecular interactions, in an infinite arrangement of those pairs (Figure S2b). Crystallisation of **II** in inert atmosphere was unsuccessful, being the crystals only obtained when air moisture was present (Figure S2c).

Crystallisation in air allowed the iminopyrrole molecules to interact with water molecules from moisture, which worked as a crystallisation template, providing two hydrogen atoms and electronic pairs for the formation of intermolecular hydrogen-bonds. Whether at room temperature in an open vessel (**II**) or at -20 °C in a closed vessel without inert atmosphere (**II<sub>A</sub>**), the formation of a co-crystal containing one water molecule per two iminopyrrole molecules was observed. The only difference to be stated is that the dihedral angle between 5-phenyl and pyrrole rings in **II<sub>A</sub>** are about half of the values of the ones of **II** (Figure S3a).

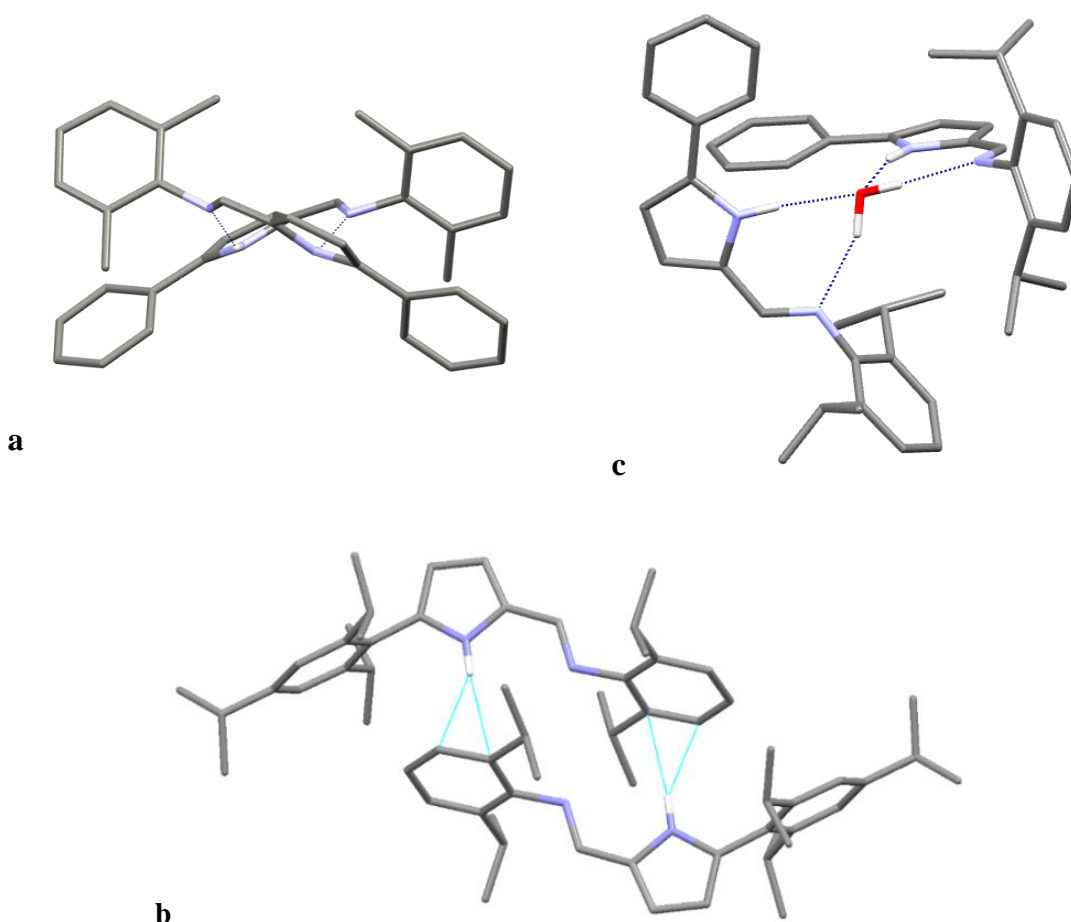


**Figure S2** (a) Complementary N-H...N hydrogen-bonds between sterically constrained dimers in **I**; (b) pseudo-dimerisation through N-H... $\pi$ C intermolecular interactions in **VI**; and (c) asymmetric unit of **II**, containing one water molecule as template for crystallisation.

The high affinity demonstrated by these compounds to establish hydrogen-bond interactions is also observed in co-crystal **I<sub>A</sub>** (Figure S3b). For **I<sub>A</sub>**, the iminopyrrolyl fragment is very similar to **I**, the only difference lying in the dihedral angle between the

5-phenyl and the pyrrole rings, lower in **I<sub>A</sub>** owing to the increased space available (13.73° for **I<sub>A</sub>** vs. 27.76 and 28.89° for **I**, molecules A and B, respectively).

For **III**, in spite of the lower bulkiness and higher electron withdrawing character of the *N*-pentafluorophenylimine substituent, no classical hydrogen-bonds are formed and the typical supramolecular pattern dictated by the formation of dimers is not observed.

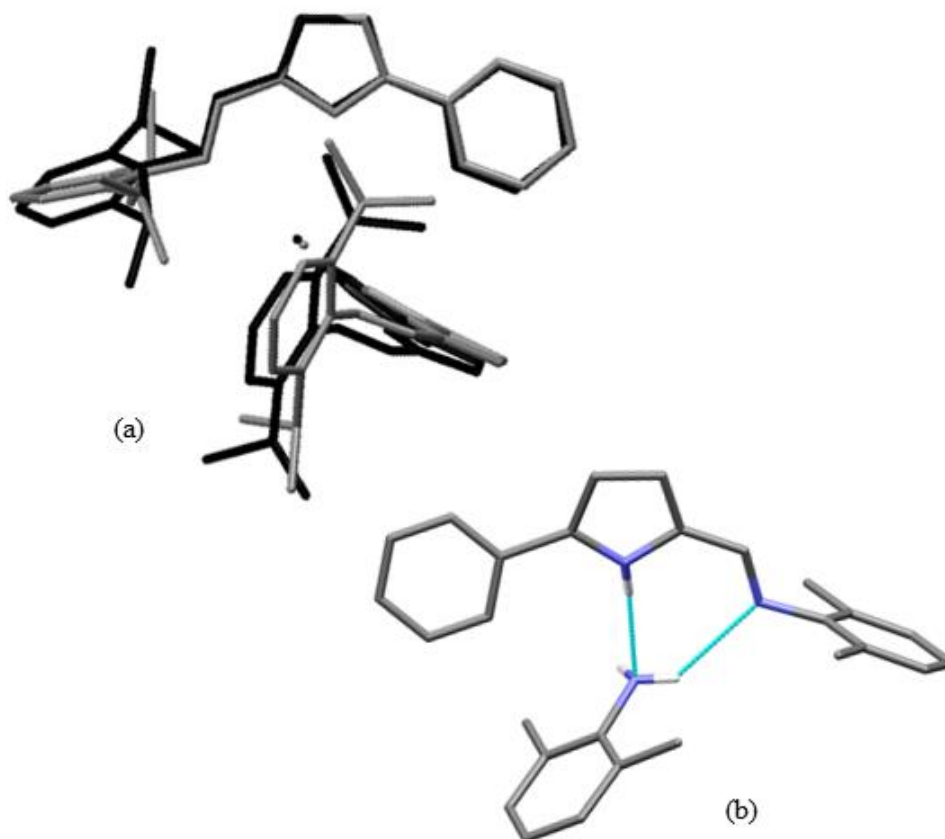


**Figure S3** (a) Superimposed views of **II** and its polymorph **II<sub>A</sub>**, and (b) molecular structure of **I<sub>A</sub>** (1:1 co-crystal of **I** with 2,6-dimethylaniline), showing the N-H...N hydrogen-bonds.

All the details of the crystal structure determinations are presented at Tables S1-S2, the selected bond distances and angles at Tables S3-S4 and other particular features at Tables S5-S6. However, it should be noticed that the molecular structure of ligand precursor **I<sub>A</sub>** results from poor crystallographic data (high  $R_{\text{int}}$ , poor diffracting power, low ratio of observed/unique reflections (37%) and low completeness).

**Table S1** Crystallographic data and refinement details for the structures of 5-aryl-2-(*N*-arylformimino)-1*H*-pyrroles **I** and **II**, for the co-crystal **I<sub>A</sub>** and for the polymorph **II<sub>A</sub>**.

	<b>I</b>	<b>I<sub>A</sub></b>	<b>II</b>	<b>II<sub>A</sub></b>
Formula	C <sub>19</sub> H <sub>18</sub> N <sub>2</sub>	C <sub>19</sub> H <sub>18</sub> N <sub>2</sub> ·C <sub>8</sub> H <sub>11</sub> N	2(C <sub>23</sub> H <sub>26</sub> N <sub>2</sub> )·H <sub>2</sub> O	2(C <sub>23</sub> H <sub>26</sub> N <sub>2</sub> )·H <sub>2</sub> O
<i>M</i>	274.35	395.53	678.93	678.93
λ (Å)	0.71073	0.71073	0.71073	0.71073
<i>T</i> (K)	150(2)	150(2)	150(2)	150(2)
Crystal system	Monoclinic	Monoclinic	Triclinic	Orthorhombic
Space group	<i>P</i> 2 <sub>1</sub> / <i>c</i>	<i>P</i> 2 <sub>1</sub> / <i>n</i>	<i>P</i> -1	<i>P</i> 2 <sub>1</sub> 2 <sub>1</sub> 2 <sub>1</sub>
<i>a</i> (Å)	14.8246(15)	13.74(2)	10.7581(8)	13.5296(4)
<i>b</i> (Å)	13.5546(15)	8.779(15)	11.5604(9)	15.0823(5)
<i>c</i> (Å)	15.4910(16)	22.72(4)	16.0156(12)	19.7874(6)
α (°)	90	90	81.266(4)	90
β (°)	101.881(6)	104.18(7)	88.811(4)	90
γ (°)	90	90	86.331(5)	90
<i>V</i> (Å <sup>3</sup> )	3046.1(6)	2658(8)	1964.6(3)	4037.8(2)
<i>Z</i>	8	4	2	4
ρ <sub>calc</sub> (g·cm <sup>-3</sup> )	1.196	0.988	1.148	1.117
μ (mm <sup>-1</sup> )	0.071	0.058	0.069	0.067
Crystal size	0.50×0.30×0.25	0.14×0.10×0.07	0.12×0.10×0.06	0.40×0.35×0.30
Crystal colour	Colourless	Colourless	Colourless	Brown
Crystal description	Prism	Prism	Prism	Block
θ <sub>max</sub> (°)	29.101	25.026	26.471	25.740
Total data	54156	19434	43215	39980
Unique data	8139	4378	8056	7652
<i>R</i> <sub>int</sub>	0.0483	0.1789	0.0664	0.0428
<i>R</i> [ <i>I</i> >2σ( <i>I</i> )]	0.0454	0.0877	0.0500	0.0366
<i>R</i> <sub>w</sub>	0.1166	0.2178	0.1153	0.0770
Goodness of fit	1.061	0.866	1.041	1.015
ρ <sub>min</sub>	-0.265	-0.438	-0.252	-0.184
ρ <sub>max</sub>	0.256	0.508	0.303	0.111

**Table S2** Crystallographic data and refinement details for the structures of 5-aryl-2-(*N*-arylformimino)-1*H*-pyrroles **III**, **IV** and **VII**.

	<b>III</b>	<b>IV</b>	<b>VII</b>
Formula	C <sub>17</sub> H <sub>9</sub> F <sub>5</sub> N <sub>2</sub>	C <sub>21</sub> H <sub>22</sub> N <sub>2</sub>	C <sub>32</sub> H <sub>44</sub> N <sub>2</sub>
<i>M</i>	336.26	302.41	456.69
λ (Å)	0.71073	0.71073	0.71073
<i>T</i> (K)	150(2)	150(2)	150(2)
Crystal system	Orthorhombic	Monoclinic	Triclinic
Space group	<i>P</i> 2 <sub>1</sub> 2 <sub>1</sub> 2 <sub>1</sub>	<i>C</i> 2/ <i>c</i>	<i>P</i> -1
<i>a</i> (Å)	4.79220(10)	11.818(2)	9.8624(9)
<i>b</i> (Å)	13.7718(3)	11.243(2)	12.9884(12)
<i>c</i> (Å)	20.8410(6)	26.174(5)	13.0264(11)
α (°)	90	90	70.021(5)
β (°)	90	92.984(10)	74.259(5)
γ (°)	90	90	68.722(4)
<i>V</i> (Å <sup>3</sup> )	1375.45(6)	3473.2(11)	1440.5(2)
<i>Z</i>	4	8	2
$\rho_{calc}$ (g.cm <sup>-3</sup> )	1.624	1.157	1.053
μ (mm <sup>-1</sup> )	0.145	0.068	0.060
Crystal size	0.30×0.30×0.20	0.26×0.20×0.20	0.30×0.20×0.15
Crystal colour	Yellow	Yellow	Orange
Crystal description	Block	Block	Prism
θ <sub>max</sub> (°)	37.805	25.694	25.920
Total data	26413	11759	12975
Unique data	7277	3269	5428
<i>R</i> <sub>int</sub>	0.0484	0.0553	0.0487
<i>R</i> [ <i>I</i> >2σ( <i>I</i> )]	0.0503	0.0516	0.0501
<i>R</i> <sub>w</sub>	0.1094	0.1206	0.1085
Goodness of fit	0.982	1.045	1.015
ρ <sub>min</sub>	-0.231	-0.242	-0.199
ρ <sub>max</sub>	0.444	0.320	0.163

**Table S3** Selected bond distances (Å) and angles (°) for 5-aryl-2-(*N*-arylformimino)-1*H*-pyrroles **I**, **II** and for the co-crystal **I<sub>A</sub>**.

	<b>I</b>		<b>I<sub>A</sub><sup>a</sup></b>	<b>II</b>	
	A	B		A	B
<i>Distances (Å)</i>					
N1-C2	1.3746(14)	1.3762(15)	1.451(7)	1.370(2)	1.373(2)
C2-C3	1.3796(17)	1.3839(17)	1.448(8)	1.380(2)	1.380(3)
C3-C4	1.3940(17)	1.4046(17)	1.467(8)	1.395(3)	1.395(3)
C4-C5	1.3848(17)	1.3824(16)	1.476(7)	1.383(2)	1.392(3)
C5-N1	1.3675(15)	1.3695(14)	1.432(7)	1.363(2)	1.363(2)
C5-C7	1.4609(17)	1.4623(15)	1.634(7)	1.464(2)	1.469(3)
C2-C6	1.4310(17)	1.4350(17)	1.496(8)	1.432(2)	1.429(2)
C6-N2	1.2763(15)	1.2794(15)	1.360(7)	1.275(2)	1.280(2)
N2-Cipso	1.4300(15)	1.4325(15)	1.504(7)	1.430(2)	1.426(2)
<i>Angles (°)</i>					
C5-N1-C2	109.39(9)	109.33(9)	110.6(4)	110.41(14)	110.86(15)
N1-C2-C3	107.51(10)	107.84(10)	107.1(5)	106.85(15)	106.89(16)
C2-C3-C4	107.85(11)	107.21(11)	108.0(5)	107.95(15)	107.72(17)
C3-C4-C5	107.70(11)	107.94(10)	108.0(4)	107.87(15)	108.35(16)
C4-C5-N1	107.56(10)	107.66(10)	106.4(5)	106.92(15)	106.19(16)
C7-C5-N1	123.74(11)	122.77(10)	123.7(4)	122.27(15)	121.30(16)
N1-C2-C6	125.62(10)	124.09(10)	124.3(4)	123.02(15)	122.64(16)
C2-C6-N2	125.68(10)	123.86(10)	126.2(5)	123.05(15)	123.72(16)
C6-N2-Cipso	116.76(9)	115.35(10)	121.2(4)	119.54(14)	120.82(15)

<sup>a</sup> Values resulting from poor crystallographic data.

**Table S4** Selected bond distances (Å) and angles (°) for 5-aryl-2-(*N*-arylformimino)-1*H*-pyrroles **III**, **IV** and **VII** and of the polymorph **II<sub>A</sub>**.

	<b>II<sub>A</sub></b>		<b>III</b>	<b>IV</b>	<b>VII</b>
	A	B			
<i>Distances (Å)</i>					
N1-C2	1.375(3)	1.371(3)	1.373(2)	1.382(2)	1.370(2)
C2-C3	1.375(3)	1.377(3)	1.381(2)	1.381(3)	1.377(3)
C3-C4	1.395(3)	1.396(3)	1.398(3)	1.399(3)	1.401(3)
C4-C5	1.382(3)	1.384(3)	1.392(2)	1.382(3)	1.372(3)
C5-N1	1.362(3)	1.364(2)	1.364(2)	1.370(2)	1.362(2)
C5-C7	1.458(3)	1.464(3)	1.460(2)	1.461(3)	1.487(3)
C2-C6	1.430(3)	1.432(3)	1.427(2)	1.430(3)	1.431(2)
C6-N2	1.282(3)	1.281(3)	1.293(2)	1.282(2)	1.272(2)
N2-Cipso	1.431(3)	1.430(2)	1.401(2)	1.435(2)	1.425(2)
<i>Angles (°)</i>					
C5-N1-C2	109.85(17)	110.26(18)	110.19(13)	109.37(16)	110.31(15)
N1-C2-C3	107.19(18)	106.87(17)	107.25(13)	107.38(16)	107.05(15)
C2-C3-C4	107.9(2)	108.2(2)	107.83(15)	107.78(17)	107.41(18)
C3-C4-C5	107.8(2)	107.57(19)	107.68(15)	107.94(17)	108.22(17)
C4-C5-N1	107.26(19)	107.11(18)	107.05(14)	107.53(16)	107.01(16)
C7-C5-N1	123.03(19)	121.38(19)	123.14(14)	122.91(16)	122.67(17)
N1-C2-C6	124.53(19)	122.56(18)	122.54(14)	123.16(17)	123.07(16)
C2-C6-N2	125.59(19)	123.53(19)	121.69(15)	123.35(17)	122.77(17)
C6-N2-Cipso	116.35(17)	118.55(17)	118.66(14)	118.62(16)	117.70(15)

**Table S5** Dihedral angles between the: (a) *N*-arylimino and 2-iminopyrrole<sup>a</sup> ring planes, (b) 5-aryl and pyrrole ring planes and, where appropriate, (c) the 2-iminopyrrole planes of a dimer, for compounds **I-IV** and **VII**, for the co-crystal **I<sub>A</sub>** and for the polymorph **II<sub>A</sub>**.

Compound	Dihedral Angle (°)		
	<i>N</i> -Ar vs. Pyrr <sub>C=N</sub> <sup>a</sup>	5-Ar vs. Pyrr	Dimer
<b>I</b> <i>mol. A</i>	76.38(6) 72.265(042)	27.79(7)	59.93(8)
<b>I</b> <i>mol. B</i>	83.25(5) 82.104(038)	28.80(6)	57.400(046)
<b>I<sub>A</sub></b> <sup>b</sup>	75.19(20) 75.369(156)	13.7(2)	
<b>II</b> <i>mol. A</i>	87.53(8) 86.915(055)	10.94(10)	
<b>II</b> <i>mol. B</i>	85.93(7) 86.885(058)	18.67(10)	
<b>II<sub>A</sub></b> <i>mol. A</i>	82.40(10) 80.927(070)	4.78(11)	
<b>II<sub>A</sub></b> <i>mol. B</i>	86.58(10) 84.924(074)	9.14(12)	
<b>III</b>	41.82(8) 40.931(058)	14.26(9)	
<b>IV</b>	72.28(7) 69.999(055)	25.56(10)	62.59
<b>VII</b>	69.81(8) 70.842(060)	89.64(10)	

<sup>a</sup> The 2-iminopyrrole ring plane is defined by atoms N1-C2-C6-N2, thus including part of the pyrrole ring (atoms N1 and C2) and of the iminic bond (atoms C6 and N2).

<sup>b</sup> Values resulting from poor crystallographic data.

**Table S6** Intermolecular hydrogen-bond interactions observed in the crystal structure of compounds **I-IV**, of the co-crystal **I<sub>A</sub>** and of the polymorph **II<sub>A</sub>**.

Compound	D-H...A	d(D-H) (Å)	d(H...A) (Å)	d(D...A) (Å)	(DĤA) (°)
<b>I</b>	N1 <sub>A</sub> -H1 <sub>A</sub> ...N2 <sub>B</sub>	0.851(14)	2.348(14)	3.1287(14)	152.8(12)
	N1 <sub>B</sub> -H1 <sub>B</sub> ...N2 <sub>A</sub>	0.868(15)	2.223(15)	3.0212(13)	152.8(14)
<b>I<sub>A</sub></b> <sup>a</sup>	N1-H1...N3	0.86(6)	2.32(6)	3.175(8)	170(6)
	N3-H2 <sub>N</sub> ...N2	0.98(6)	2.55(5)	3.362(9)	141(3)
<b>II</b>	N1 <sub>A</sub> -H1 <sub>A</sub> ...O1	0.845(18)	2.126(18)	2.951(2)	164.9(16)
	O1-H1...N2 <sub>A</sub>	0.92(2)	1.90(2)	2.7796(19)	159(2)
	N1 <sub>B</sub> -H1 <sub>B</sub> ...O1	0.89(2)	2.03(2)	2.841(2)	149.4(18)
	O1-H2...N2 <sub>B</sub>	0.91(2)	2.00(2)	2.853(2)	157(2)
<b>II<sub>A</sub></b>	N1 <sub>A</sub> -H1 <sub>A</sub> ...O1	0.88(2)	2.10(2)	2.954(2)	163.0(19)
	O1-H2...N2 <sub>A</sub>	0.94(3)	1.90(3)	2.807(2)	161(2)
	N1 <sub>B</sub> -H1 <sub>B</sub> ...O1	0.89(2)	2.03(2)	2.876(2)	159(2)
	O1-H1...N2 <sub>B</sub>	0.94(3)	1.92(3)	2.814(2)	160(2)
<b>III</b>	C10-H10...F5	0.95	2.44	3.216(2)	138
	C12-H12...F1	0.95	2.52	3.403(2)	155
<b>IV</b>	N1-H1...N2	0.93(2)	2.11(2)	2.955(2)	149(2)

<sup>a</sup> Values resulting from poor crystallographic data.

Crystals of complex **6** were of poor quality and showed a weak diffracting power for resolutions better than 0.82 Å. This led to a high  $R_{\text{int}}$  (0.299), a relatively low ratio of observed/unique reflections (28%) and a final low completeness of 94.9%. Due to the poor quality of the crystal and corresponding data, although all the atoms were correctly assigned and no twinning was found, two larger than expected residual density maxima of 2.09 and 3.03 eÅ<sup>-3</sup> were present close to the metal atom (nickel) location after completion of the structure refinement. All this led to a final high wR2 value of 0.3910 and to a low bond precision on C-C bonds of 0.01845 Å. Nevertheless, it was possible to undoubtedly solve the molecular structure with a  $R = 11.70\%$ .

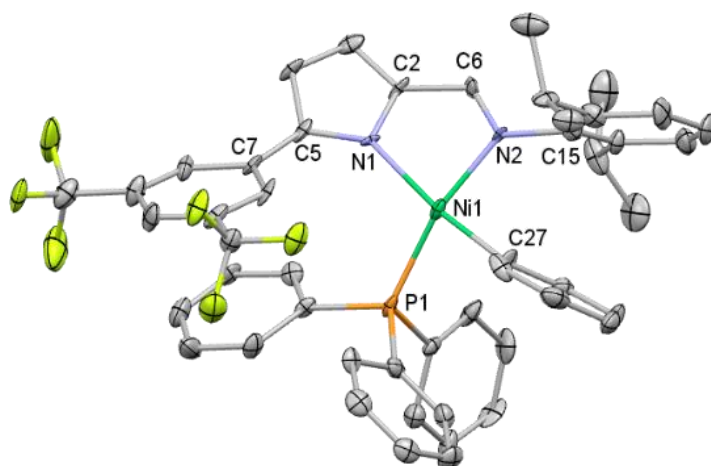


**Figure S4.** Perspective view of the molecular structure of the phenyl nickel iminopyrrolyl complex **6**, using 30% probability level ellipsoids. All the calculated hydrogen atoms were omitted for clarity. Owing to the poor quality of the crystal data, the picture is not presented in the article.

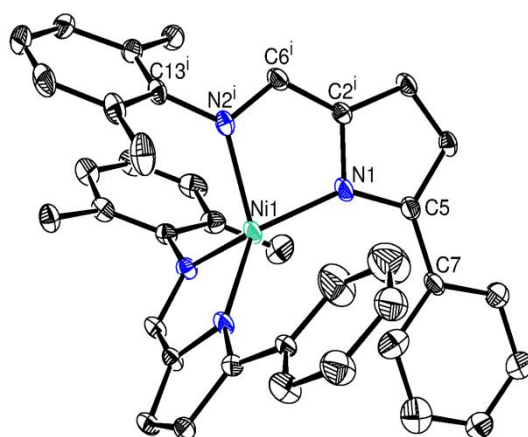


**Figure S5** ORTEP-3 diagram of the homoleptic complex bis[5-phenyl-2-(*N*-2,6-dimethylphenylformimino)pyrrolyl] nickel(II) (**1<sub>A</sub>**), using 10% probability level ellipsoids. Half molecule is generated by the symmetry operation  $1/2-x, 3/2-y, z$ . Hydrogen atoms have been omitted for clarity.

**Table S7** Crystallographic data and refinement details for the structures of iminopyrrolyl nickel complexes **1-3** and of bis(iminopyrrolyl)nickel complex **1<sub>A</sub>**.

	<b>1</b>	<b>1<sub>A</sub></b>	<b>2</b>	<b>3</b>
Formula	2(C <sub>43</sub> H <sub>37</sub> N <sub>2</sub> NiP)·C <sub>6</sub> H <sub>14</sub>	C <sub>38</sub> H <sub>34</sub> N <sub>4</sub> Ni	C <sub>47</sub> H <sub>45</sub> N <sub>2</sub> NiP	C <sub>41</sub> H <sub>28</sub> F <sub>5</sub> N <sub>2</sub> NiP
<i>M</i>	1429.02	605.38	727.53	733.33
λ (Å)	0.71073	0.71073	0.71073	0.71073
<i>T</i> (K)	150(2)	150(2)	150(2)	150(2)
Crystal system	Monoclinic	Tetragonal	Monoclinic	Monoclinic
Space group	<i>P</i> 2 <sub>1</sub>	<i>P</i> 4 <sub>2</sub> / <i>n</i>	<i>P</i> 2 <sub>1</sub> / <i>c</i>	<i>P</i> 2 <sub>1</sub> / <i>n</i>
<i>a</i> (Å)	10.3715(15)	11.600(3)	11.4768(8)	13.1214(7)
<i>b</i> (Å)	33.585(5)	11.600(3)	14.1372(11)	8.8622(4)
<i>c</i> (Å)	10.5727(17)	23.772(6)	23.4360(16)	31.0382(15)
α (°)	90	90	90	90
β (°)	94.5720(10)	90	93.967(3)	101.361(2)
γ (°)	90	90	90	90
<i>V</i> (Å <sup>3</sup> )	3671.0(10)	3198.8(18)	3793.4(5)	3538.5(3)
<i>Z</i>	2	4	4	4
ρ <sub>calc</sub> (g.cm <sup>-3</sup> )	1.293	1.257	1.274	1.377
μ (mm <sup>-1</sup> )	0.608	0.639	0.589	0.652
Crystal size	0.14×0.12×0.10	0.20×0.12×0.10	0.40×0.30×0.25	0.20×0.16×0.16
Crystal colour	Red	Green	Orange	Red
Crystal description	Block	Prism	Block	Block
θ <sub>max</sub> (°)	25.349	25.345	25.726	25.767
Total data	37217	36591	97172	29088
Unique data	13022	2915	7232	6736
<i>R</i> <sub>int</sub>	0.1798	0.1516	0.0621	0.0821
<i>R</i> [ <i>I</i> >2σ( <i>I</i> )]	0.0861	0.0974	0.0313	0.0497
<i>R</i> <sub>w</sub>	0.1720	0.2898	0.0671	0.1080
Goodness of fit	0.910	0.996	1.026	1.028
ρ <sub>min</sub>	-0.510	-0.789	-0.387	-0.376
ρ <sub>max</sub>	1.051	1.048	0.314	0.443

**Table S8** Crystallographic data and refinement details for the structures of iminopyrrolyl nickel complexes **4-7**.

	<b>4</b>	<b>5</b>	<b>6</b> <sup>a</sup>	<b>7</b>
Formula	C <sub>45</sub> H <sub>41</sub> N <sub>2</sub> NiP	C <sub>49</sub> H <sub>49</sub> N <sub>2</sub> NiP	C <sub>49</sub> H <sub>43</sub> N <sub>2</sub> F <sub>6</sub> NiP	C <sub>56</sub> H <sub>63</sub> N <sub>2</sub> NiP
<i>M</i>	699.48	755.58	863.53	853.76
$\lambda$ (Å)	0.71073	0.71073	0.71073	0.71073
<i>T</i> (K)	150(2)	150(2)	150(2)	150(2)
Crystal system	Monoclinic	Monoclinic	Monoclinic	Triclinic
Space group	<i>P2</i> <sub>1</sub> / <i>c</i>	<i>C2</i> / <i>c</i>	<i>P2</i> <sub>1</sub> / <i>c</i>	<i>P</i> -1
<i>a</i> (Å)	11.9364(3)	40.613(4)	20.749(4)	10.1181(8)
<i>b</i> (Å)	32.1736(9)	11.4486(12)	11.3247(19)	13.5337(9)
<i>c</i> (Å)	10.3382(3)	18.1713(18)	17.904(3)	19.3762(16)
$\alpha$ (°)	90	90	90	108.714(3)
$\beta$ (°)	108.6030(10)	107.820(4)	93.833(8)	94.968(3)
$\gamma$ (°)	90	90	90	106.611(3)
<i>V</i> (Å <sup>3</sup> )	3762.81(18)	8043.6(14)	4197.6(12)	2361.2(3)
<i>Z</i>	4	8	4	2
$\rho_{calc}$ (g.cm <sup>-3</sup> )	1.235	1.248	1.366	1.201
$\mu$ (mm <sup>-1</sup> )	0.591	0.558	0.564	0.483
Crystal size	0.28×0.22×0.22	0.25×0.25×0.20	0.20×0.10×0.10	0.30×0.30×0.28
Crystal colour	Red	Orange	Orange	Red
Crystal description	Block	Block	Needle	Prism
$\theta_{max}$ (°)	28.037	25.651	25.772	25.761
Total data	83151	58869	16545	24486
Unique data	9051	7578	7570	9000
<i>R</i> <sub>int</sub>	0.0537	0.0941	0.2995	0.0631
<i>R</i> [ <i>I</i> >2 $\sigma$ ( <i>I</i> )]	0.0382	0.0526	0.1170	0.0504
<i>R</i> <sub>w</sub>	0.0923	0.1101	0.2564	0.1115
Goodness of fit	1.043	1.050	0.951	1.001
$\rho_{min}$	-0.433	-0.378	-2.537	-0.429
$\rho_{max}$	0.357	0.527	3.031	0.429

<sup>a</sup> Values resulting from poor crystallographic data.

**Table S9** Selected bond distances (Å) and angles (°) for compounds **1** to **3**.

	<b>1</b>		<b>2</b>	<b>3</b>
	Molecule A	Molecule B		
<i>Distances (Å)</i>				
Ni1-N1	1.926(12)	1.969(12)	1.9310(15)	1.989(3)
Ni1-N2	1.966(14)	1.986(13)	1.9795(14)	1.985(3)
Ni1-P1	2.174(5)	2.170(5)	2.1540(5)	2.1677(11)
Ni1-C <sub>ipso2</sub> <sup>a</sup>	1.915(14)	1.899(16)	1.9027(17)	1.888(3)
N1-C2	1.39(2)	1.41(2)	1.382(2)	1.389(4)
N1-C5	1.37(2)	1.34(2)	1.354(2)	1.364(5)
C5-C7	1.49(2)	1.44(2)	1.462(2)	1.461(5)
C2-C6	1.43(2)	1.39(3)	1.410(2)	1.400(6)
C6-N2	1.30(2)	1.31(2)	1.309(2)	1.308(5)
N2-C <sub>ipso1</sub> <sup>b</sup>	1.43(2)	1.44(2)	1.431(2)	1.408(4)
<i>Angles (°)</i>				
N1-Ni1-N2	83.1(5)	84.0(5)	82.52(6)	82.76(11)
N1-Ni1-P1	105.8(4)	106.2(4)	102.98(5)	102.17(8)
P1-Ni1-C <sub>ipso2</sub>	84.2(4)	84.9(4)	85.60(6)	87.73(10)
N2-Ni1-C <sub>ipso2</sub>	93.2(6)	90.8(6)	93.77(7)	88.55(13)
Ni1-N1-C2	111.8(9)	108.4(10)	109.81(11)	106.6(2)
Ni1-N1-C5	146.3(11)	143.9(11)	142.81(12)	146.4(2)
Ni1-N2-C6	111.8(11)	110.2(11)	109.55(11)	109.5(2)
Ni1-N2-C <sub>ipso1</sub>	129.3(11)	129.9(11)	129.78(11)	130.1(2)
C5-N1-C2	101.9(12)	107.6(13)	106.55(14)	105.2(3)
N1-C5-C7	120.7(15)	124.3(15)	122.33(15)	124.4(3)
N1-C2-C6	113.3(14)	115.9(15)	113.78(14)	116.8(3)
C2-C6-N2	117.7(15)	119.4(16)	117.72(15)	117.3(3)
C6-N2-C <sub>ipso1</sub>	118.9(14)	119.9(14)	120.34(14)	118.6(3)
N2-Ni1-P1	152.1(4)	152.7(4)	152.06(5)	160.33(8)
N1-Ni1-C <sub>ipso2</sub>	165.0(6)	164.6(6)	168.10(7)	169.89(13)

<sup>a</sup>C<sub>ipso2</sub> corresponds to the *ipso* carbon of the phenyl ring directly bonded to the nickel;<sup>b</sup>C<sub>ipso1</sub> corresponds to the *ipso* carbon of the *N*-aryl ring in the iminopyrrolyl chelating ligand.

**Table S10** Selected bond distances (Å) and angles (°) for compounds **4** to **7**.

	<b>4</b>	<b>5</b>	<b>6<sup>c</sup></b>	<b>7</b>
<i>Distances (Å)</i>				
Ni1-N1	1.9494(15)	1.963(3)	1.985(8)	1.966(2)
Ni1-N2	1.9865(15)	1.978(2)	1.957(10)	1.980(2)
Ni1-P1	2.1661(5)	2.1650(9)	2.162(4)	2.1518(8)
Ni1-C <sub>ipso2</sub> <sup>a</sup>	1.8987(19)	1.908(3)	1.897(12)	1.889(3)
N1-C2	1.382(2)	1.385(4)	1.322(15)	1.389(4)
N1-C5	1.358(2)	1.364(4)	1.356(14)	1.365(4)
C5-C7	1.469(2)	1.472(5)	1.436(17)	1.493(4)
C2-C6	1.404(3)	1.408(5)	1.454(16)	1.405(4)
C6-N2	1.307(2)	1.307(4)	1.278(15)	1.307(4)
N2-C <sub>ipso1</sub> <sup>b</sup>	1.431(2)	1.440(4)	1.476(15)	1.428(4)
<i>Angles (°)</i>				
N1-Ni1-N2	82.89(6)	82.63(10)	81.9(4)	82.93(9)
N1-Ni1-P1	104.91(5)	103.07(7)	105.9(3)	104.21(7)
P1-Ni1-C <sub>ipso2</sub>	85.28(5)	85.20(11)	83.8(5)	88.26(9)
N2-Ni1-C <sub>ipso2</sub>	94.36(7)	93.57(13)	92.0(5)	96.10(11)
Ni1-N1-C2	110.09(11)	108.4(2)	111.0(7)	108.90(17)
Ni1-N1-C5	143.16(13)	144.3(2)	140.5(8)	145.15(19)
Ni1-N2-C6	110.62(12)	110.0(2)	112.1(8)	110.40(19)
Ni1-N2-C <sub>ipso1</sub>	128.71(12)	129.2(2)	130.1(7)	130.57(17)
C5-N1-C2	106.33(15)	105.9(3)	108.4(9)	105.5(2)
N1-C5-C7	123.70(16)	124.1(3)	128.5(10)	123.9(3)
N1-C2-C6	115.26(16)	115.0(3)	114.8(10)	115.1(2)
C2-C6-N2	117.81(16)	117.6(3)	116.8(11)	118.1(3)
C6-N2-C <sub>ipso1</sub>	118.97(15)	119.9(3)	117.0(10)	118.4(2)
N2-Ni1-P1	151.36(6)	154.15(8)	156.4(3)	142.11(7)
N1-Ni1-C <sub>ipso2</sub>	163.52(8)	168.23(12)	167.9(5)	160.99(11)

<sup>a</sup> C<sub>ipso2</sub> corresponds to the *ipso* carbon of the phenyl ring directly bonded to the nickel;

<sup>b</sup> C<sub>ipso1</sub> corresponds to the *ipso* carbon of the *N*-aryl ring in the iminopyrrolyl chelating ligand.

<sup>c</sup> Values resulting from poor crystallographic data.

**Table S11** Dihedral angles (°) for compounds **1** to **7**.

Dihedral Angles(°)	2- <i>N</i> -2,6-Ar/NC <sub>4</sub> H <sub>2</sub> <sup>a</sup>	5-Ar/NC <sub>4</sub> H <sub>2</sub>	N1-Ni1-N2/P1-Ni1-C <sub>ipso2</sub>
<b>1</b> <i>mol. A</i>	80.2(5)	36.7(6)	32.14(57)
<b>1</b> <i>mol. B</i>	81.1(5)	33.8(6)	30.38(61)
<b>2</b>	70.34(8)	33.73(10)	30.74(7)
<b>3</b>	63.99(16)	26.9(2)	19.91(15)
<b>4</b>	73.64(9)	38.41(11)	33.81(4)
<b>5</b>	74.12(18)	31.5(2)	28.71(18)
<b>6</b> <sup>b</sup>	71.9(5)	36.9(5)	25.7(3)
<b>7</b>	75.35(11)	77.44(10)	43.46(9)

<sup>a</sup> The iminopyrrole ring plane is defined by atoms N1-C2-C6-N2, thus including part of the pyrrole ring (atoms N1 and C2) and of the imino bond (atoms C6 and N2).

<sup>b</sup> Values resulting from poor crystallographic data.

**Table S12** Selected bond distances (Å) and angles (°) for bis(iminopyrrolyl)nickel complex **1<sub>A</sub>**.

Distances (Å)		Angles (°)	
Ni1-N1	1.945(6)	N1-Ni1-N2 <sup>i</sup>	129.4(3)
Ni1-N2 <sup>i</sup>	2.038(6)	Ni1-N1-C2 <sup>i</sup>	110.2(5)
N1-C2 <sup>i</sup>	1.380(10)	Ni1-N1-C5	142.8(5)
N1-C5	1.385(10)	Ni1-N2 <sup>i</sup> -C6 <sup>i</sup>	110.7(5)
C5-C7	1.475(11)	Ni1-N2 <sup>i</sup> -C13 <sup>i</sup>	128.0(5)
C2 <sup>i</sup> -C6 <sup>i</sup>	1.413(11)	N1-C2 <sup>i</sup> -C6 <sup>i</sup>	117.9(6)
C6 <sup>i</sup> -N2 <sup>i</sup>	1.297(9)	N1-C5-C7	123.7(7)
N2 <sup>i</sup> -C13 <sup>i</sup>	1.416(10)	C2 <sup>i</sup> -N1-C5	106.8(6)
		C2 <sup>i</sup> -C6 <sup>i</sup> -N2 <sup>i</sup>	117.4(6)
		C6 <sup>i</sup> -N2 <sup>i</sup> -C13 <sup>i</sup>	120.5(6)
		N1-Ni1-N1 <sup>i</sup>	129.6(3)
		N2 <sup>i</sup> -Ni1-N2	104.0(2)
		N1-Ni1-N2	129.4(3)

## NMR spectra of complexes 1-7

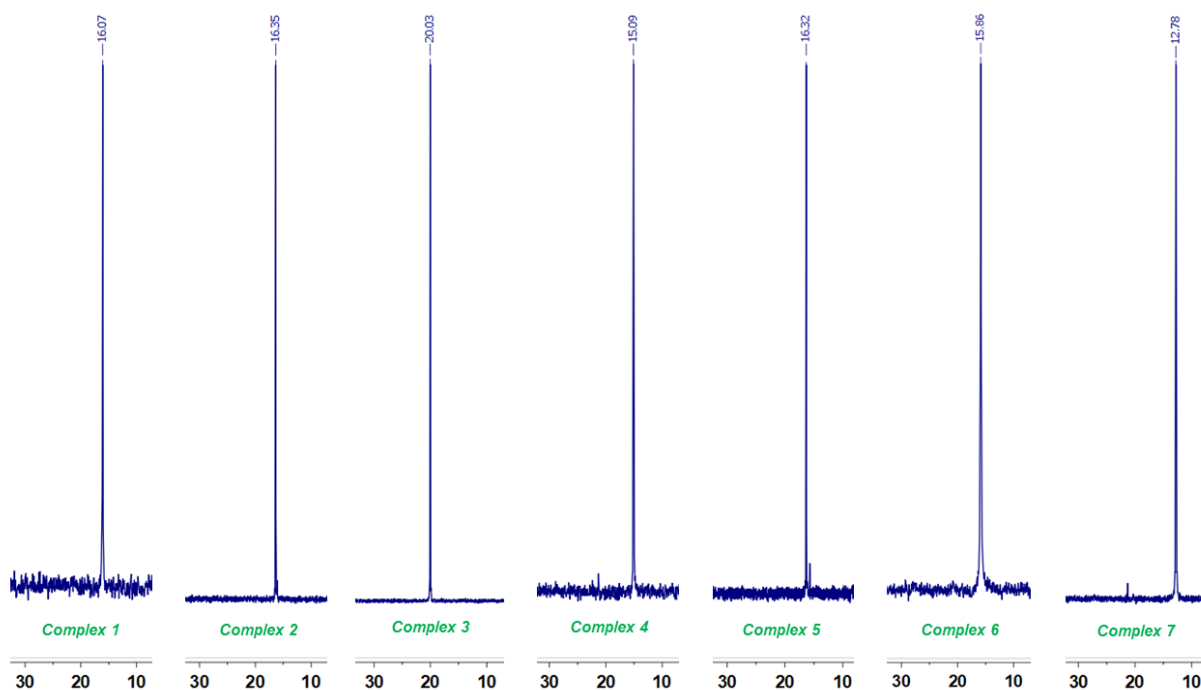


Figure S6  $^{31}\text{P}\{^1\text{H}\}$  NMR (121 MHz,  $\text{CD}_2\text{Cl}_2$ ) spectra of complexes 1-7 (162 MHz for 3 and 6).

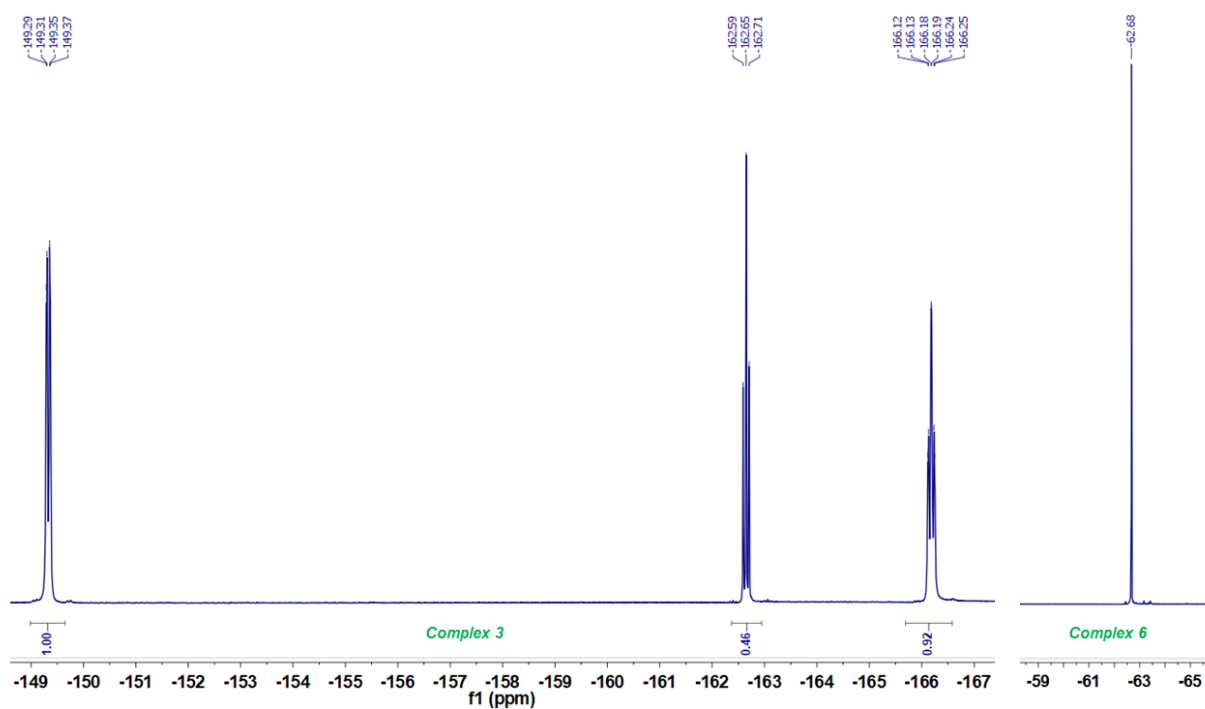


Figure S7  $^{19}\text{F}\{^1\text{H}\}$  NMR (376 MHz,  $\text{CD}_2\text{Cl}_2$ ) spectra of complexes 3 and 6.

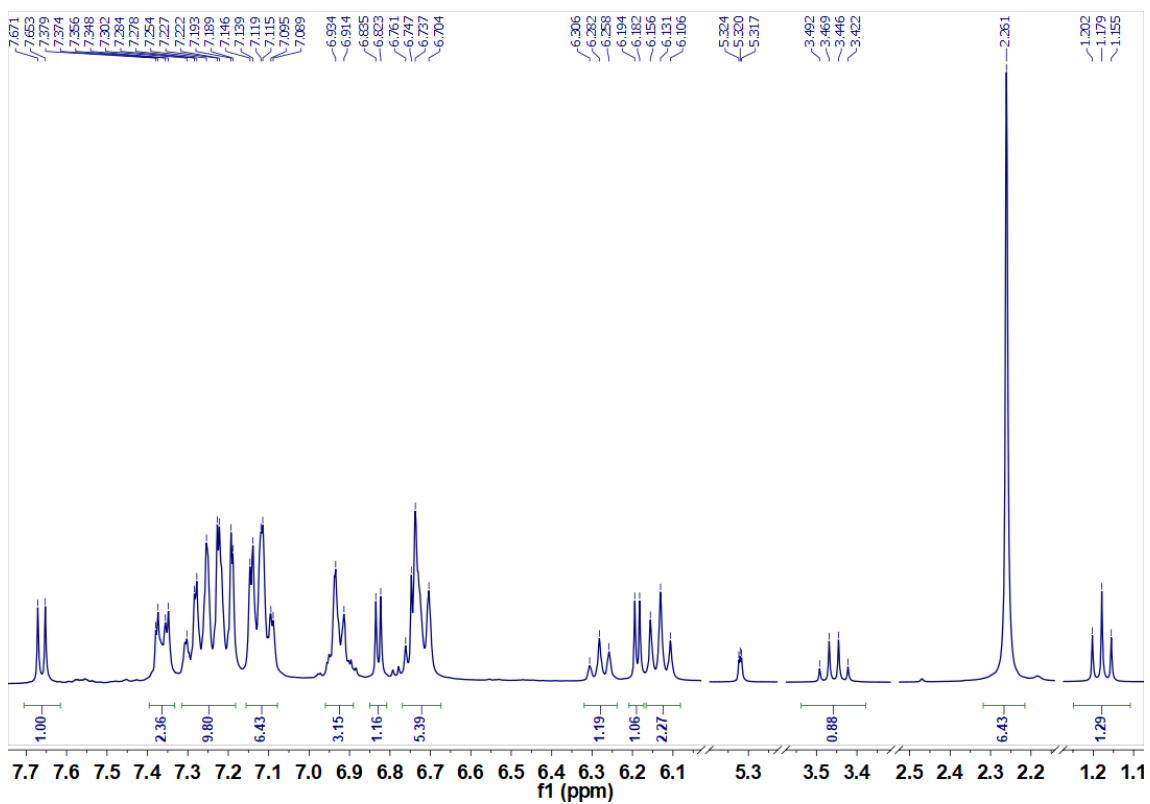


Figure S8  $^1\text{H}$  NMR (300 MHz,  $\text{CD}_2\text{Cl}_2$ ) spectrum of complex **1**.

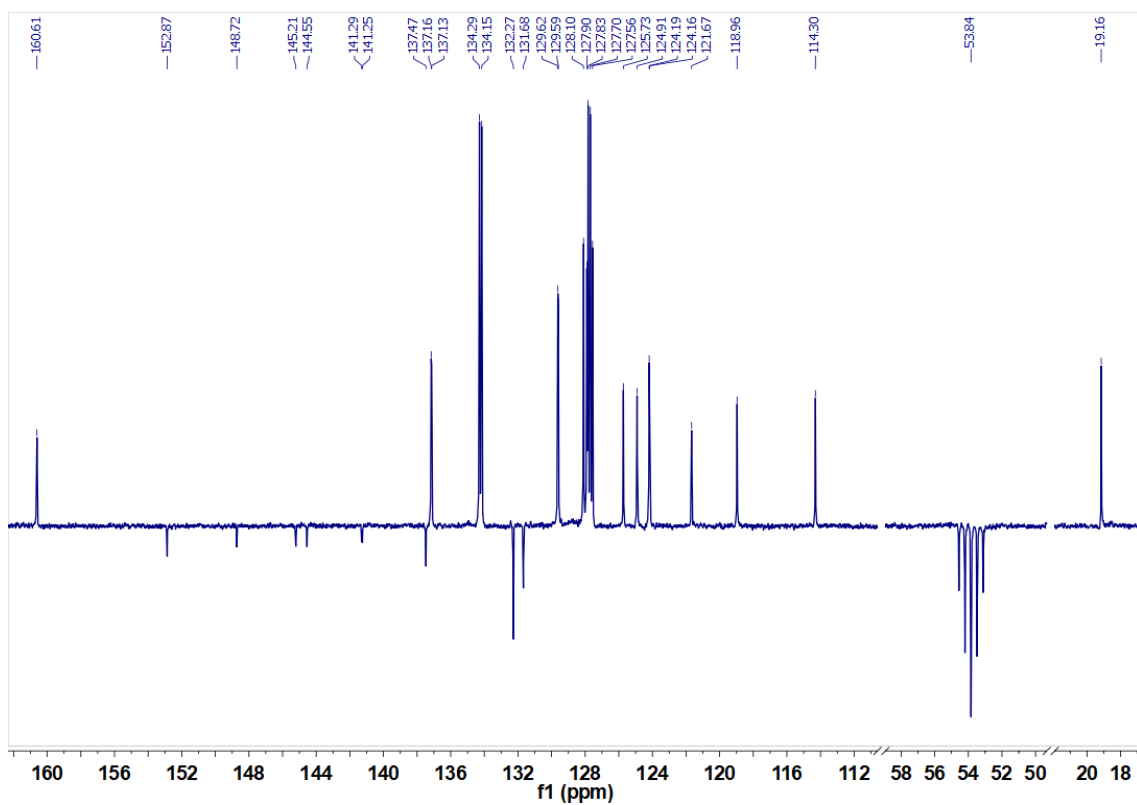


Figure S9  $^{13}\text{C}$  APT NMR (75 MHz,  $\text{CD}_2\text{Cl}_2$ ) spectrum of complex **1**.

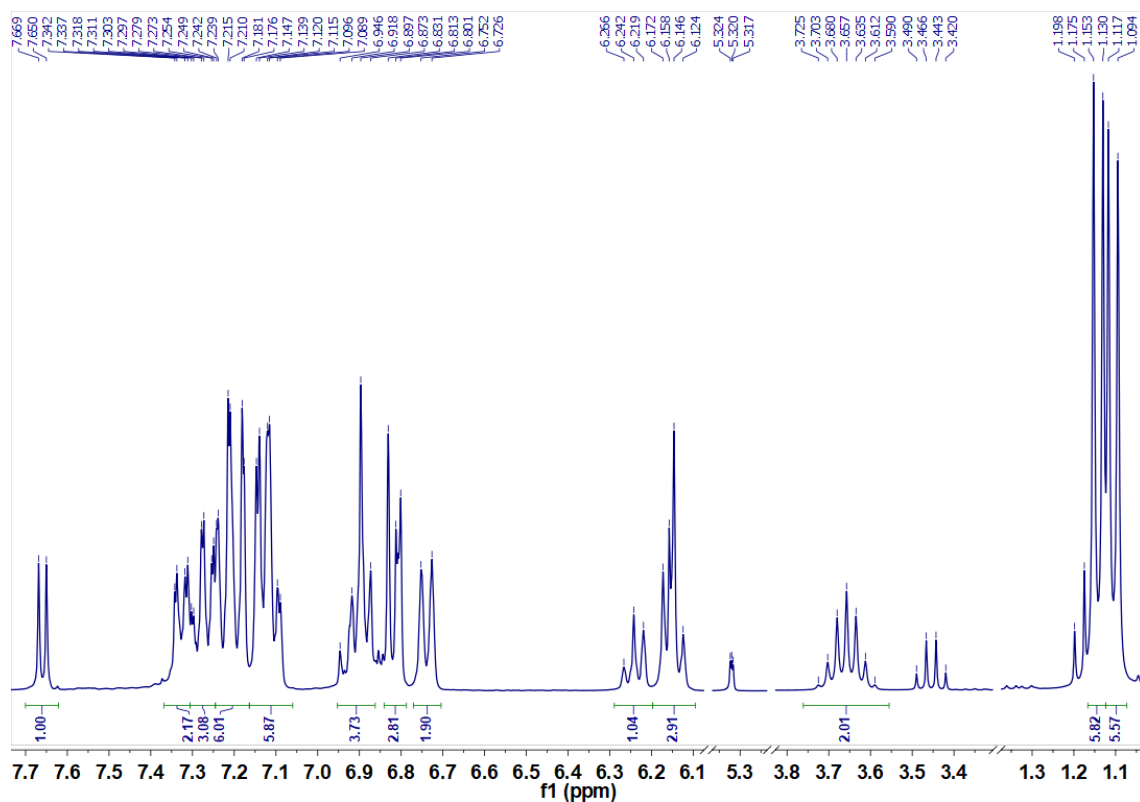


Figure S10  $^1\text{H}$  NMR (300 MHz,  $\text{CD}_2\text{Cl}_2$ ) spectrum of complex **2**.

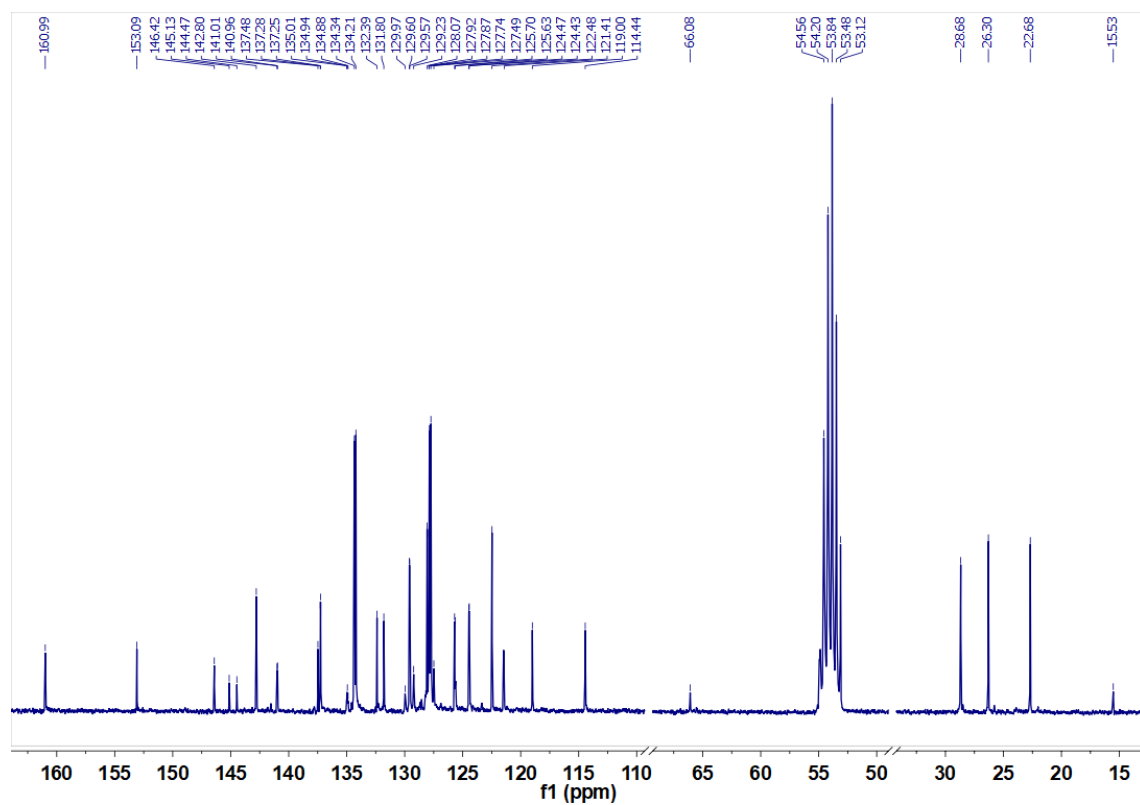


Figure 11  $^{13}\text{C}$   $\{^1\text{H}\}$  NMR (75 MHz,  $\text{CD}_2\text{Cl}_2$ ) spectrum of complex **2**.

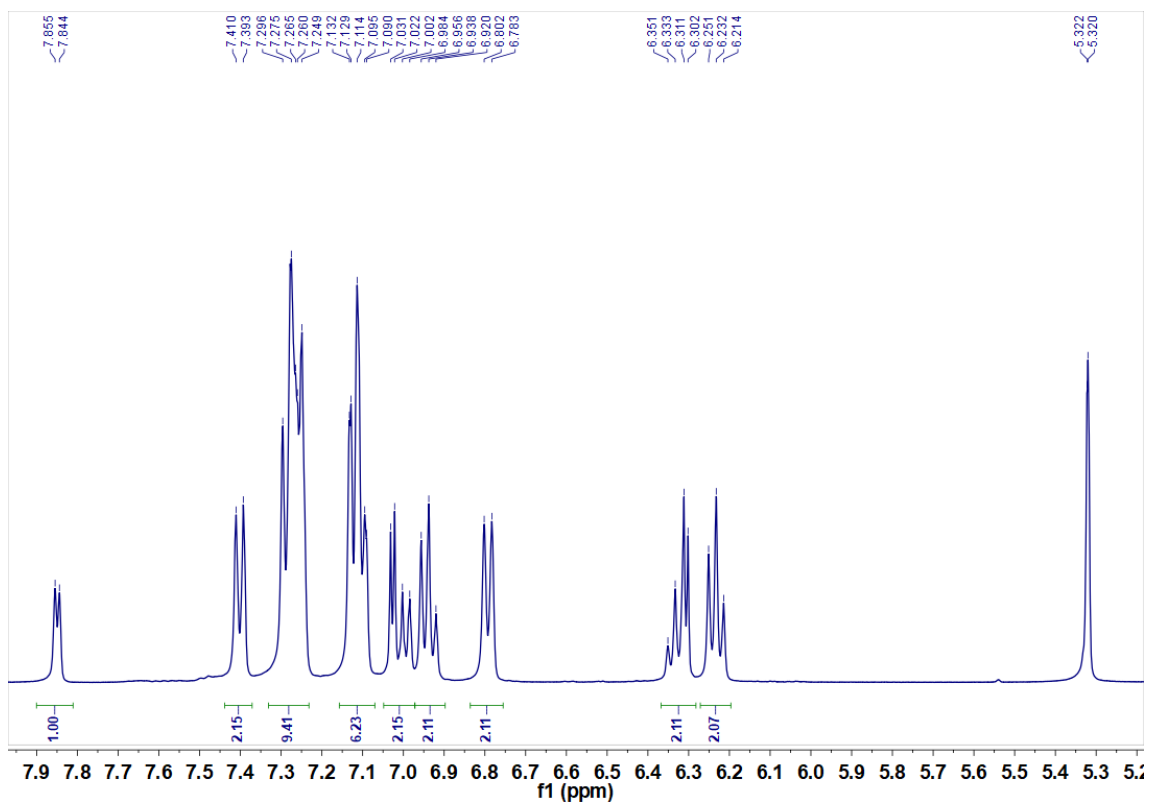


Figure S12  $^1\text{H}$  NMR (400 MHz,  $\text{CD}_2\text{Cl}_2$ ) spectrum of complex **3**.

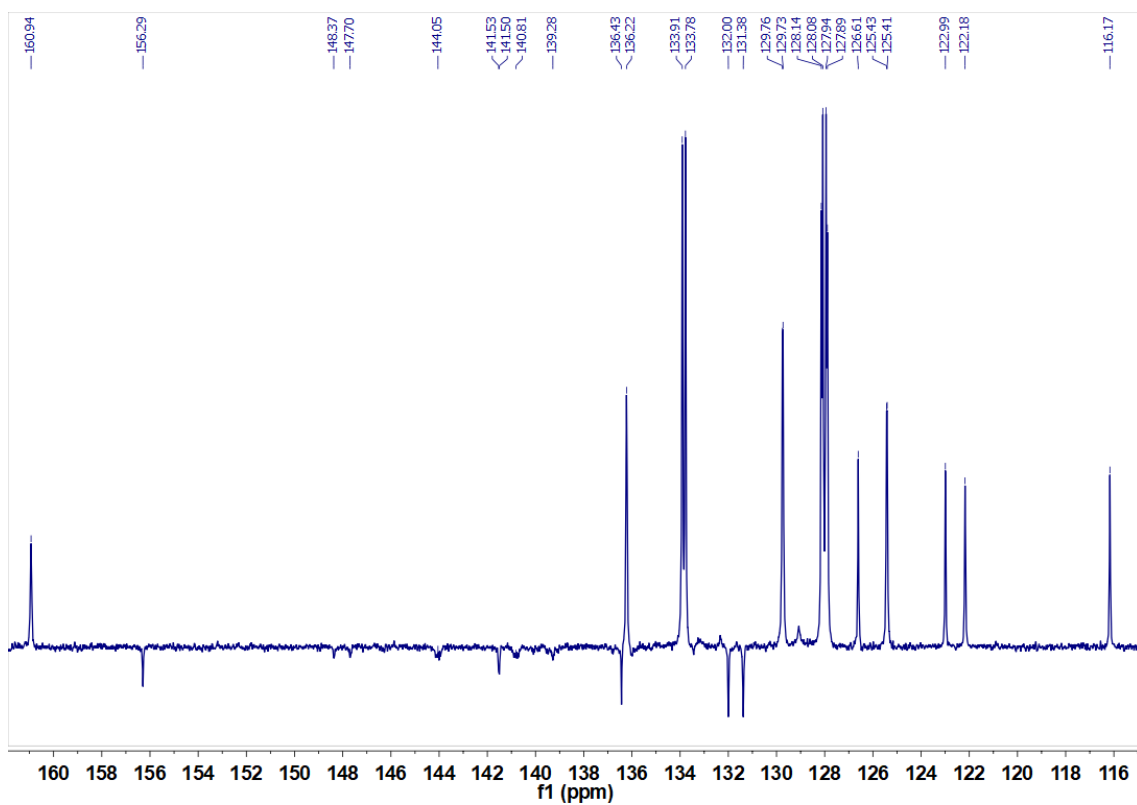


Figure S13  $^{13}\text{C}$  APT NMR (101 MHz,  $\text{CD}_2\text{Cl}_2$ ) spectrum of complex **3**.

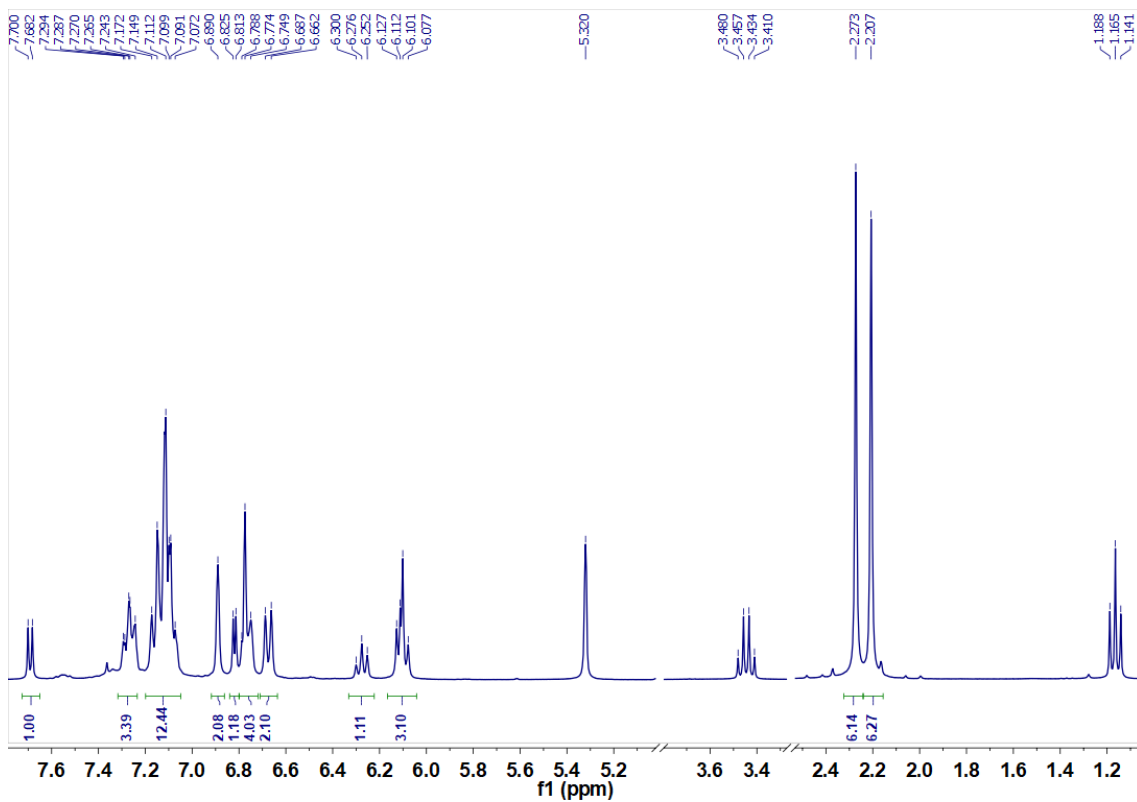


Figure S14  $^1\text{H}$  NMR (300 MHz,  $\text{CD}_2\text{Cl}_2$ ) spectrum of complex 4.

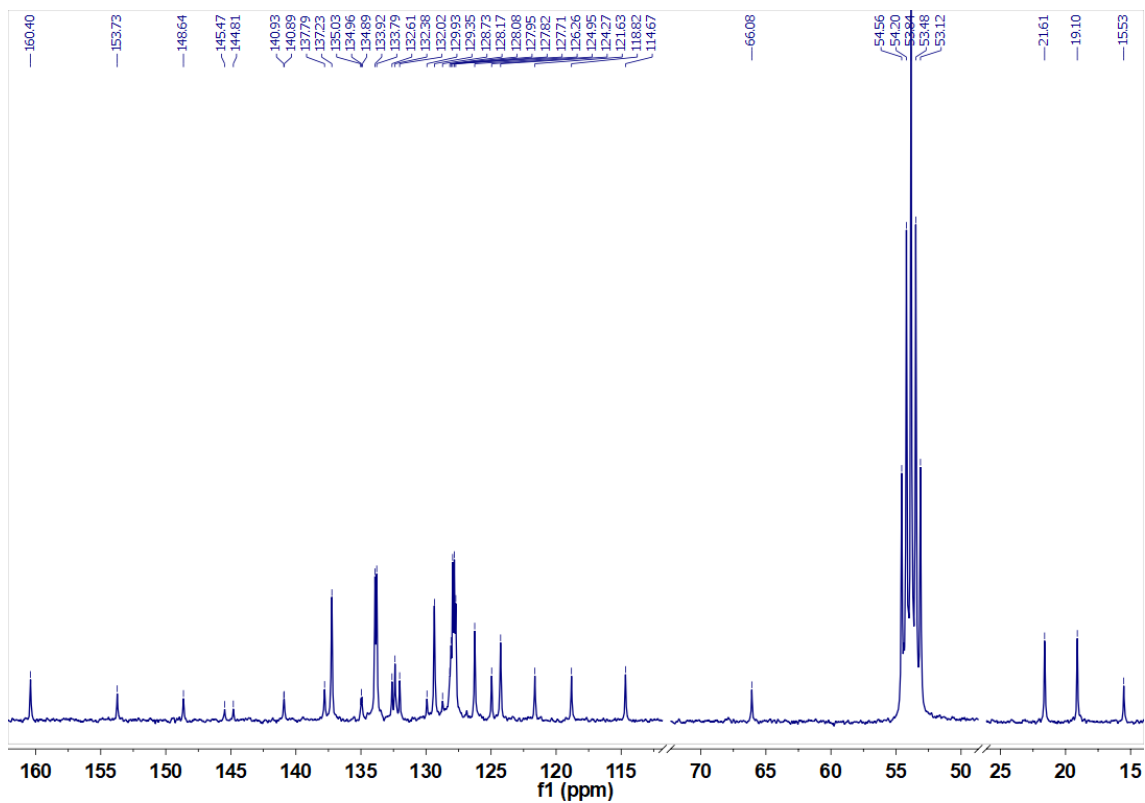


Figure S15  $^{13}\text{C}\{^1\text{H}\}$  NMR (75 MHz,  $\text{CD}_2\text{Cl}_2$ ) spectrum of complex 4.

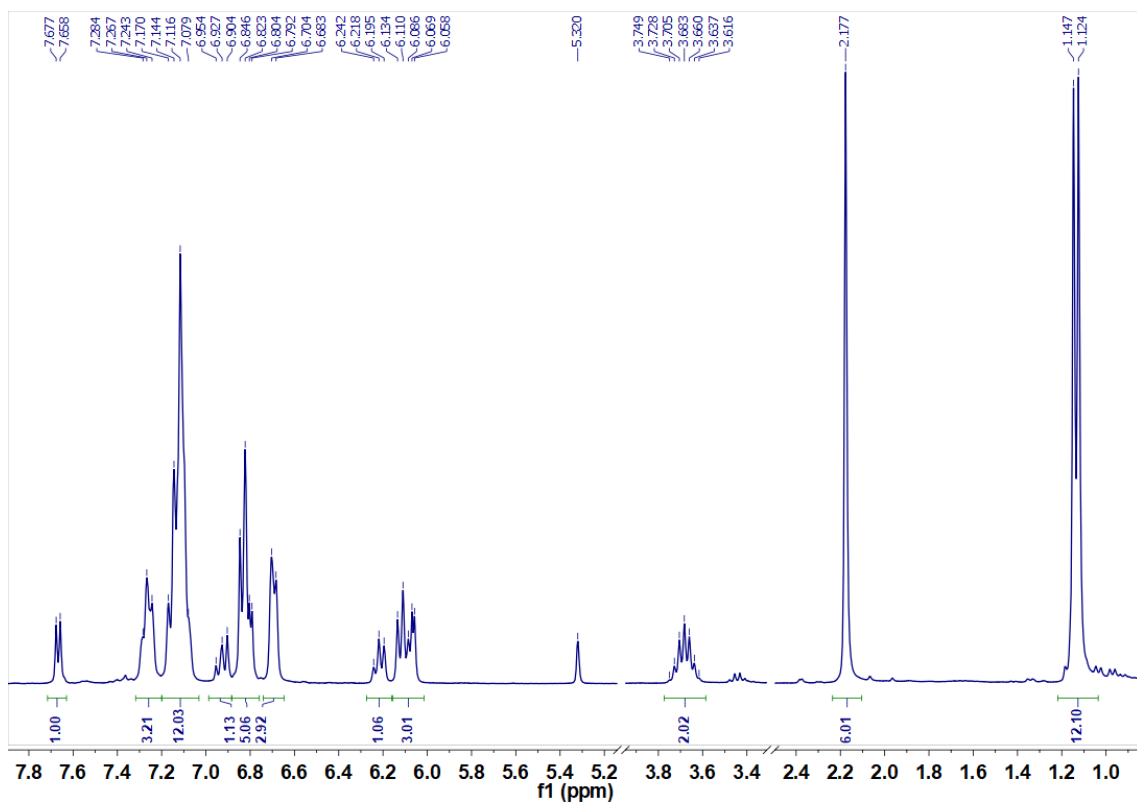


Figure S16  $^1\text{H}$  NMR (300 MHz,  $\text{CD}_2\text{Cl}_2$ ) spectrum of complex **5**.

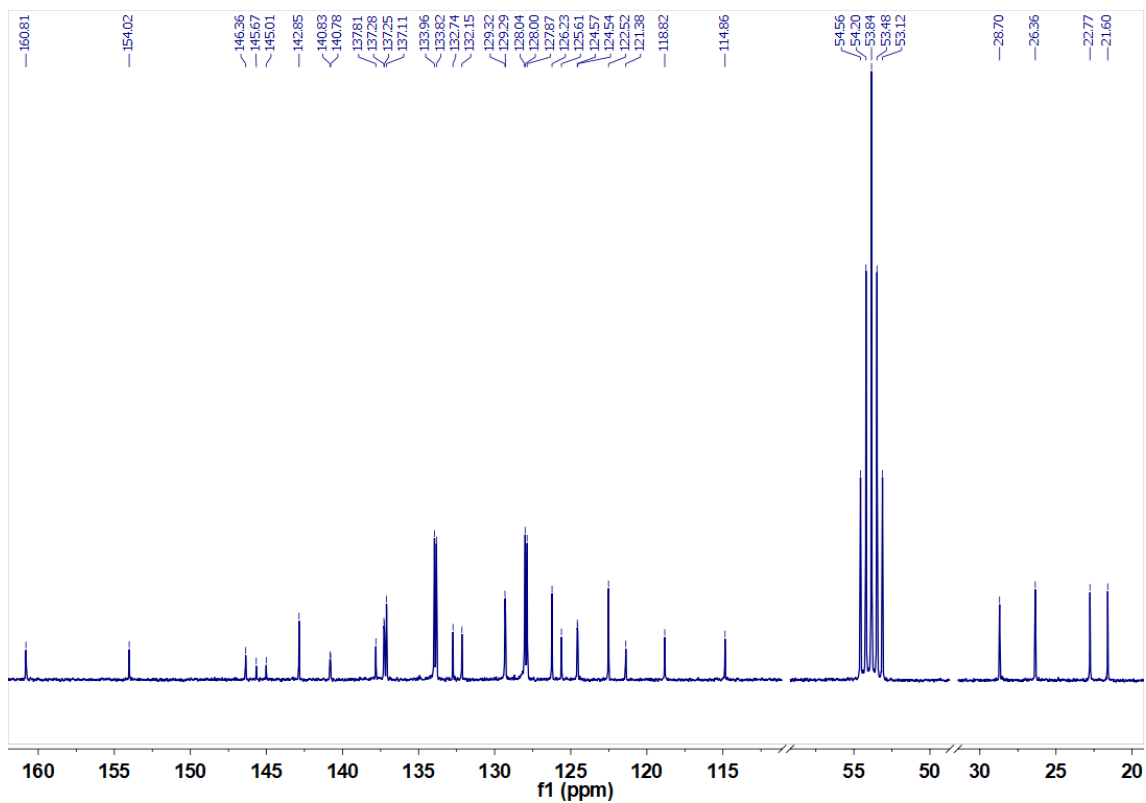


Figure S17  $^{13}\text{C}\{^1\text{H}\}$  NMR (75 MHz,  $\text{CD}_2\text{Cl}_2$ ) spectrum of complex **5**.

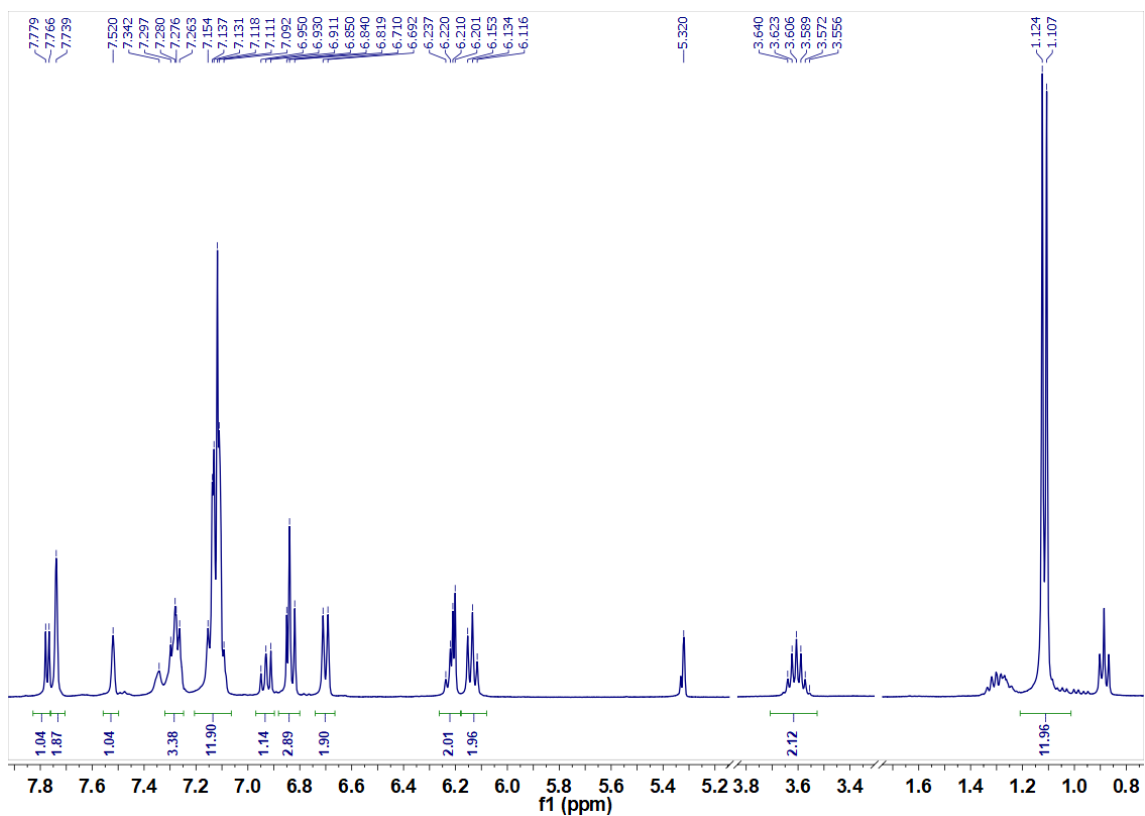


Figure S18  $^1\text{H}$  NMR (400 MHz,  $\text{CD}_2\text{Cl}_2$ ) spectrum of complex **6**.

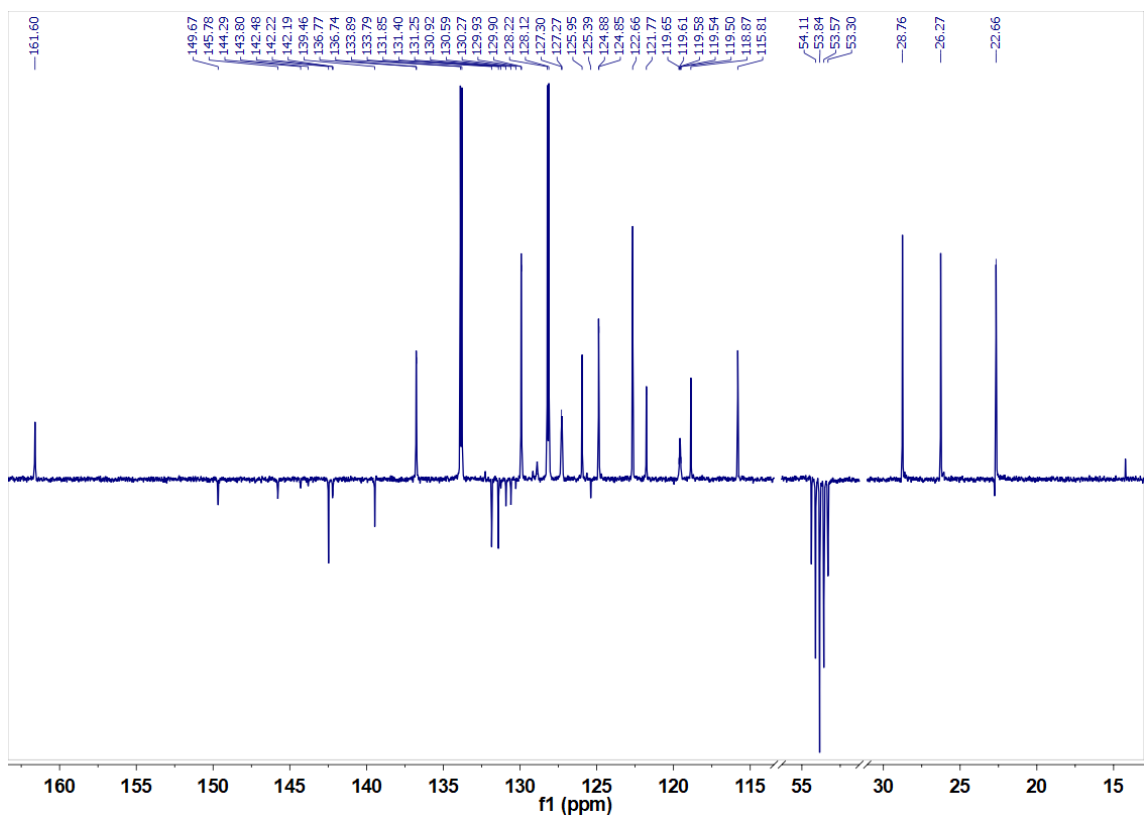


Figure S19  $^{13}\text{C}$  APT NMR (101 MHz,  $\text{CD}_2\text{Cl}_2$ ) spectrum of complex **6**.

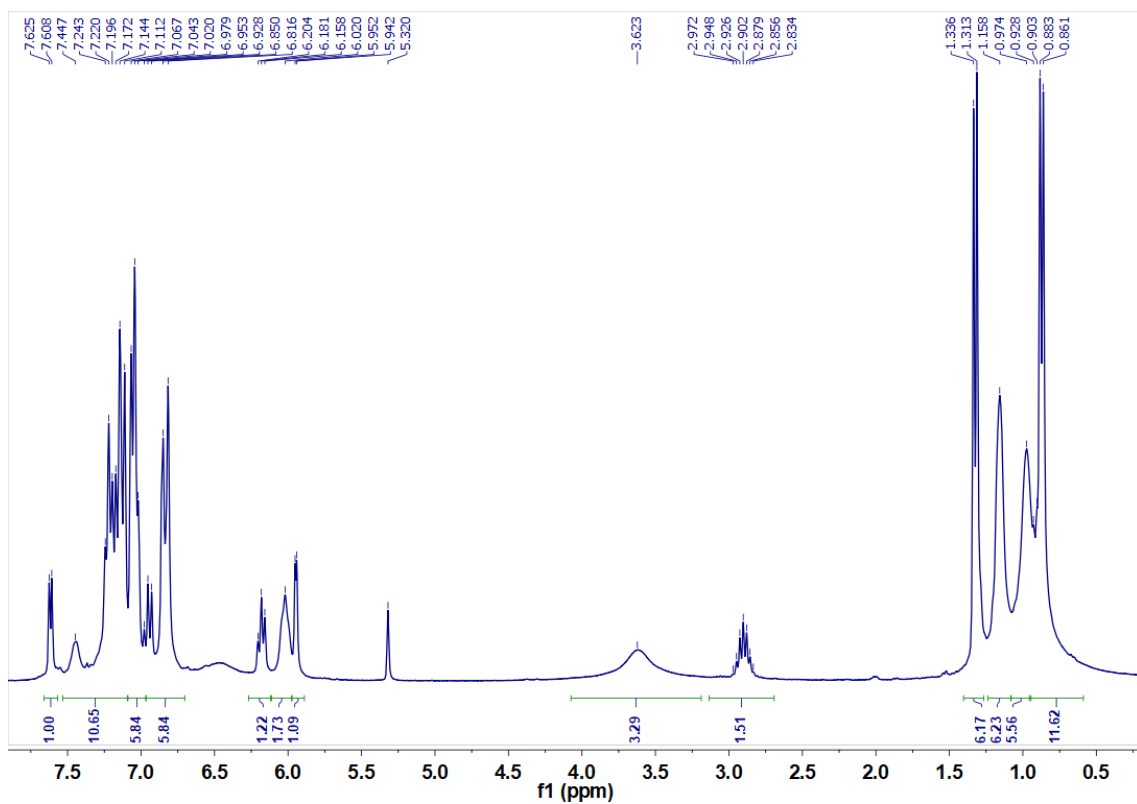


Figure S20  $^1\text{H}$  NMR (300 MHz,  $\text{CD}_2\text{Cl}_2$ ) spectrum of complex 7.

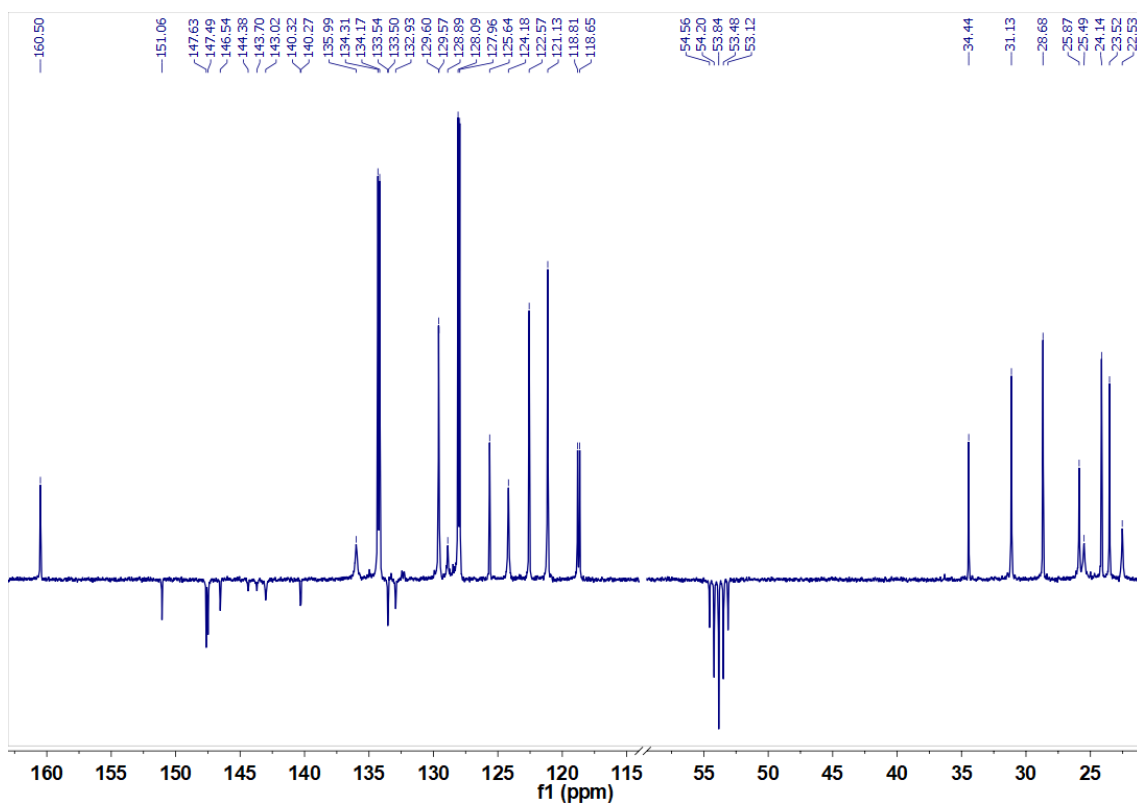
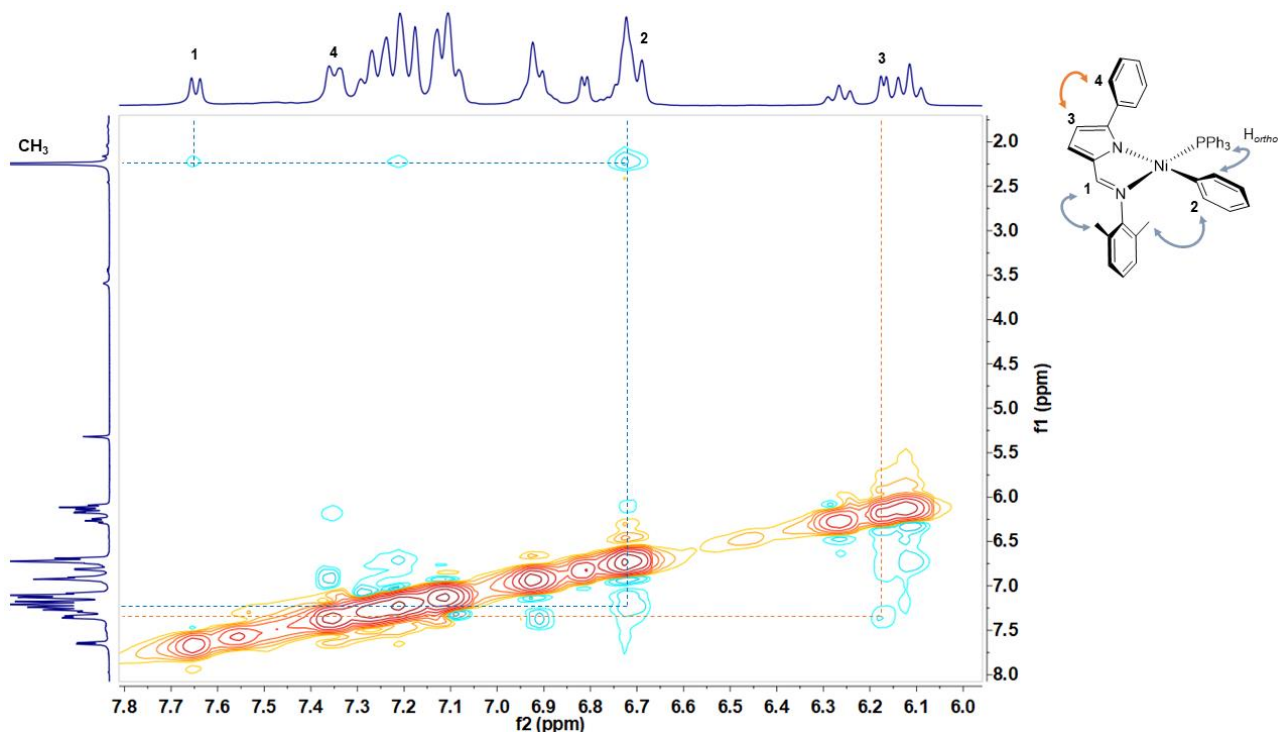
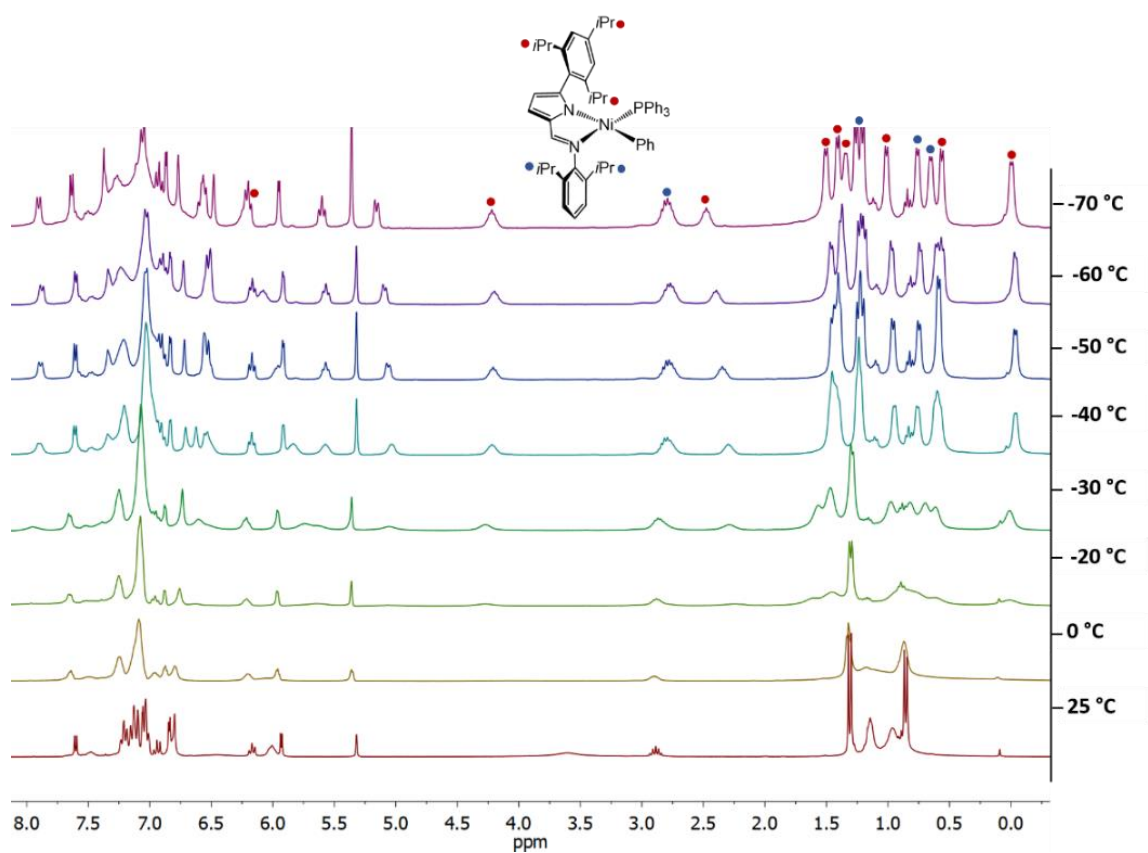


Figure S21  $^{13}\text{C}$  APT NMR (75 MHz,  $\text{CD}_2\text{Cl}_2$ ) spectrum of complex 7.



**Figure S22** Partial view of the  $^1\text{H}$ - $^1\text{H}$  NOESY NMR (300 MHz,  $\text{CD}_2\text{Cl}_2$ ) spectrum of complex **1**.



**Figure S23** VT- $^1\text{H}$  NMR (300 MHz,  $\text{CD}_2\text{Cl}_2$ ) experiments for complex **7**.

## Catalytic kinetic profiles for the polymerisation of ethylene

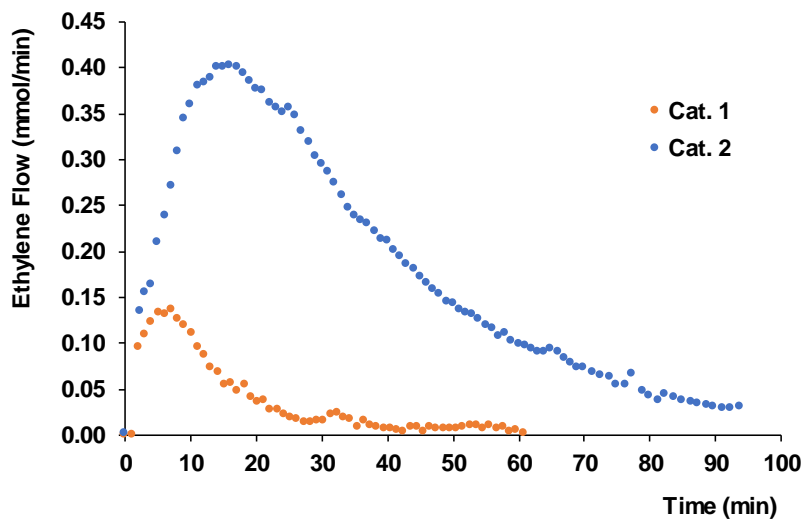


**Figure S24** Preliminary tests of ethylene consumption vs. reaction time for catalysts **1** and **2**, at 3 bar and 50 °C.

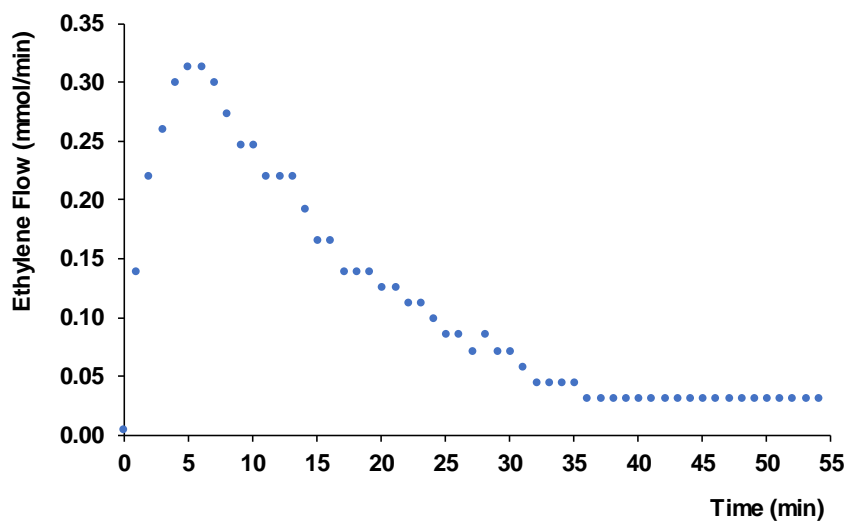


**Figure S25** Reaction profile for catalyst **3** obtained by the mass flow meter (ethylene flow vs. time), when acting as single-component at 3 bar and 25 °C.

## GC chromatograms

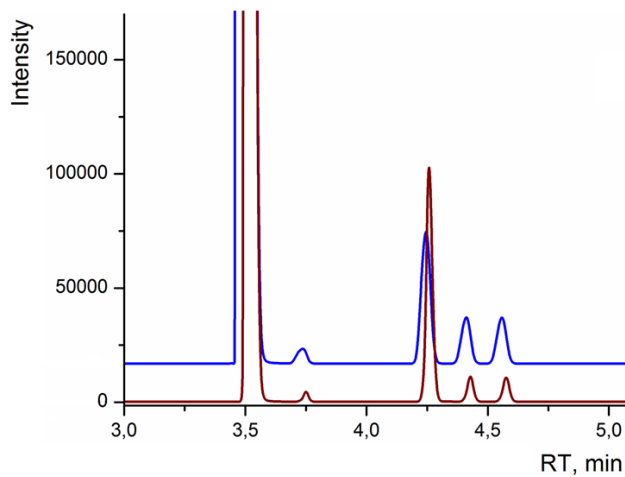


**Figure S26** GC chromatogram of the gas phase collected at the end of catalytic test with the system **3**/[Ni(COD)<sub>2</sub>] (in blue) and after the addition *cis*-2-butene as an internal standard (in brown).

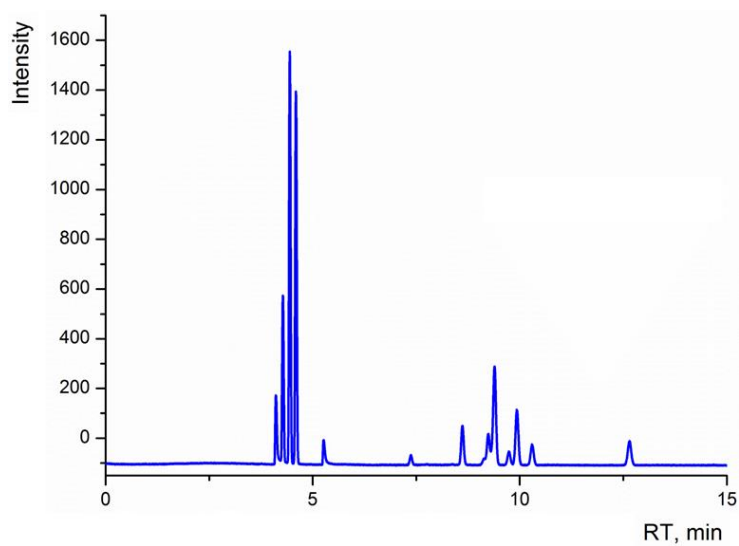


**Figure S27** GC chromatogram of the liquid phase collected at the end of the catalytic test with the system **3**/[Ni(COD)<sub>2</sub>].

## Polyethylene characterisation by $^1\text{H}$ NMR: Determination of $M_n$ and branching degree

### A. Determination of polyethylene $M_n$ by end-group analysis

The determination of the  $M_n$  was performed according to Mecking and co-workers, using the equation:<sup>4</sup>

$$M_n = \frac{\left(\frac{I_{\text{tot}}}{4}\right)}{\left(\frac{I_2 + 2I_3 + 2I_4 + I_5 + I_6}{2}\right)} \times 28 \text{ g/mol} \quad (\text{S1})$$

where  $I_2$ - $I_6$  represents the integrals of the several types of vinyl groups which can be found in a particular sample of PE. In the samples obtained in the present work only the internal end-group protons B and the vinyl terminal end-group protons A are observed (see Figure 4 of the article).

### B. Determination of the polyethylene branching degree

The determination of the branching degree,  $N_{\text{branches}}$  (number of branches/1000 C atoms) is normally given by the equation:<sup>5</sup>

$$N_{\text{branches}} = \frac{I_{\text{CH}_3}}{I_{\text{tot}}} \times \frac{2}{3} \times 1000 \quad (\text{branches/1000C atoms}) \quad (\text{S2})$$

where  $I_{\text{CH}_3}$  represents the integral of the methyl protons  $^1\text{H}$  NMR resonances and  $I_{\text{tot}}$  the overall integral of all proton resonances. However, for *low molecular weight oligomers* (typically  $< 10^4$  g/mol), a correction has to be introduced to discount the two methyl terminal end-groups (in this work most of the terminal unsaturated end-groups are internal – see below Figures S27-S49):<sup>4</sup>

$$N = \left[ \frac{N_{\text{branches}}}{1000} \times \frac{M_n}{14 \text{ g mol}^{-1}} - 2 \right] \times \frac{1000}{M_n} \times 14 \text{ g mol}^{-1} \quad (\text{branches/1000C atoms}) \quad (\text{S3})$$

Therefore, only the  $I_2$  integral, corresponding to the internal end-group protons ( $-\text{CH}=\text{CH}-$ ), and  $I_5$  integral, corresponding to the vinyl terminal end-group geminal protons ( $\text{CH}_2=\text{CH}-$ ), are used in the calculation.

<sup>4</sup> T. Wiedemann, G. Voit, A. Tchernook, P. Roesle, I. Göttker-Schnetmann, S. Mecking *J. Am. Chem. Soc.* 2014, **136**, 2078.

<sup>5</sup> A. C. Gottfried and M. Brookhart, *Macromolecules* 2003, **36**, 3085.

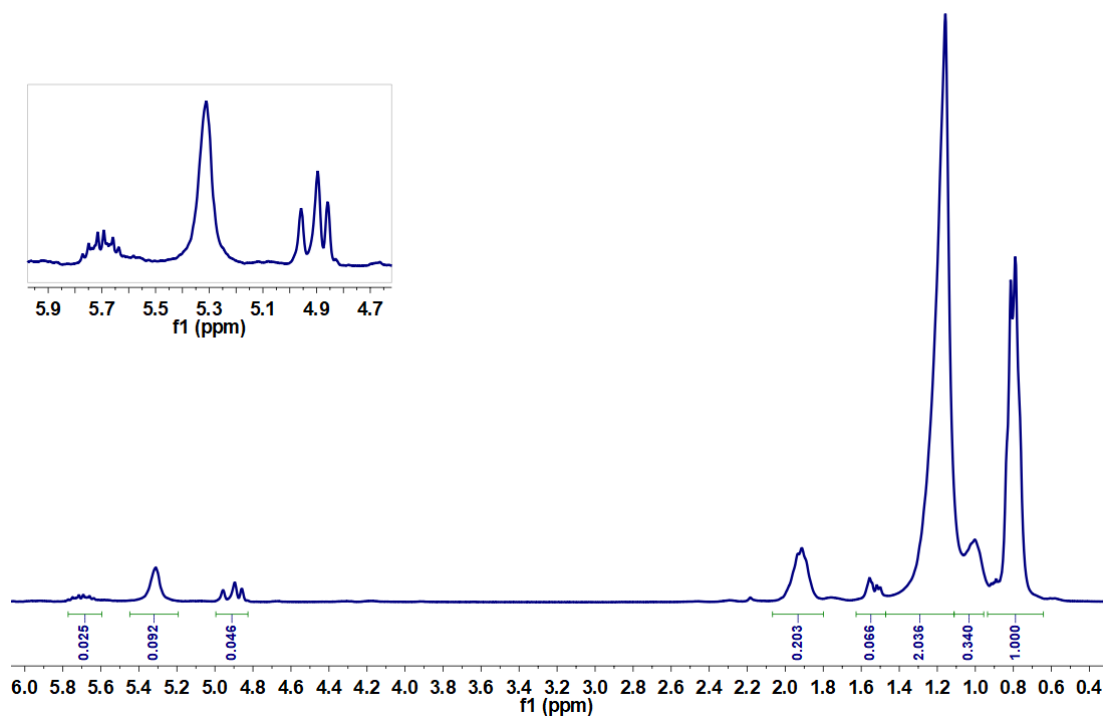


**Figure S28** <sup>1</sup>H NMR spectrum (300 MHz, C<sub>6</sub>D<sub>6</sub>:1,2,4-trichlorobenzene (1:3), 25 °C) of the PE obtained using the catalyst **1**, at 50 °C and 9 bar of ethylene.

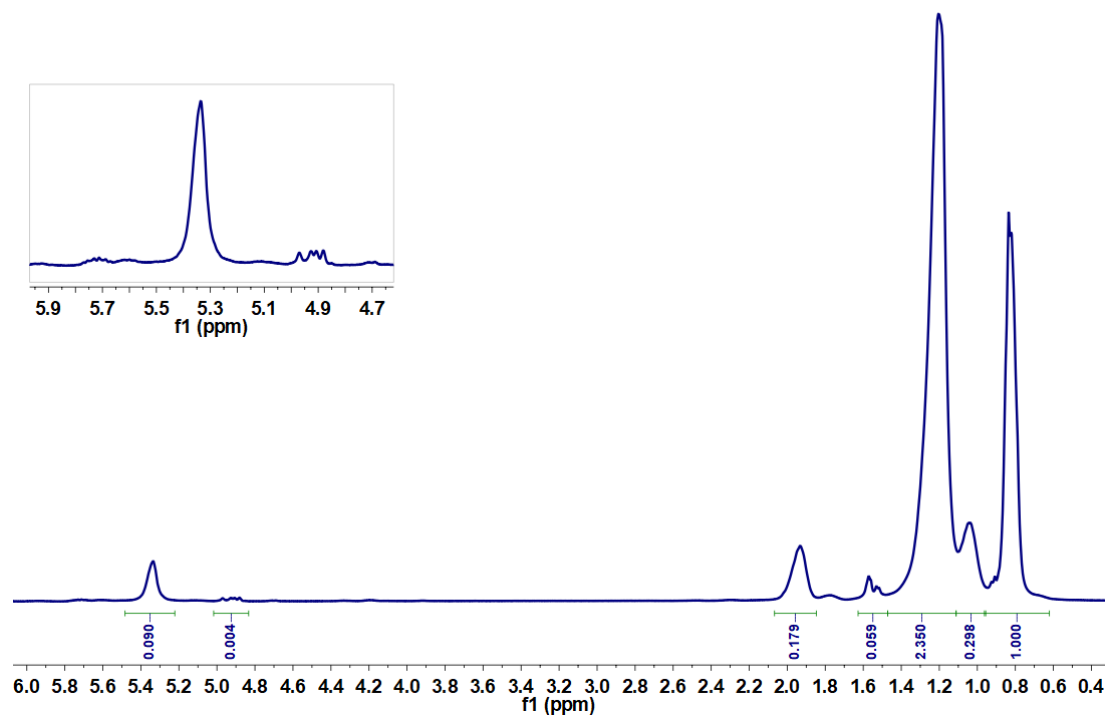


**Figure S29** <sup>1</sup>H NMR spectrum (300 MHz, C<sub>6</sub>D<sub>6</sub>:1,2,4-trichlorobenzene (1:3), 90 °C) of the PE obtained using the catalyst **1\***, at 25 °C and 9 bar of ethylene.

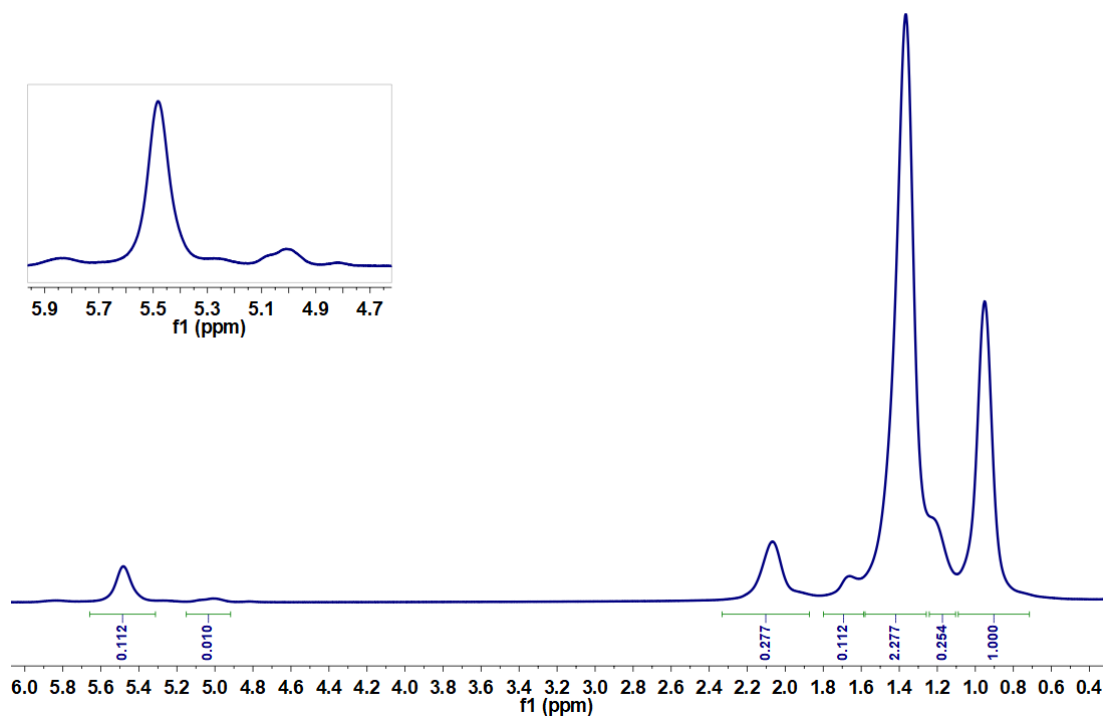


**Figure S30** <sup>1</sup>H NMR spectrum (300 MHz, C<sub>6</sub>D<sub>6</sub>:1,2,4-trichlorobenzene (1:3), 90 °C) of the PE obtained using the catalyst **1**\*, at 50 °C and 9 bar of ethylene.

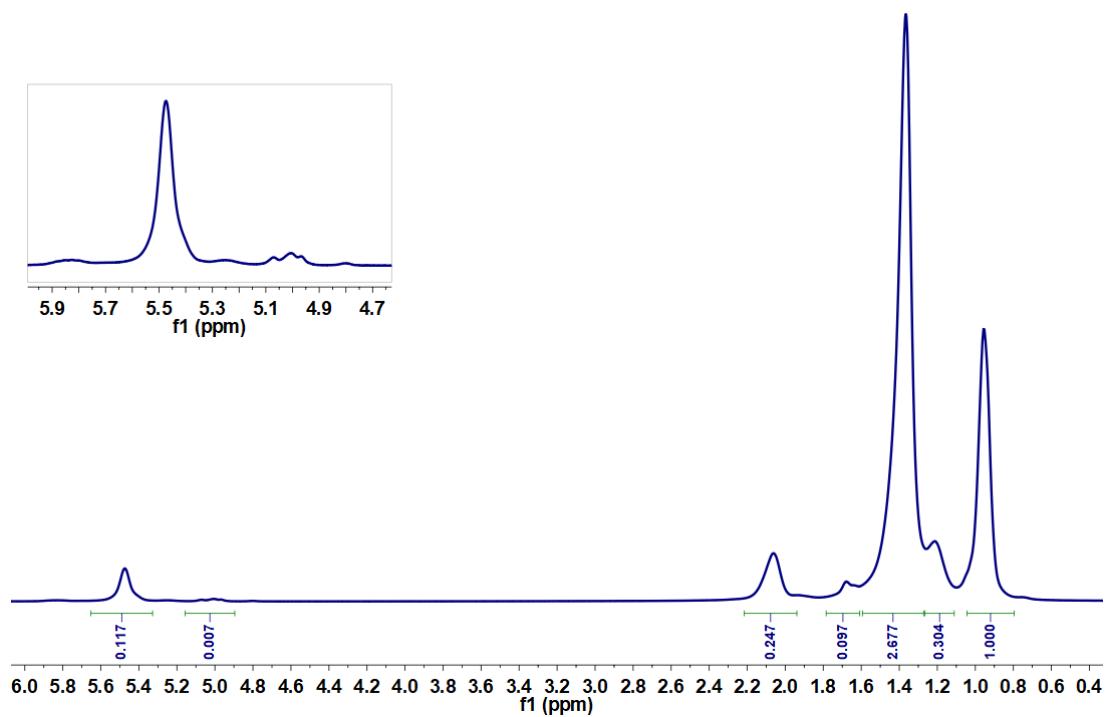


**Figure S31** <sup>1</sup>H NMR spectrum (300 MHz, C<sub>6</sub>D<sub>6</sub>:1,2,4-trichlorobenzene (1:3), 90 °C) of the PE obtained using the catalyst **2**\*, at 50 °C and 9 bar of ethylene.

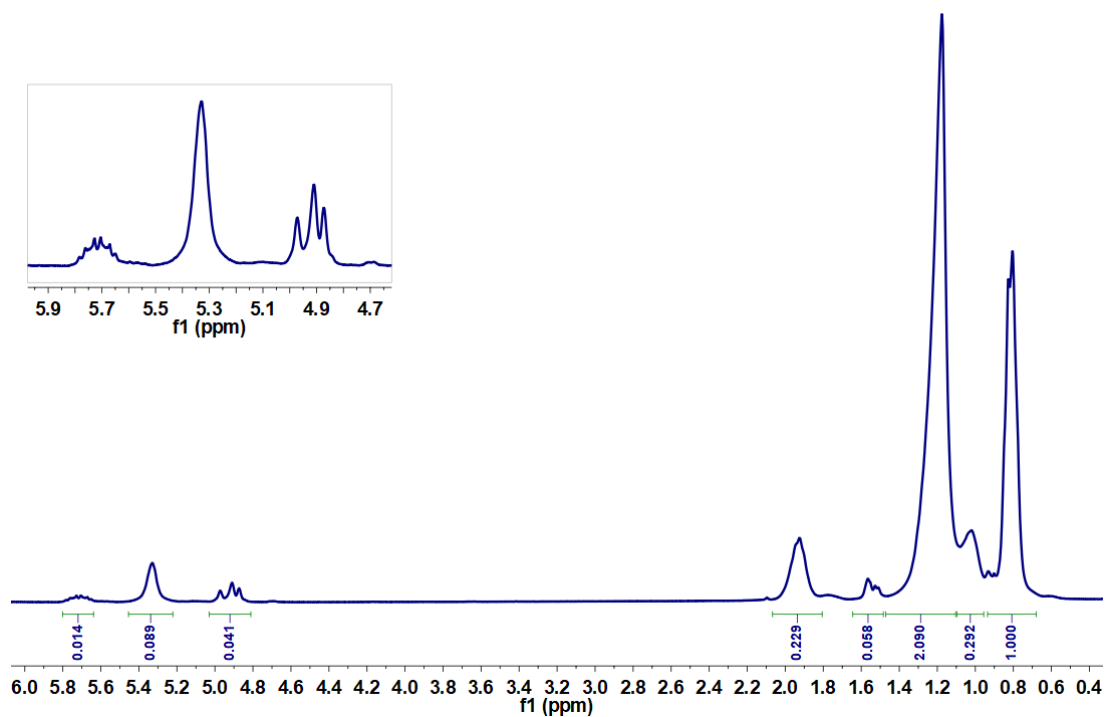


**Figure S32**  $^1\text{H}$  NMR spectrum (300 MHz,  $\text{C}_6\text{D}_6$ :1,2,4-trichlorobenzene (1:3), 25 °C) of the PE obtained using the catalyst **4**, at 50 °C and 9 bar of ethylene.

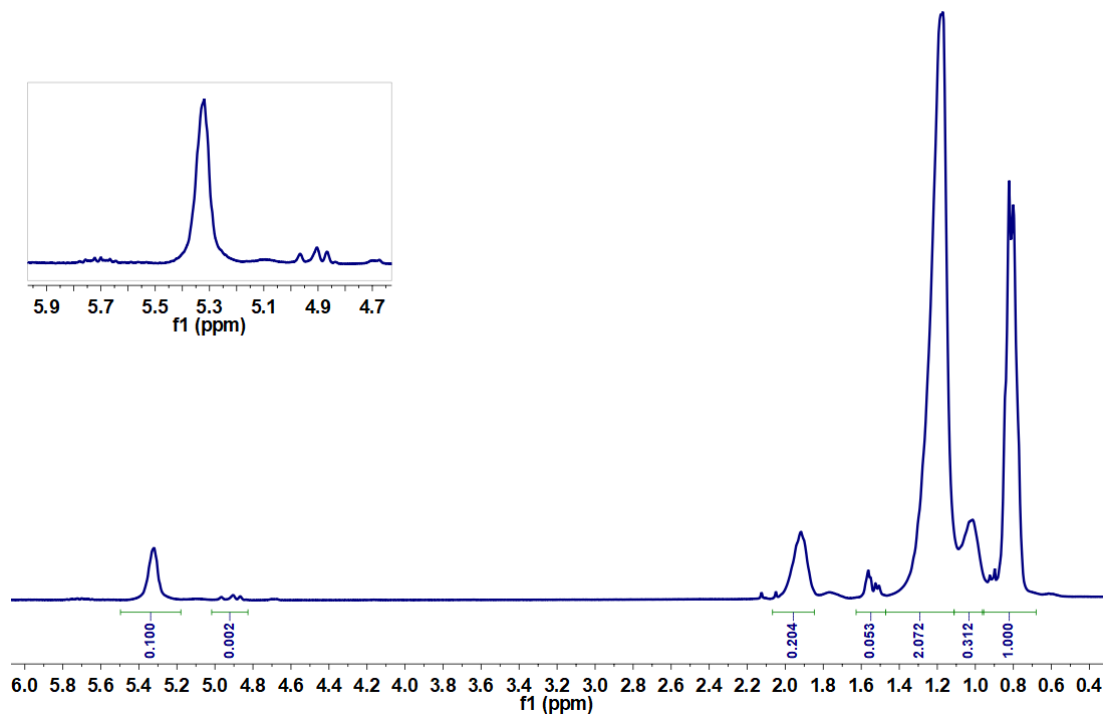


**Figure S33**  $^1\text{H}$  NMR spectrum (300 MHz,  $\text{C}_6\text{D}_6$ :1,2,4-trichlorobenzene (1:3), 25 °C) of the PE obtained using the catalyst **4\***, at 25 °C and 9 bar of ethylene.

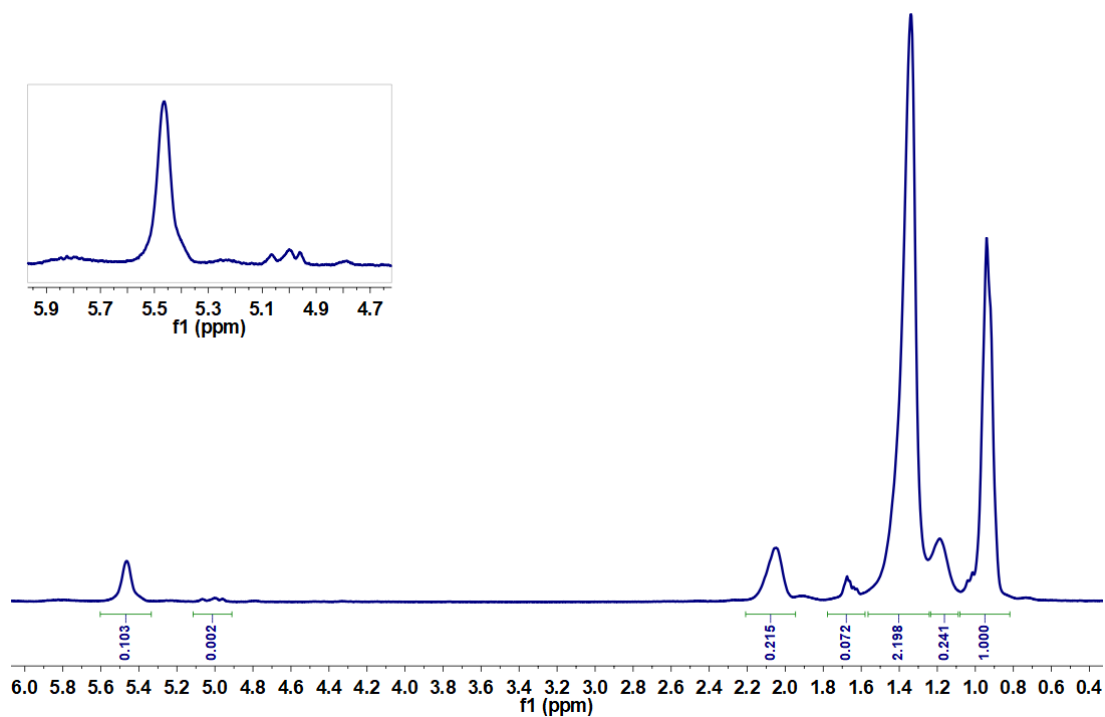


**Figure S34** <sup>1</sup>H NMR spectrum (300 MHz, C<sub>6</sub>D<sub>6</sub>:1,2,4-trichlorobenzene (1:3), 90 °C) of the PE obtained using the catalyst **4\***, at 50 °C and 9 bar of ethylene.

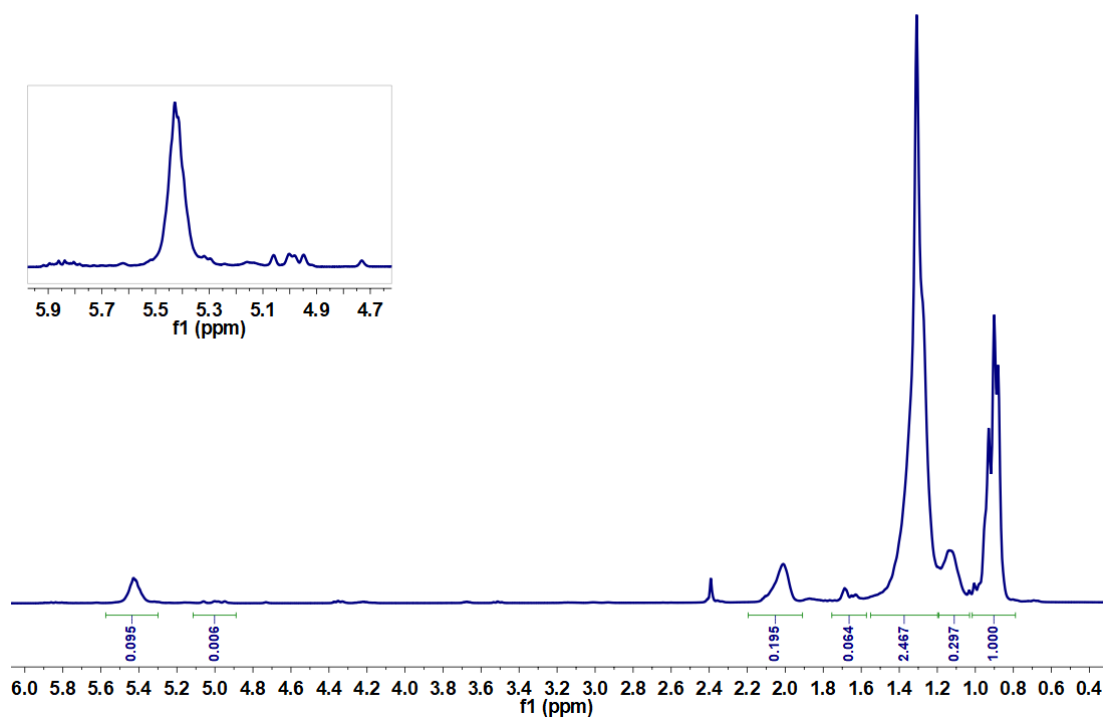


**Figure S35** <sup>1</sup>H NMR spectrum (300 MHz, CDCl<sub>3</sub>, 25 °C) of the PE obtained using the catalyst **5\***, at 25 °C and 3 bar of ethylene.

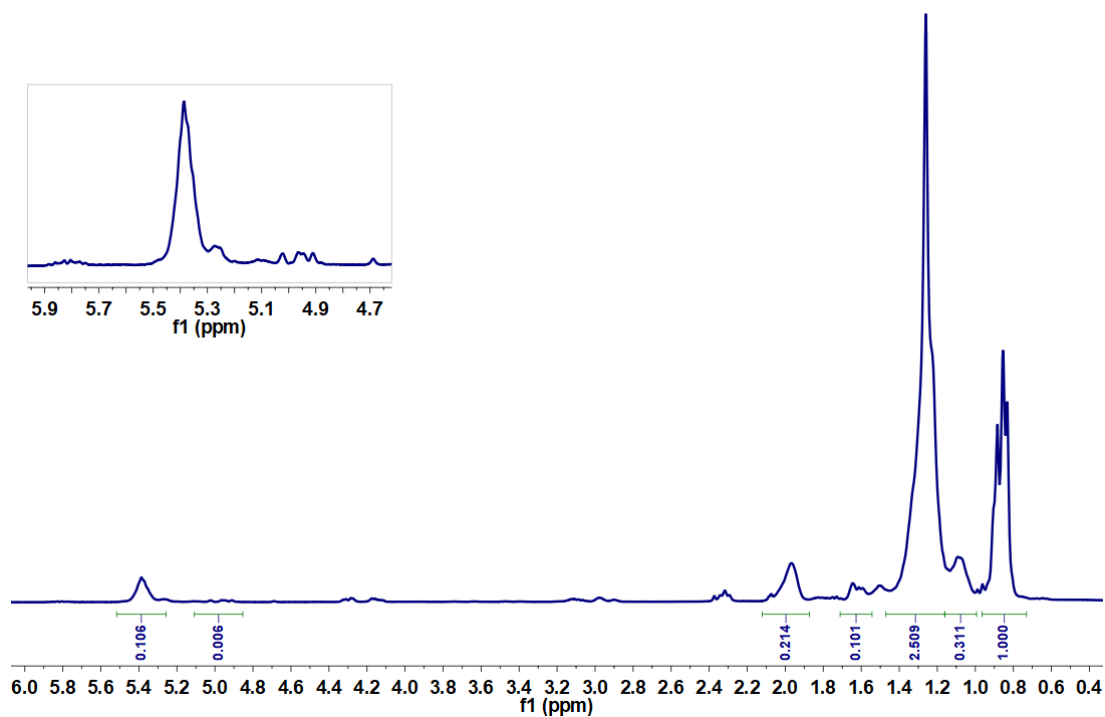


**Figure S36**  $^1\text{H}$  NMR spectrum (300 MHz,  $\text{CDCl}_3$ , 25 °C) of the PE obtained using the catalyst **5\***, at 50 °C and 3 bar of ethylene.

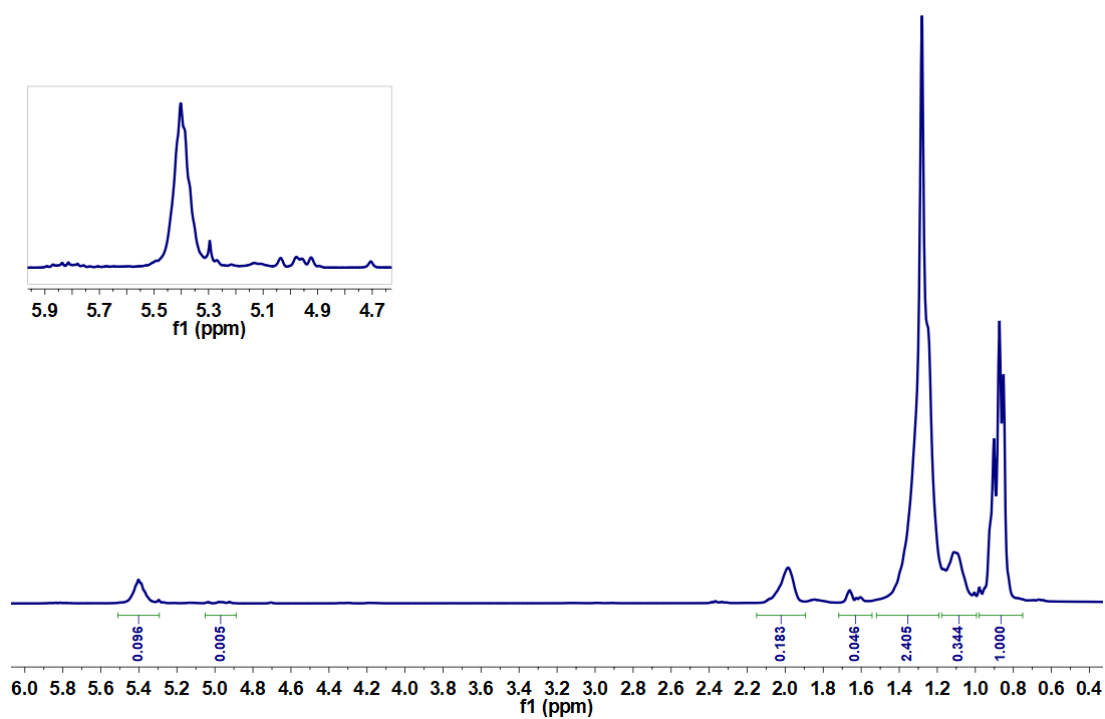


**Figure S37**  $^1\text{H}$  NMR spectrum (300 MHz,  $\text{CDCl}_3$ , 25 °C) of the PE obtained using the catalyst **5\***, at 25 °C and 9 bar of ethylene.

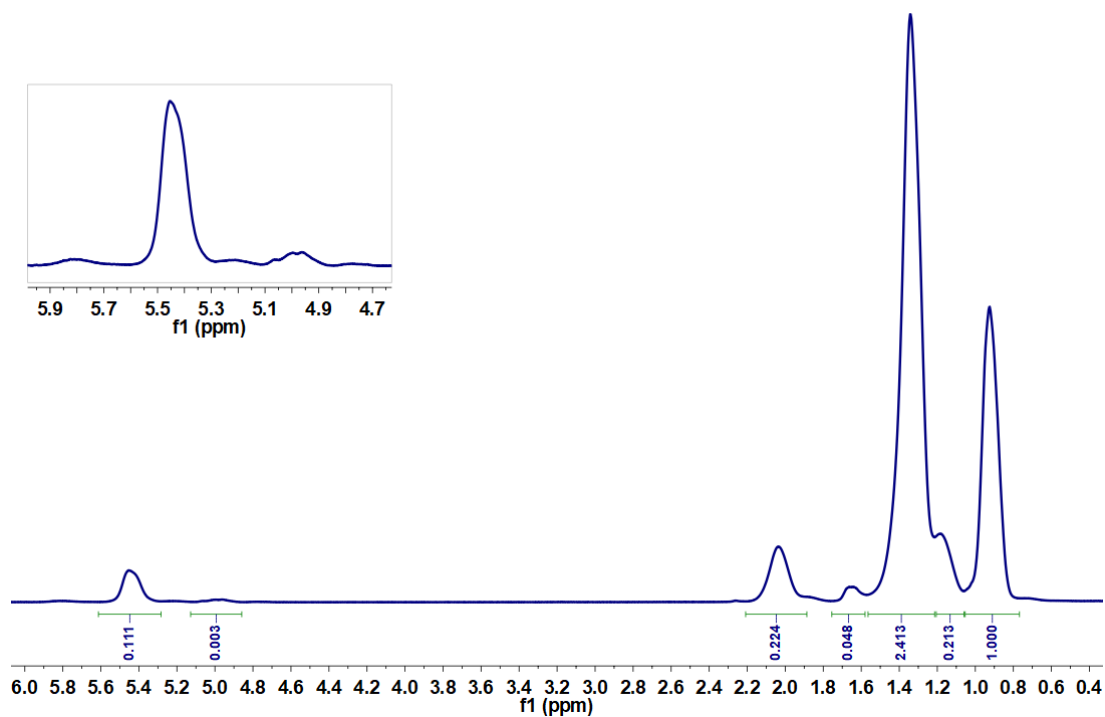


**Figure S38**  $^1\text{H}$  NMR spectrum (300 MHz,  $\text{C}_6\text{D}_6$ :1,2,4-trichlorobenzene (1:3), 90 °C) of the PE obtained using the catalyst **5\***, at 50 °C and 9 bar of ethylene.

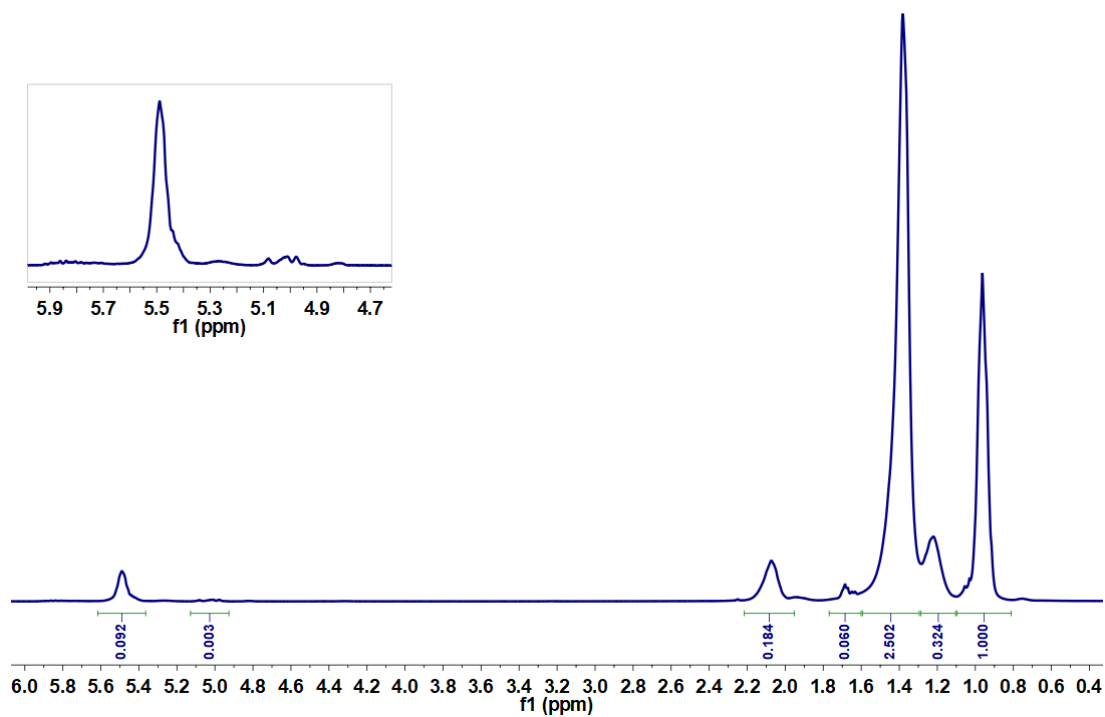


**Figure S39**  $^1\text{H}$  NMR spectrum (300 MHz,  $\text{C}_6\text{D}_6$ :1,2,4-trichlorobenzene (1:3), 90 °C) of the PE obtained using the catalyst **5\***, at 25 °C and 15 bar of ethylene.

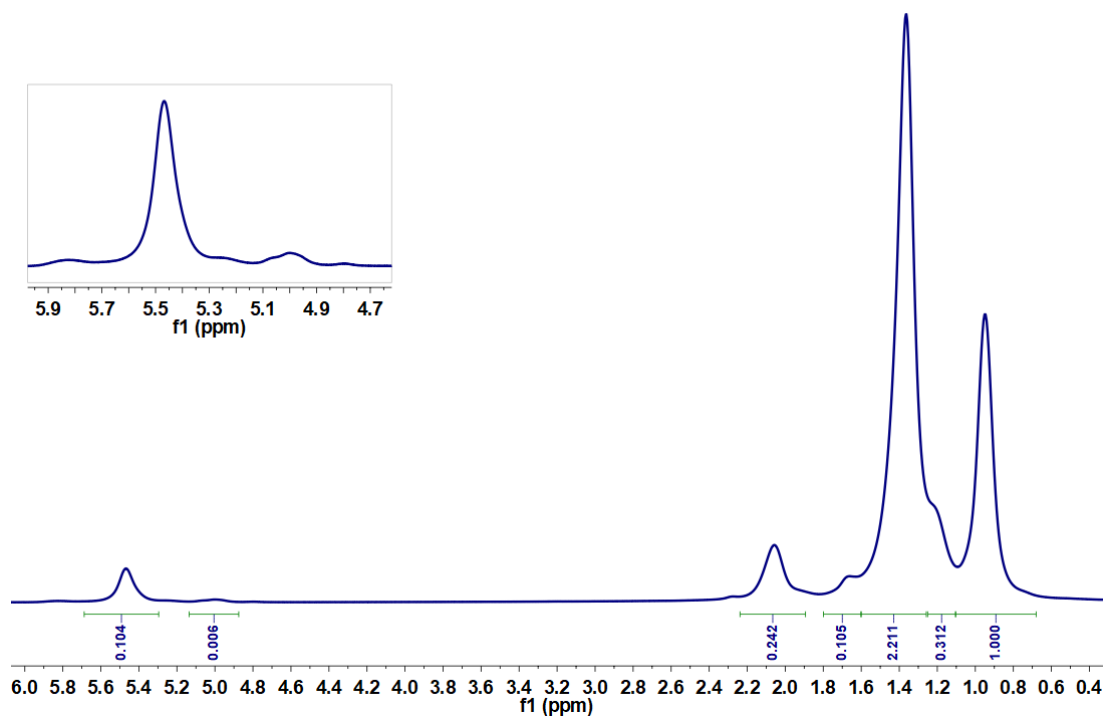


**Figure S40** <sup>1</sup>H NMR spectrum (300 MHz, C<sub>6</sub>D<sub>6</sub>:1,2,4-trichlorobenzene (1:3), 90 °C) of the PE obtained using the catalyst **5\***, at 50 °C and 15 bar of ethylene.

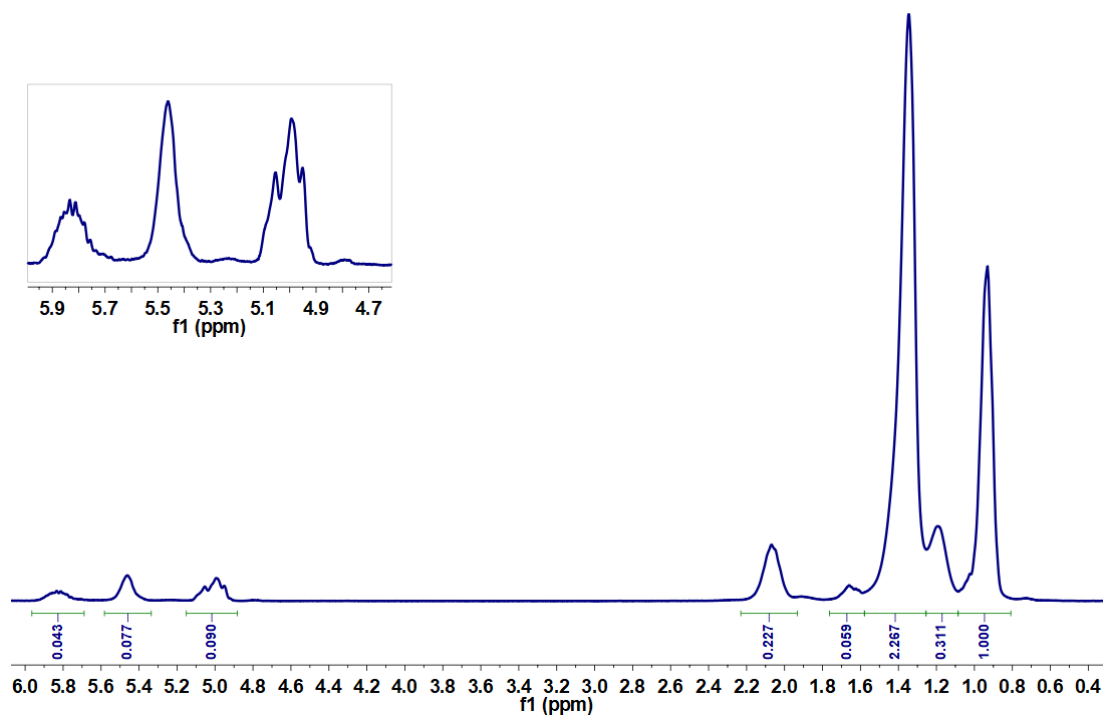


**Figure S41** <sup>1</sup>H NMR spectrum (300 MHz, C<sub>6</sub>D<sub>6</sub>:1,2,4-trichlorobenzene (1:3), 90 °C) of the PE obtained using the catalyst **6**, at 25 °C and 9 bar of ethylene.

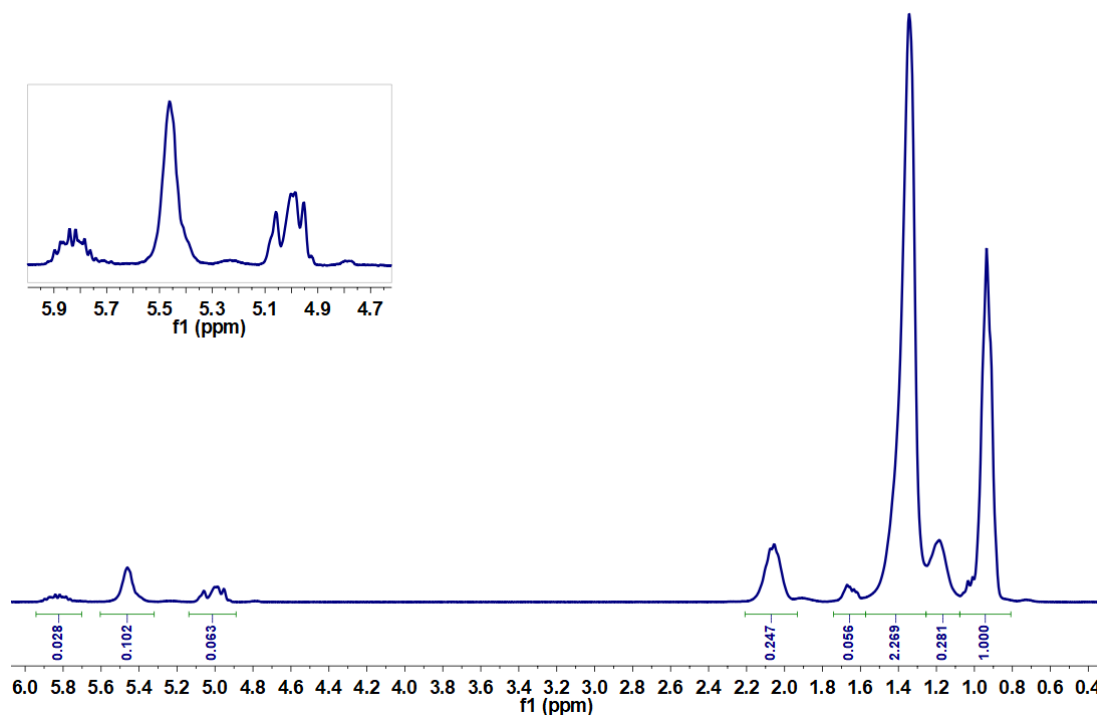


**Figure S42**  $^1\text{H}$  NMR spectrum (300 MHz,  $\text{C}_6\text{D}_6$ :1,2,4-trichlorobenzene (1:3),  $90^\circ\text{C}$ ) of the PE obtained using the catalyst **6**, at  $50^\circ\text{C}$  and 9 bar of ethylene.

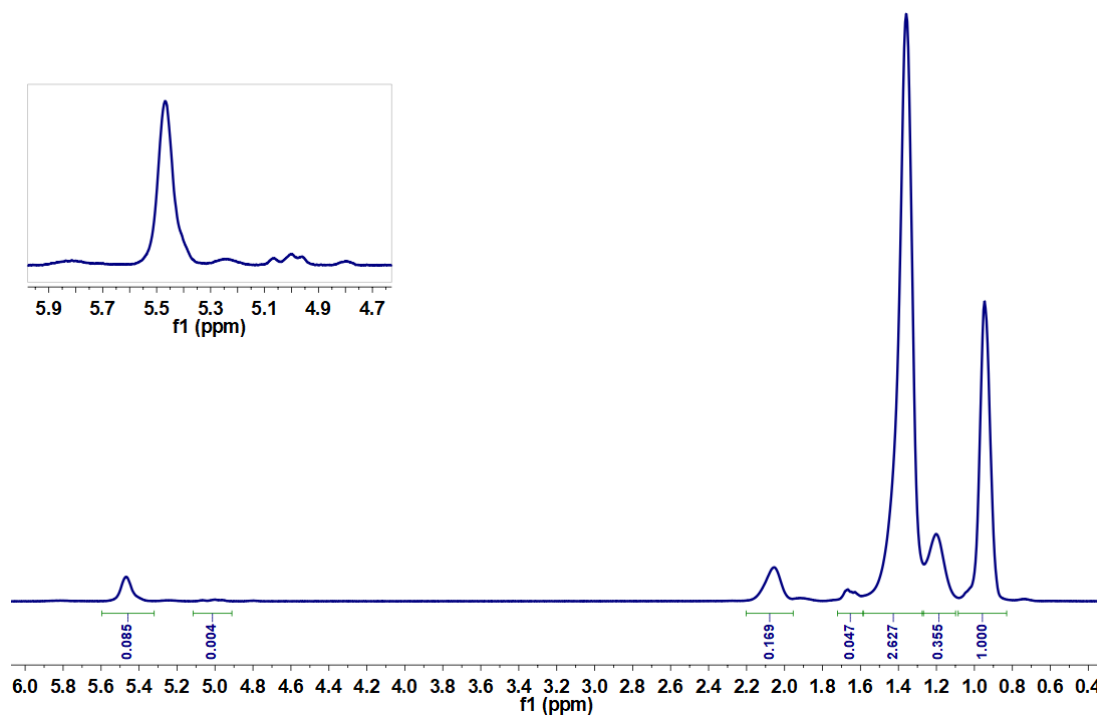


**Figure S43**  $^1\text{H}$  NMR spectrum (300 MHz,  $\text{C}_6\text{D}_6$ :1,2,4-trichlorobenzene (1:3),  $90^\circ\text{C}$ ) of the PE obtained using the catalyst **6\***, at  $25^\circ\text{C}$  and 9 bar of ethylene.

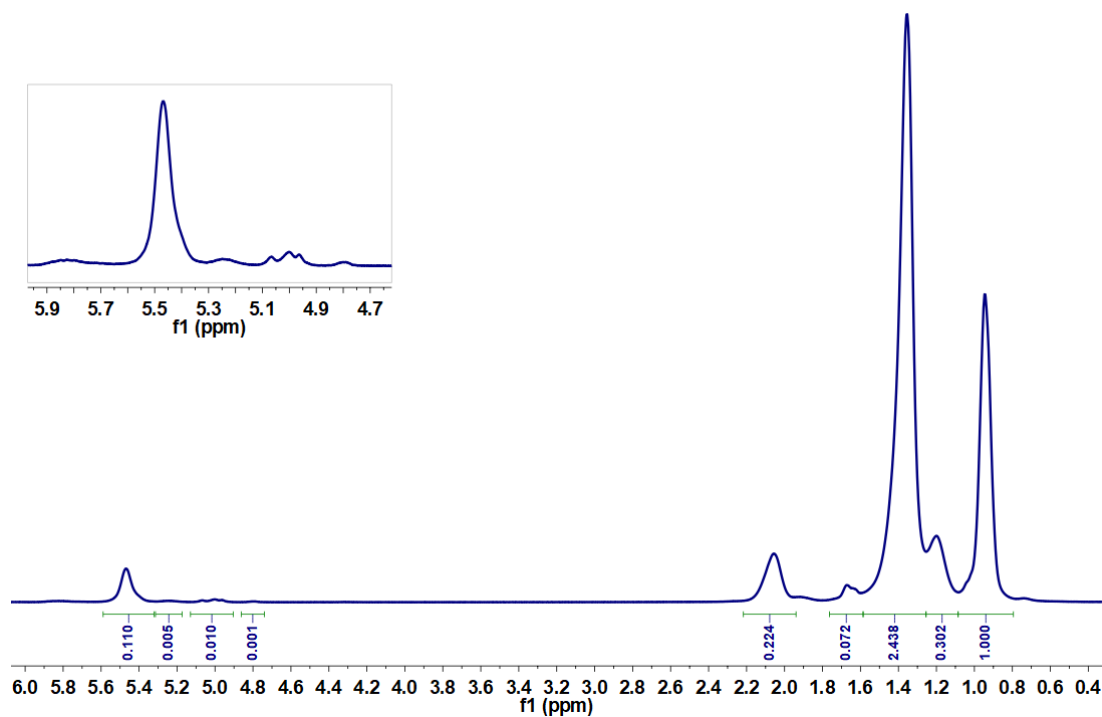


**Figure S44** <sup>1</sup>H NMR spectrum (300 MHz, C<sub>6</sub>D<sub>6</sub>:1,2,4-trichlorobenzene (1:3), 90 °C) of the PE obtained using the catalyst **6\***, at 50 °C and 9 bar of ethylene.

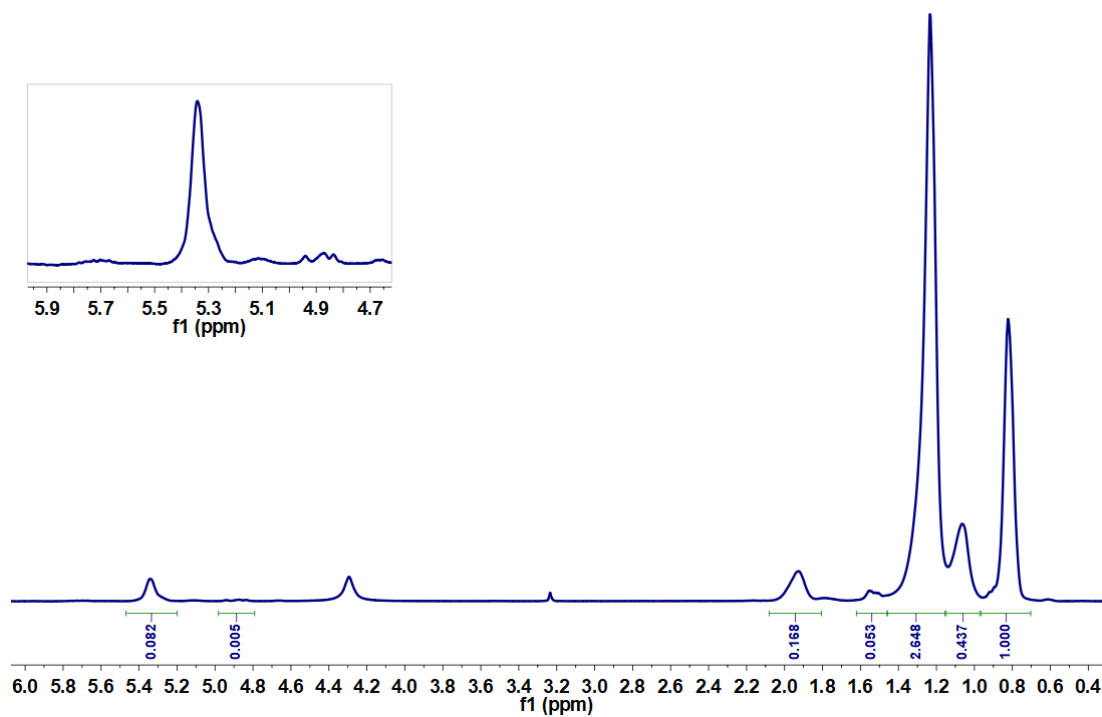


**Figure S45** <sup>1</sup>H NMR spectrum (300 MHz, C<sub>6</sub>D<sub>6</sub>:1,2,4-trichlorobenzene (1:3), 90 °C) of the PE obtained using the catalyst **6\***, at 25 °C and 15 bar of ethylene.

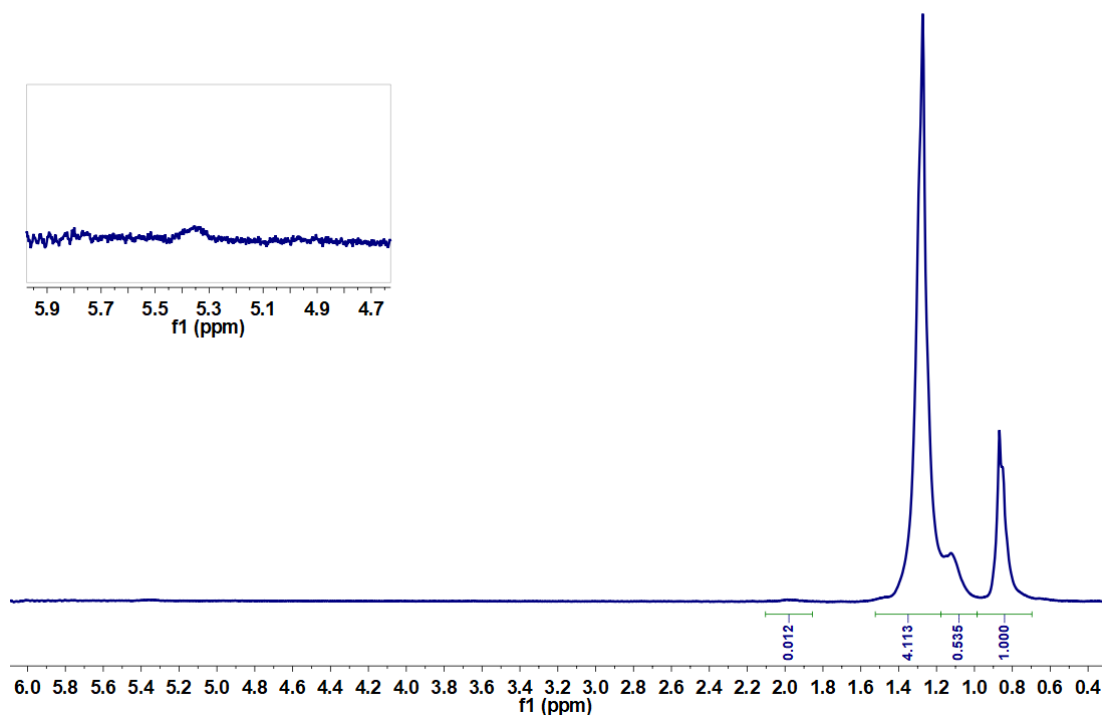


**Figure S46**  $^1\text{H}$  NMR spectrum (300 MHz,  $\text{C}_6\text{D}_6$ :1,2,4-trichlorobenzene (1:3), 90 °C) of the PE obtained using the catalyst 7, at 25 °C and 9 bar of ethylene.

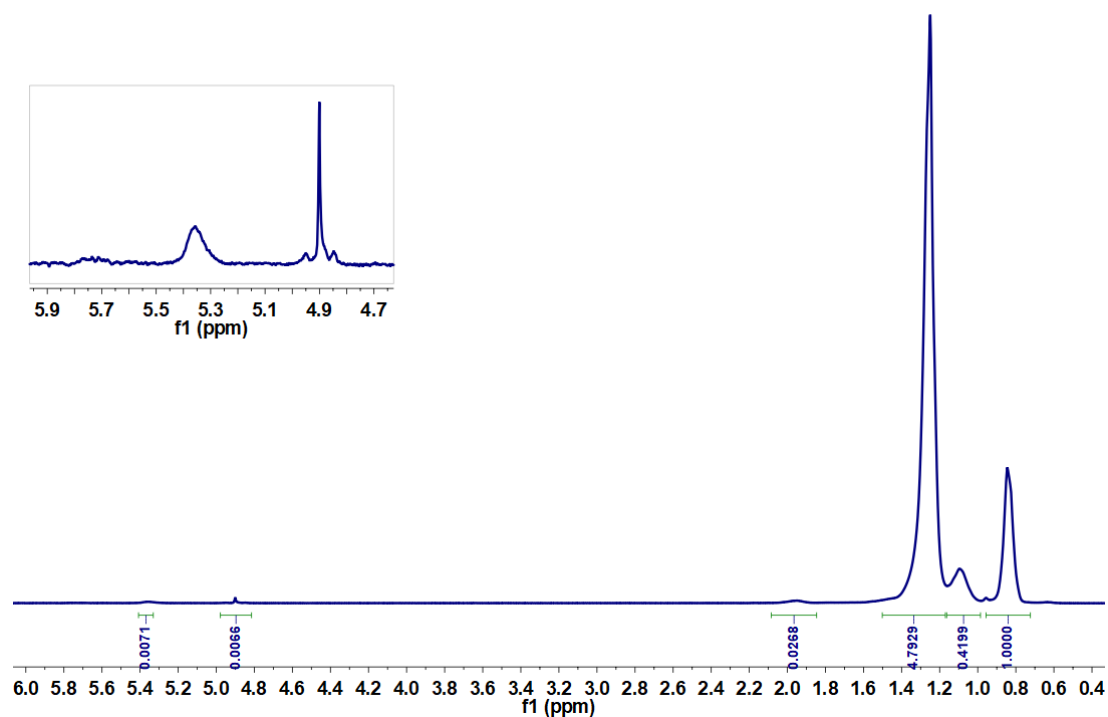


**Figure S47**  $^1\text{H}$  NMR spectrum (300 MHz,  $\text{C}_6\text{D}_6$ :1,2,4-trichlorobenzene (1:3), 90 °C) of the PE obtained using the catalyst 7, at 50 °C and 9 bar of ethylene. Note: The integral of the terminal vinyl group was corrected to 0.0011 since the overlapped singlet is probably a residual impurity.

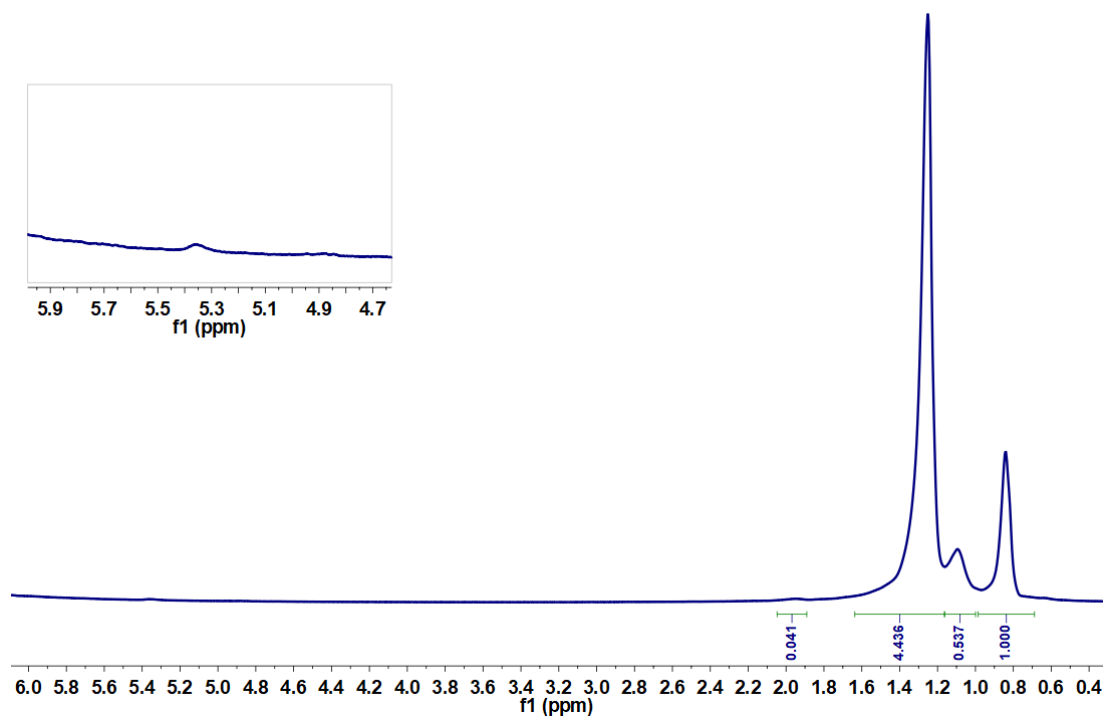


**Figure S48** <sup>1</sup>H NMR spectrum (300 MHz, C<sub>6</sub>D<sub>6</sub>:1,2,4-trichlorobenzene (1:3), 90 °C) of the PE obtained using the catalyst **7\***, at 25 °C and 9 bar of ethylene.

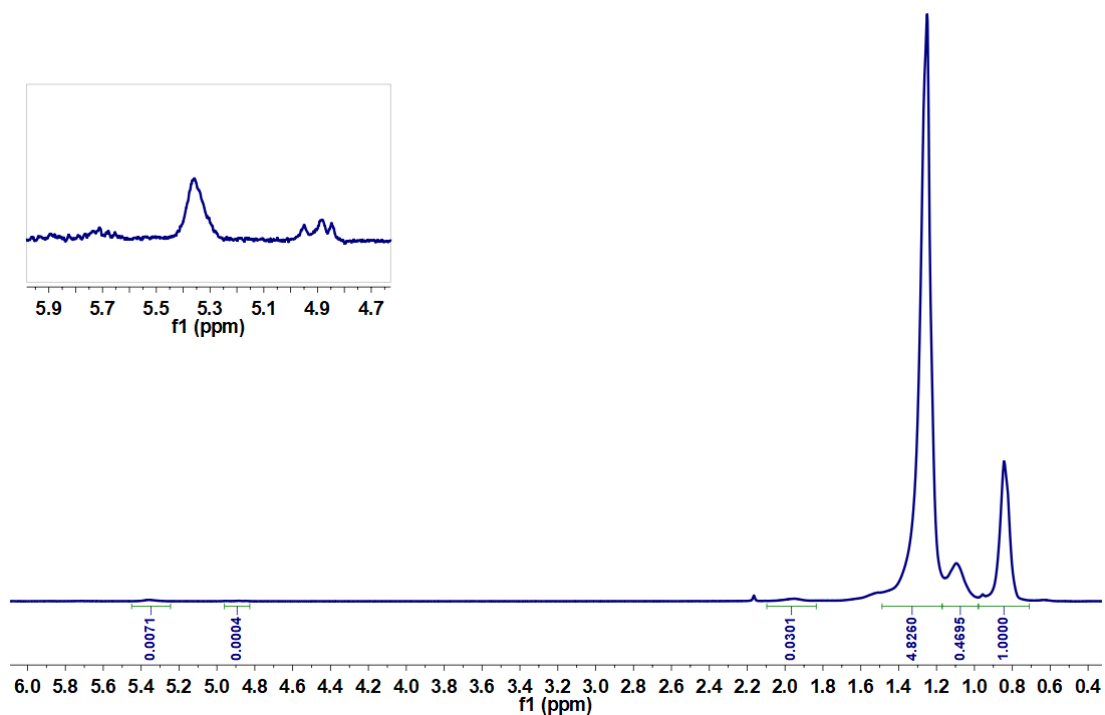


**Figure S49** <sup>1</sup>H NMR spectrum (300 MHz, C<sub>6</sub>D<sub>6</sub>:1,2,4-trichlorobenzene (1:3), 90 °C) of the PE obtained using the catalyst **7\***, at 50 °C and 9 bar of ethylene.

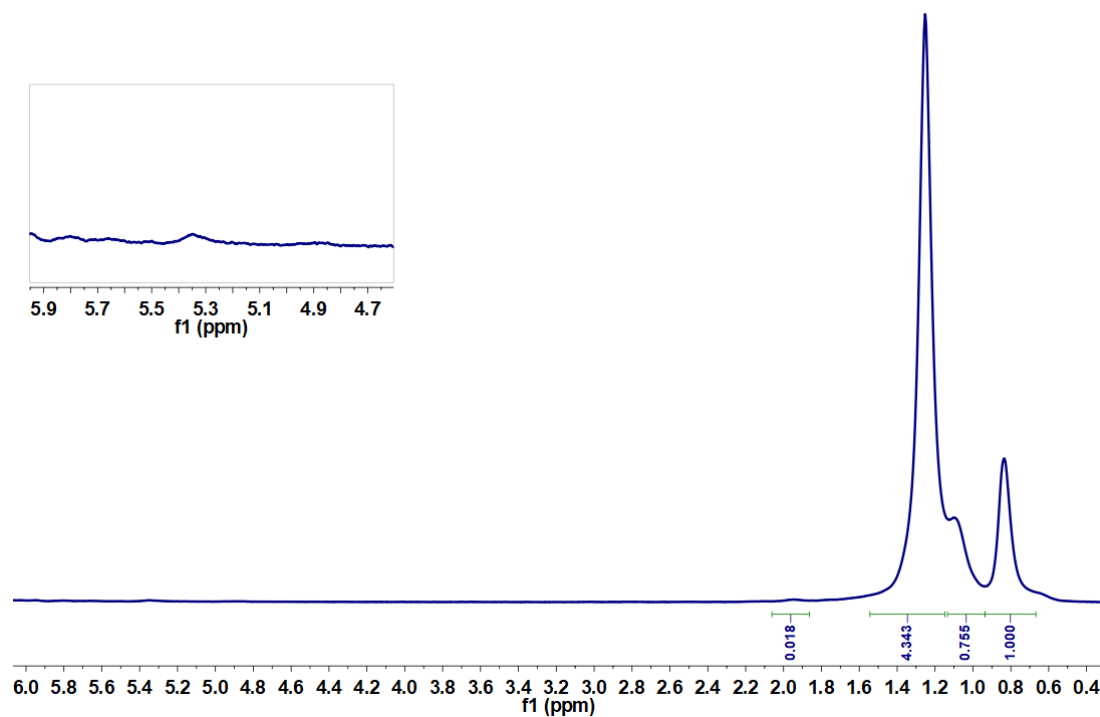


**Figure S50** <sup>1</sup>H NMR spectrum (300 MHz, C<sub>6</sub>D<sub>6</sub>:1,2,4-trichlorobenzene (1:3), 90 °C) of the PE obtained using the catalyst 7\*, at 25 °C and 15 bar of ethylene.

## Polyethylene characterisation by $^{13}\text{C}\{^1\text{H}\}$ NMR: Microstructure analysis

Although several authors had identified the majority of the resonances,<sup>6</sup> one of the PE samples was characterised by  $^{13}\text{C}\{^1\text{H}\}$ ,  $^{13}\text{C}$  APT and DEPT 90 NMR experiments in order to distinguish the several types of carbons present in the samples (methylenic, methinic, methyl and quaternary).

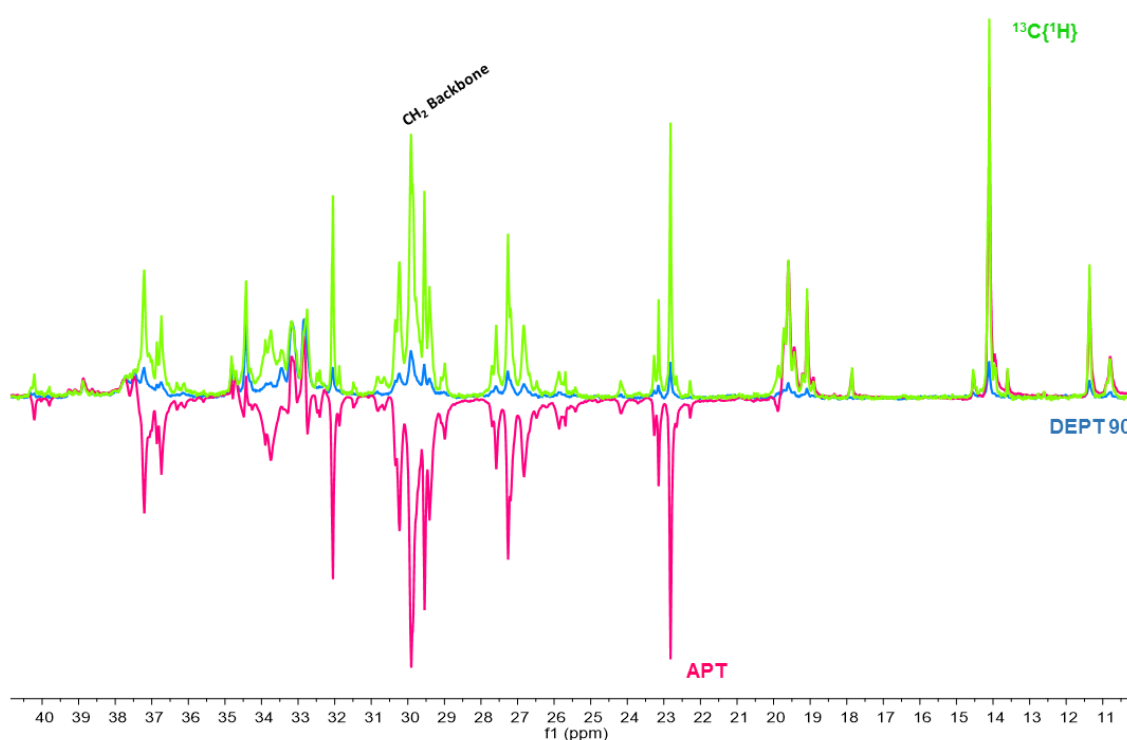


**Figure S51** Superimposition of different 1D  $^{13}\text{C}$  NMR experiments (75 MHz,  $\text{C}_6\text{D}_6$ :1,2,4-trichlorobenzene (1:3), 25 °C) obtained for the same PE sample produced by catalyst system **5\***, at 50 °C and 9 bar of ethylene.

<sup>6</sup> (a) G. B. Galland, R. F. Souza, R. S. Mauler, F. F. Nunes, *Macromolecules*, 1999, **32**, 1620; (b) W. Liu, D. G. Ray III, P. L. Rinaldi, *Macromolecules*, 1999, **32**, 3817; (c) A. Jurkiewicz, N. W. Eilerts, E. T. Hsieh, *Macromolecules*, 1999, **32**, 5471; (d) P. M. Cotts, Z. Guan, E. McCord, S. McLain, *Macromolecules*, 2000, **33**, 6945; (e) G. B. Galland, R. Quijada, R. Rojas, G. Bazan, Z. J. A. Komon, *Macromolecules*, 2002, **35**, 339; (f) J. D. Azoulay, G. C. Bazan, G. B. Galland, *Macromolecules*, 2010, **43**, 2794.

The different identifiable branches were named as  $x\text{B}_n$  where  $n$  is the length of the branch and  $x$  is the carbon number, with the methyl group as 1. For the backbone carbons, Greek letters ( $\alpha$   $\beta$   $\gamma$ ) are used instead of  $x$  for the methylenes, and  $br$  for a branch point. For paired branches of the same size prefixes (1,  $m$ ) are used ( $m$ : number of carbons between two tertiary carbons,  $2 \geq m \geq 6$ ). Backbone carbons between paired branches are designated by Greek letters with primes ( $\alpha'$   $\beta'$   $\gamma'$ ).

**Table S13** Assignments of the resonances in the  $^{13}\text{C}\{^1\text{H}\}$  NMR spectrum obtained for the PE produced with the system **6\***, at 25 °C and 9 bar of ethylene (Figure S51).

Peak	$\delta$ (ppm)	Assignments
1	11.13	1B <sub>2</sub>
2	11.39	B <sub>sec-Bu</sub>
3	14.10	1B <sub>4</sub> , 1B <sub><i>n</i></sub> , 1,4-1B <sub><i>n</i></sub>
4	14.60	1B <sub>3</sub>
5	19.36	A <sub>sec-Bu</sub>
6	19.90	1B <sub>1</sub> , 1,5-1B <sub>1</sub> , 1,6-1B <sub>1</sub>
7	19.99	1,4-1B <sub>1</sub>
8	20.27	2B <sub>3</sub>
9	22.89	2B <sub><i>n</i></sub> , 1,4-2B <sub><i>n</i></sub>
10	23.26	2B <sub>sec-Bu</sub>
11	23.38	2B <sub>4</sub>
12	24.65	1,5- $\beta'$ B <sub>1</sub>
13	26.58	2B <sub>2</sub>
14	27.23	$\beta$ B <sub>2</sub> , $\beta$ B <sub>3</sub> , $\beta$ B <sub>4</sub> , $\beta$ B <sub><i>n</i></sub> , (n-1)B <sub><i>n</i></sub> , 1,4- $\beta'$ B <sub><i>n</i></sub>
15	27.43	$\beta$ B <sub>1</sub> , 1,4- $\beta'$ B <sub>1</sub> , 1,5- $\beta'$ B <sub>1</sub>
16	27.80	1,6- $\beta'$ B <sub>1</sub>
17	29.49	3B <sub>4</sub>
18	29.60	4B <sub><i>n</i></sub> , 1,4-4B <sub><i>n</i></sub>
19	30.00	$\delta\delta\text{CH}_2$ (main chain)
20	30.37	$\gamma$ B <sub>1</sub> , 1,4- $\gamma'$ B <sub>1</sub> , 1,5- $\gamma'$ B <sub>1</sub> , 1,6- $\gamma'$ B <sub>1</sub>
21	30.48	$\gamma$ B <sub>2</sub> , $\gamma$ B <sub>3</sub> , $\gamma$ B <sub>4</sub> , 1,4- $\gamma'$ B <sub><i>n</i></sub> , $\gamma$ B <sub><i>n</i></sub>
22	31.58	1,4- $\alpha'$ B <sub><i>n</i></sub>
23	32.18	3B <sub><i>n</i></sub> , 1,4-3B <sub><i>n</i></sub>
24	33.18	brB <sub>1</sub> , 1,5-brB <sub>1</sub> , 1,6-brB <sub>1</sub>
25	33.41	1,4-brB <sub>1</sub>
26	33.90	4B <sub>4</sub>
27	34.41	$\alpha$ B <sub>3</sub> , $\alpha$ B <sub>4</sub> , $\alpha$ B <sub><i>n</i></sub> , nB <sub><i>n</i></sub> , 1,4- $\alpha'$ B <sub><i>n</i></sub> , 1,4-nB <sub><i>n</i></sub>
28	34.77	1,4- $\alpha'$ B <sub>1</sub>
29	36.81	3B <sub>3</sub>
30	37.49	$\alpha$ B <sub>1</sub> , 1,5- $\alpha'$ B <sub>1</sub> , 1,6- $\alpha'$ B <sub>1</sub>
31	38.04	brB <sub>4</sub> , brB <sub><i>n</i></sub>
32	38.31	1,4-brB <sub><i>n</i></sub>
33	39.53	brB <sub>2</sub>
34	39.97	1,3- $\alpha'$ B <sub>1</sub>

Due to the high content of methyl branches, it is also possible to identify (1,3-) to (1,6-) paired branches, as well (1,4-) paired long branches.

### Determination of the branches distribution (%)

The integration areas (I) used to quantify the different types of branches ( $I_{Branch\ type}$ ) are indicated in Figure S51 (see below), and correspond to the area of the methyl group of each type of branch (methyl, ethyl, propyl, butyl, *sec*-butyl and longer). Their calculation is performed according to the following equations:<sup>7,8</sup>

$$I_{Methyl} = I_6 - I_4 \text{ (where } I_4 = I_7)$$

$$I_{Ethyl} = I_1$$

$$I_{Propyl} = I_4$$

$$I_{Butyl} = I_3 - [(I_8 + I_{17})/2]$$

$$I_{Sec-Butyl} = (I_2 + I_5)/2$$

$$I_{Longer} = (I_8 + I_{17})/2$$

The total intensity of methyl groups,  $I_{Total\ CH_3}$ , is given by:

$$I_{Total\ CH_3} = (I_2 + I_5)/2 + I_1 + I_3 + I_6$$

where  $I_6$  is the total integral  $I_6 + I_7$ , with  $I_7 = I_4$ .

The branches distribution (%) is determined by the ratio between the intensities of each one of the branch types and the overall methyl groups intensity multiplied by 100:

$$Branchtype\ (\%) = \frac{I_{Branchtype}}{I_{Total\ CH_3}} \times 100 \quad (S4)$$

<sup>7</sup> J. D. Azoulay, G. C. Bazan, G. B. Galland, *Macromolecules*, 2010, **43**, 2794.

<sup>8</sup> F. Wang, R. Tanaka, Z. Cai, Y. Nakayama, T. Shiono, *Polymers*, 2016, **8**, 160.

$^{13}\text{C}\{^1\text{H}\}$  NMR spectra of the selected polyethylene products

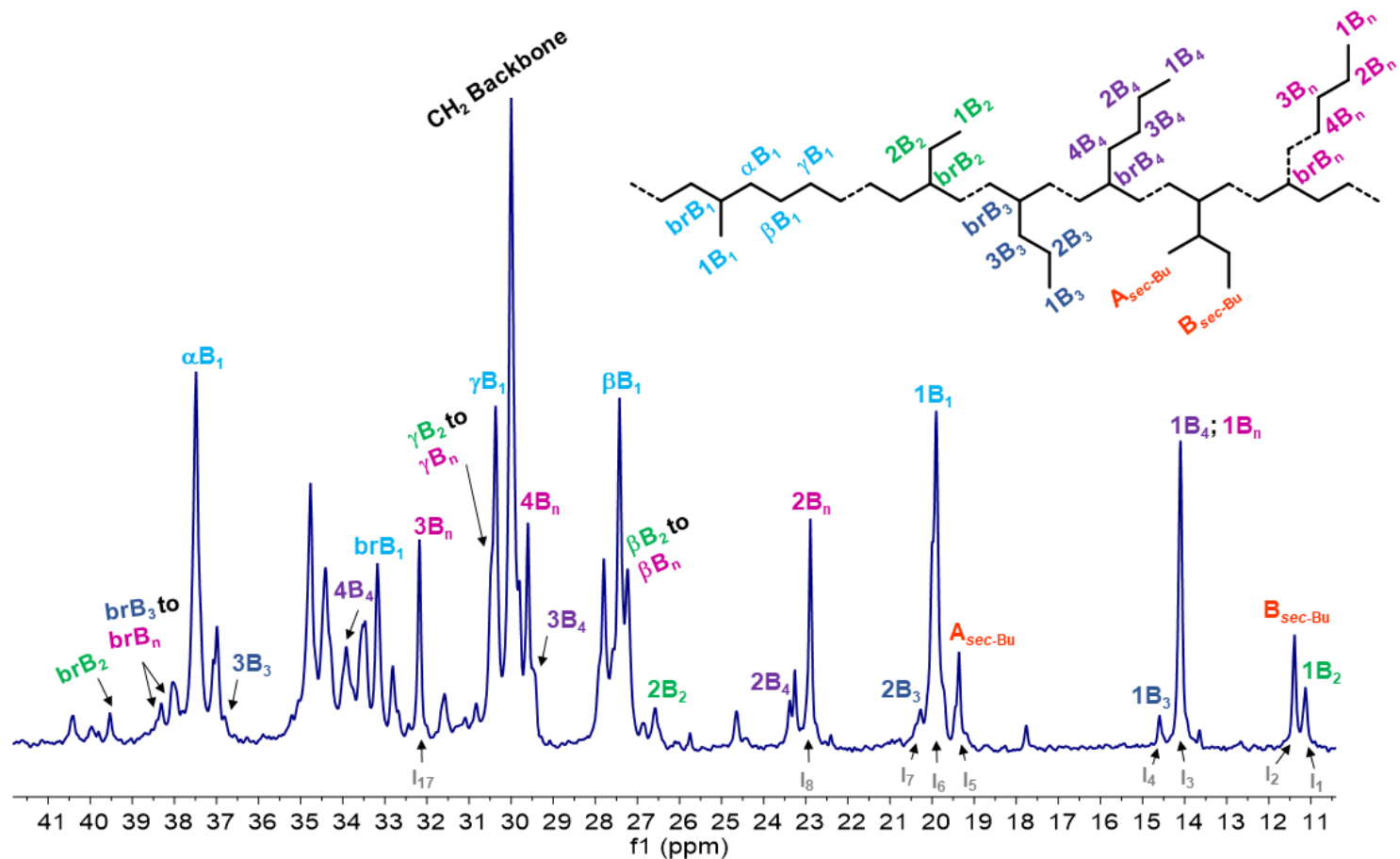


**Figure S52**  $^{13}\text{C}\{^1\text{H}\}$  NMR spectrum (75 MHz,  $\text{C}_6\text{D}_6$ :1,2,4-trichlorobenzene (1:3), 90 °C) of the PE obtained using the catalyst system **6\***, at 25 °C and 9 bar of ethylene, and the corresponding  $^{13}\text{C}$  resonances assignments (see also Table S13).

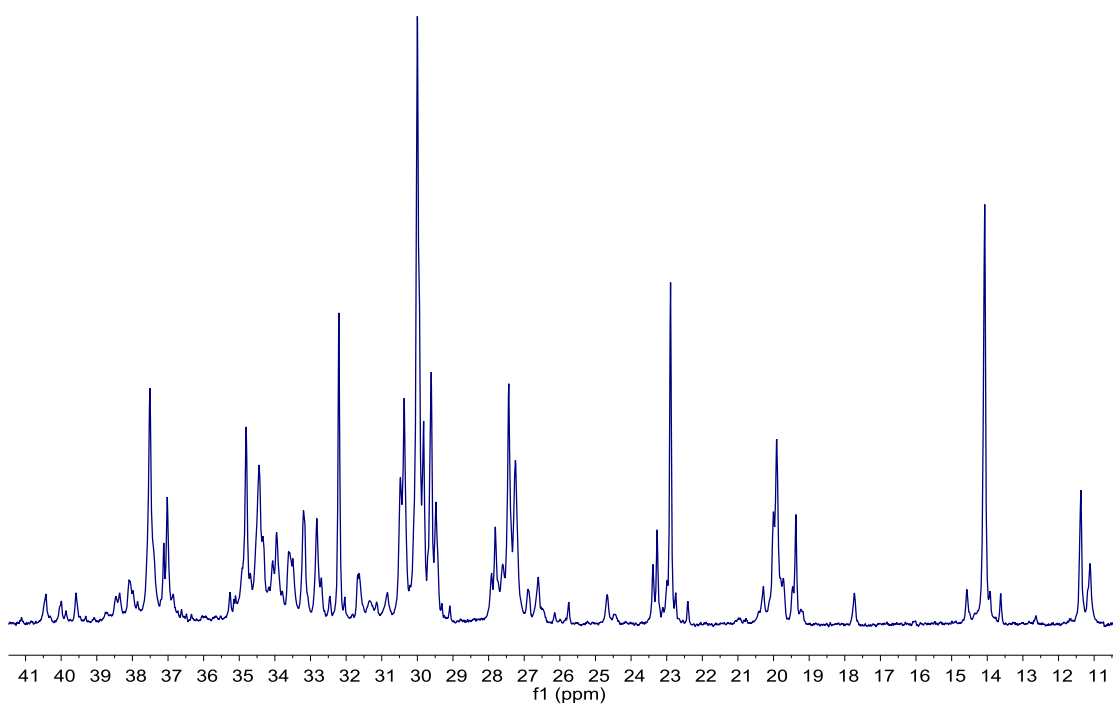


**Figure S53**  $^{13}\text{C}\{^1\text{H}\}$  NMR spectrum (75 MHz,  $\text{C}_6\text{D}_6$ :1,2,4-trichlorobenzene (1:3), 90 °C) of the PE obtained using the catalyst system **2\***, at 50 °C and 9 bar of ethylene.

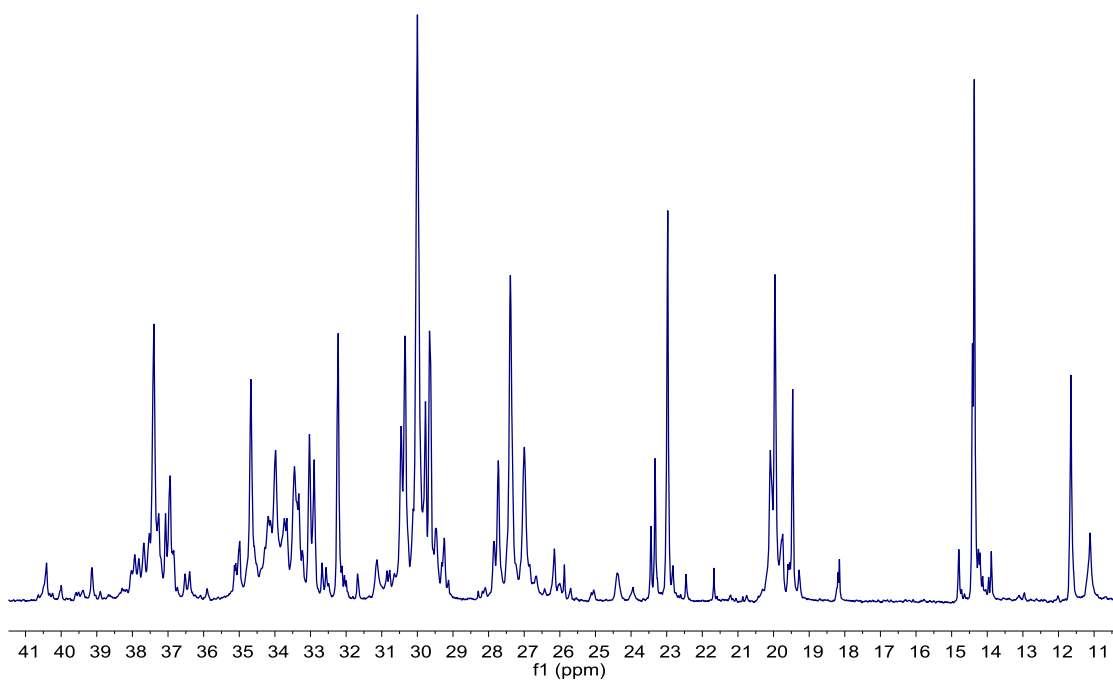


**Figure S54**  $^{13}\text{C}\{^1\text{H}\}$  NMR spectrum (75 MHz,  $\text{CDCl}_3$ , 25 °C) of the PE obtained using the catalytic system **5\***, at 25 °C and 3 bar of ethylene.

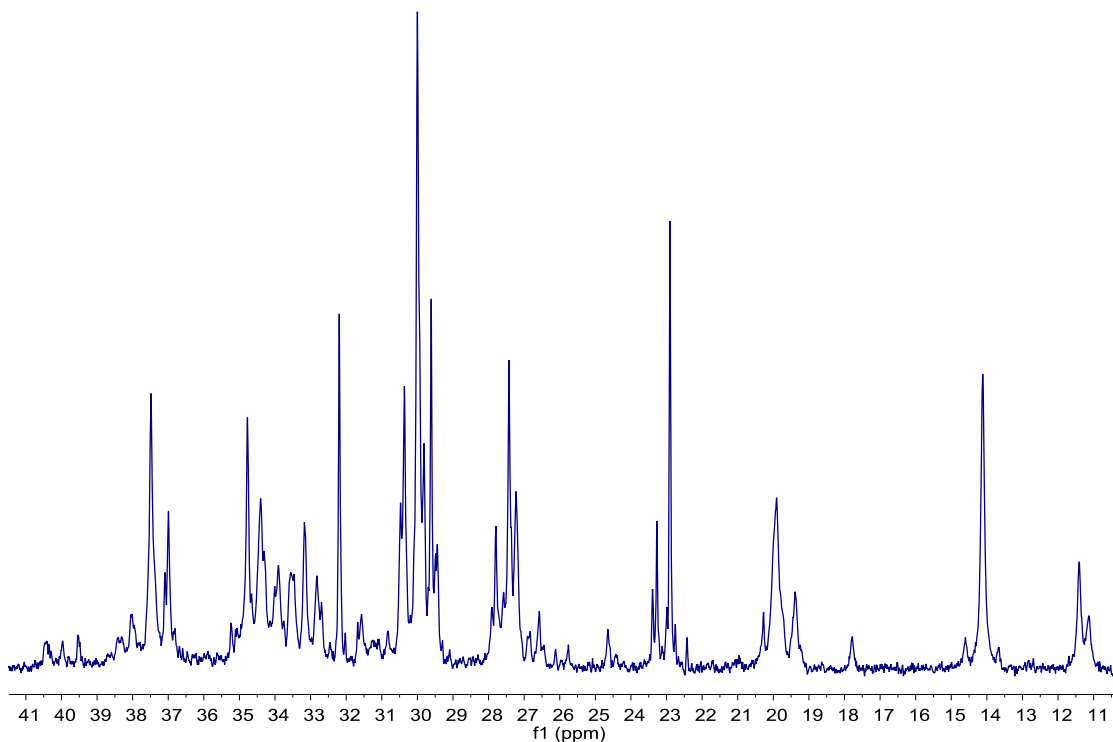


**Figure S55**  $^{13}\text{C}\{^1\text{H}\}$  NMR spectrum (75 MHz,  $\text{CDCl}_3$ , 25 °C) of the PE obtained using the catalytic system **5\***, at 50 °C and 3 bar of ethylene.

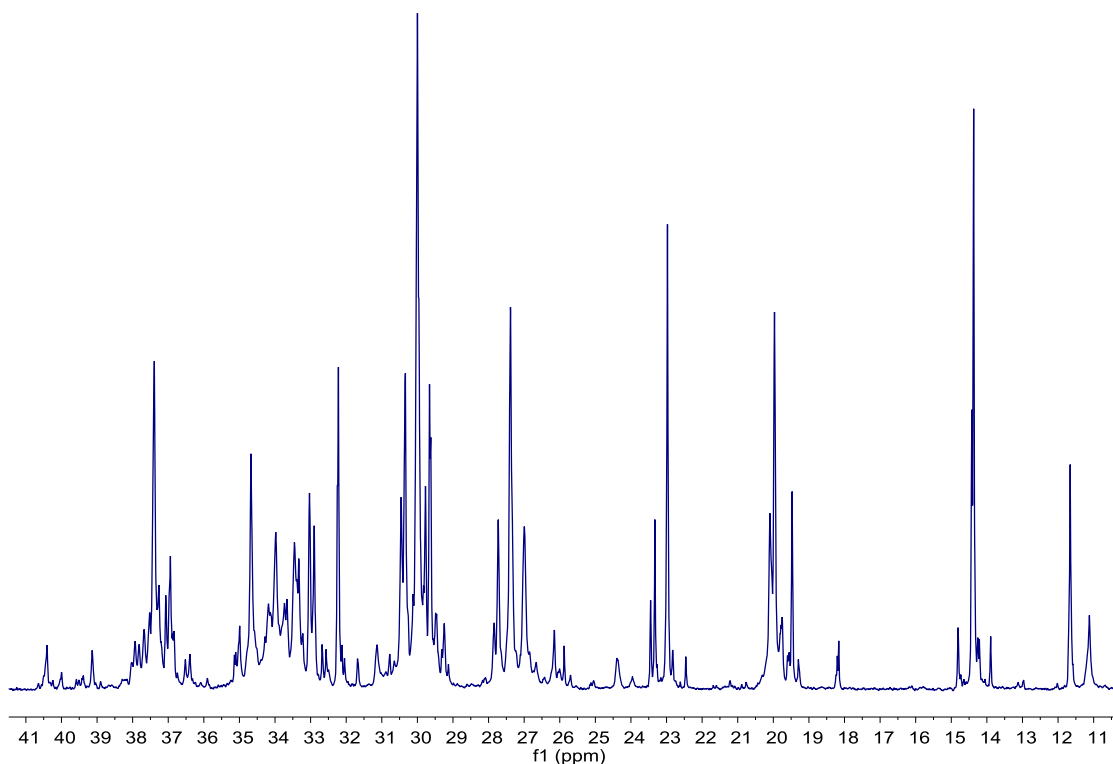


**Figure S56**  $^{13}\text{C}\{^1\text{H}\}$  NMR spectrum (75 MHz,  $\text{CDCl}_3$ , 25 °C) of the PE obtained using the catalytic system **5\***, at 25 °C and 9 bar of ethylene.

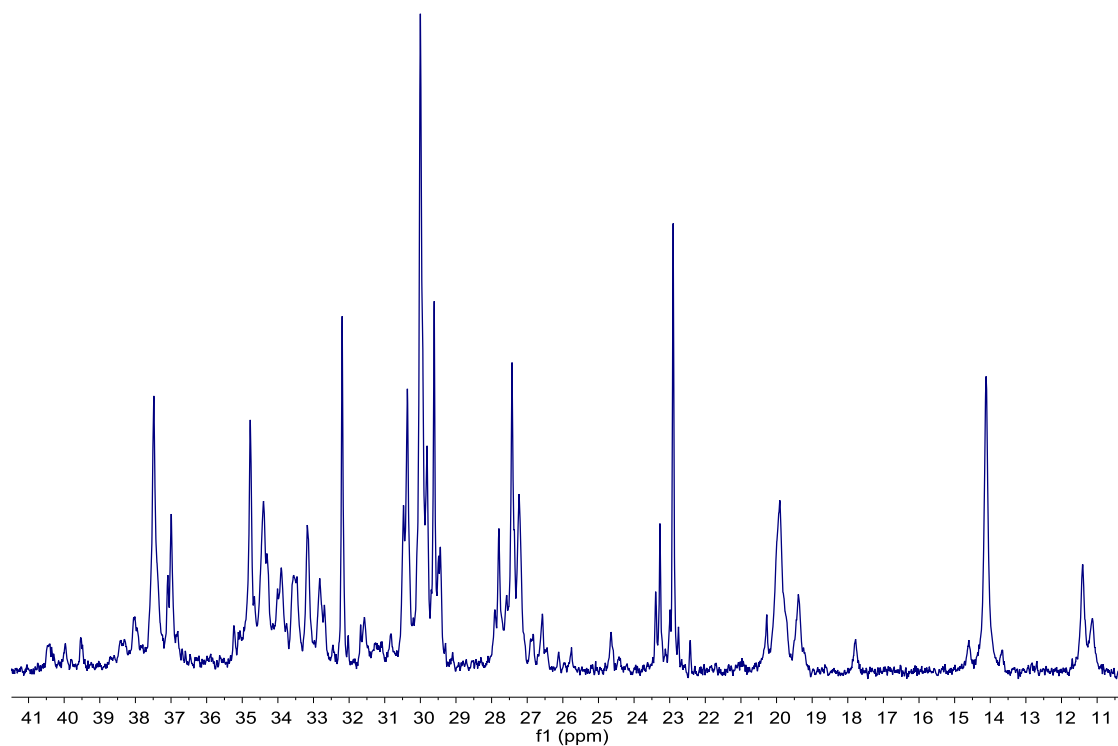


**Figure S57**  $^{13}\text{C}\{^1\text{H}\}$  NMR spectrum (75 MHz,  $\text{C}_6\text{D}_6$ :1,2,4-trichlorobenzene (1:3), 90 °C) of the PE obtained using the catalytic system **5\***, at 50 °C and 9 bar of ethylene.

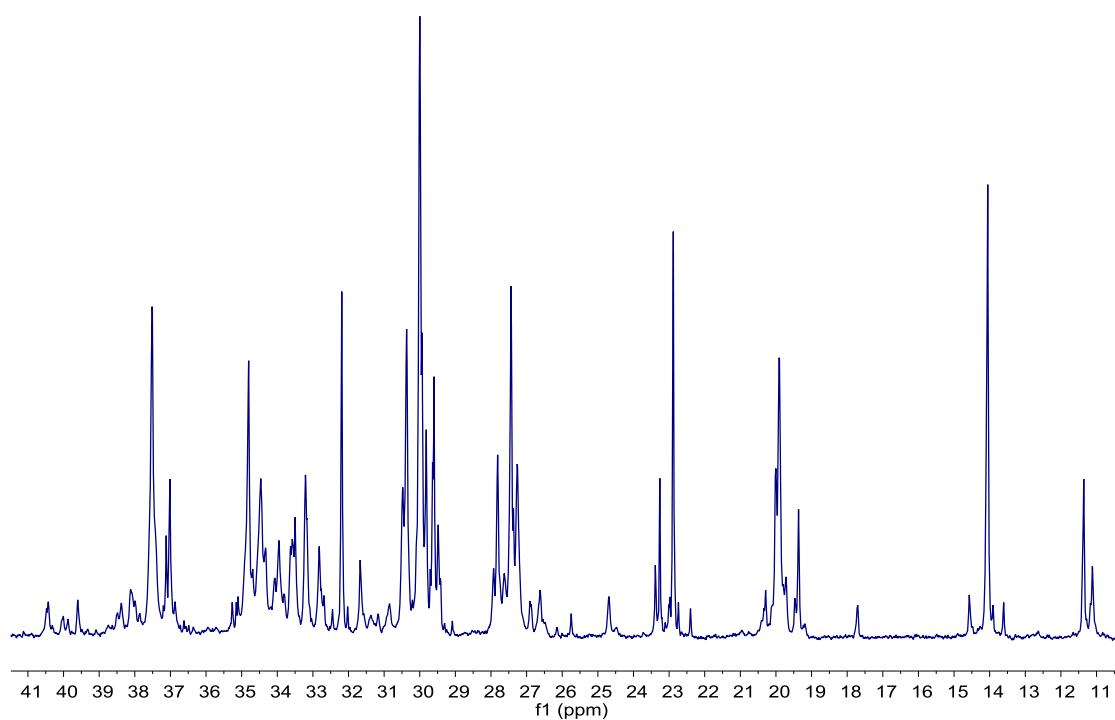


**Figure S58**  $^{13}\text{C}\{^1\text{H}\}$  NMR spectrum (75 MHz,  $\text{C}_6\text{D}_6$ :1,2,4-trichlorobenzene (1:3), 90 °C) of the PE obtained using the catalytic system **5\***, at 25 °C and 15 bar of ethylene.

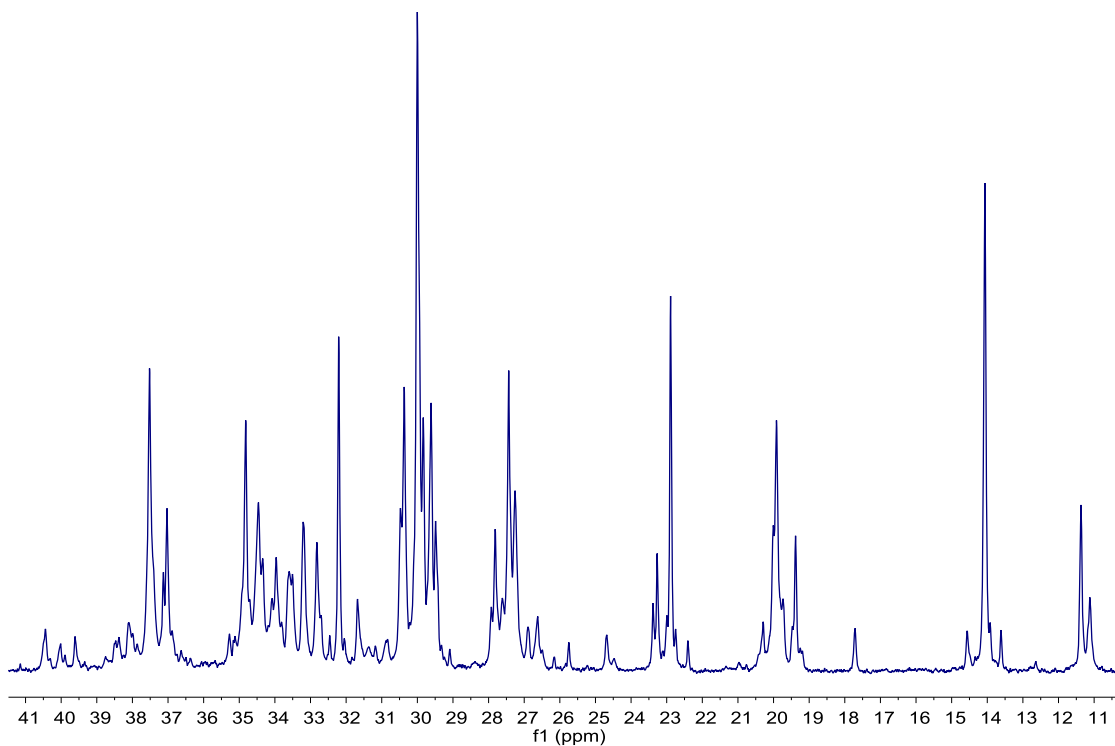


**Figure S59**  $^{13}\text{C}\{^1\text{H}\}$  NMR spectrum (75 MHz,  $\text{C}_6\text{D}_6$ :1,2,4-trichlorobenzene (1:3), 90 °C) of the PE obtained using the catalytic system **5\***, at 50 °C and 15 bar of ethylene.

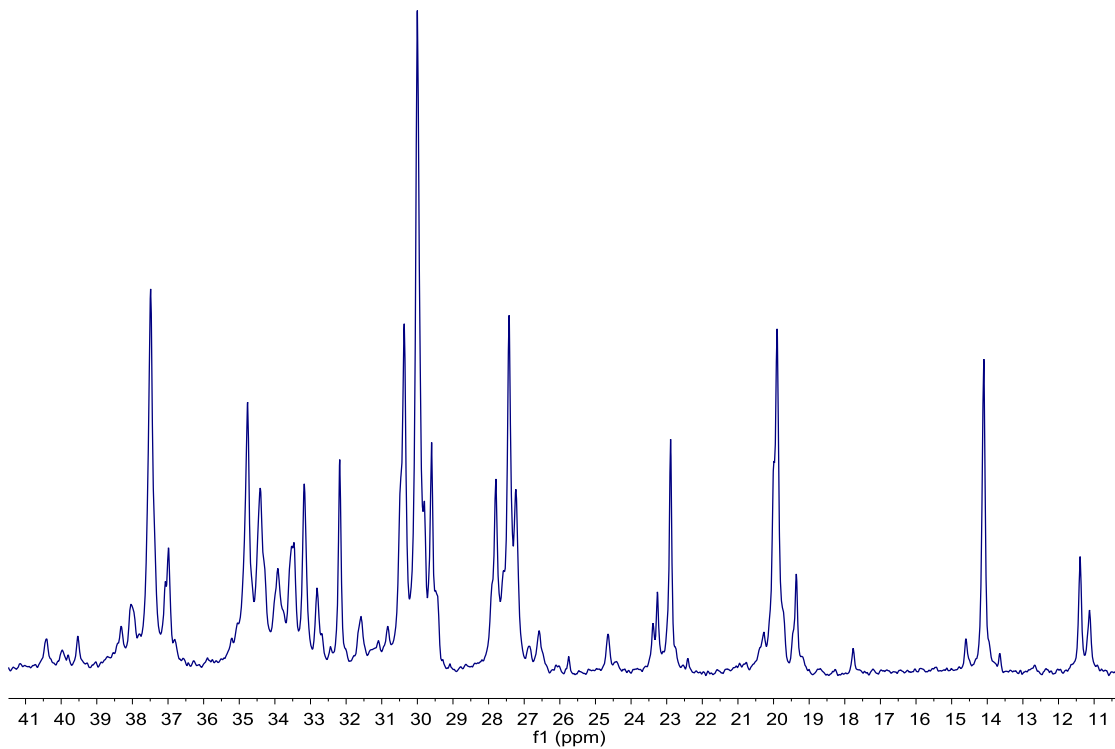


**Figure S60**  $^{13}\text{C}\{^1\text{H}\}$  NMR spectrum (75 MHz,  $\text{C}_6\text{D}_6$ :1,2,4-trichlorobenzene (1:3), 90 °C) of the PE obtained using the catalytic system **6\***, at 25 °C and 9 bar of ethylene.

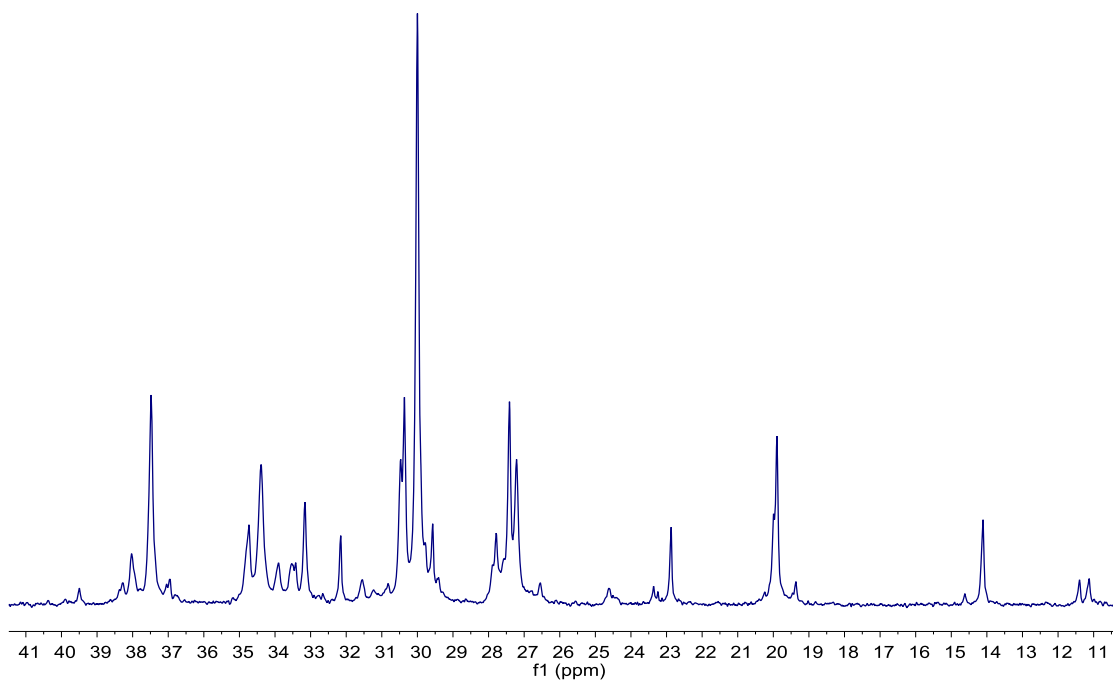


**Figure S61**  $^{13}\text{C}\{^1\text{H}\}$  NMR spectrum (75 MHz,  $\text{C}_6\text{D}_6$ :1,2,4-trichlorobenzene (1:3), 90 °C) of the PE obtained using the catalytic system **7\***, at 25 °C and 9 bar of ethylene.

## GPC/SEC chromatograms

Chromatograms of the PEs obtained with catalysts X or X\* (X/[Ni(COD)<sub>2</sub>])

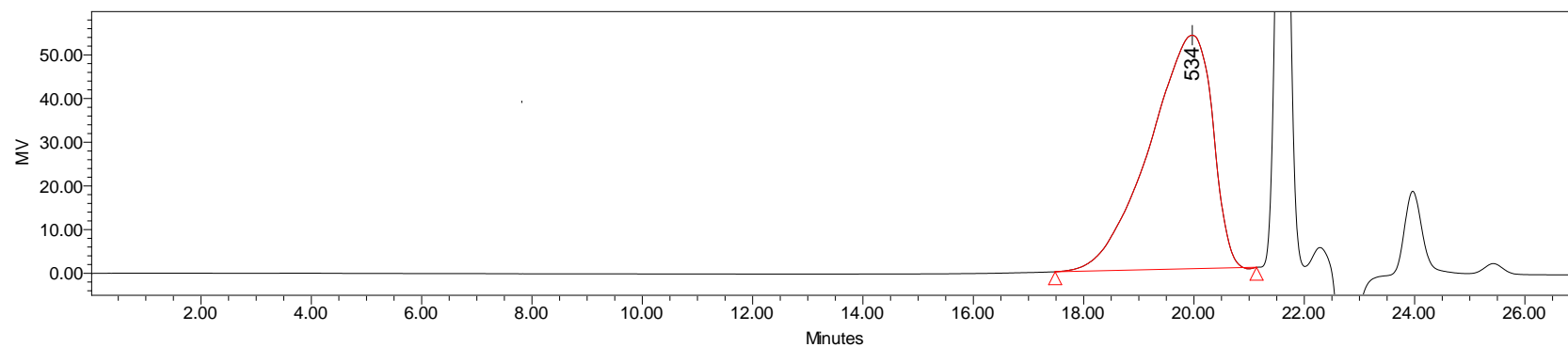


**Figure S62** GPC/SEC chromatogram of the PE obtained with catalyst **1**, at 9 bar and 50 °C.

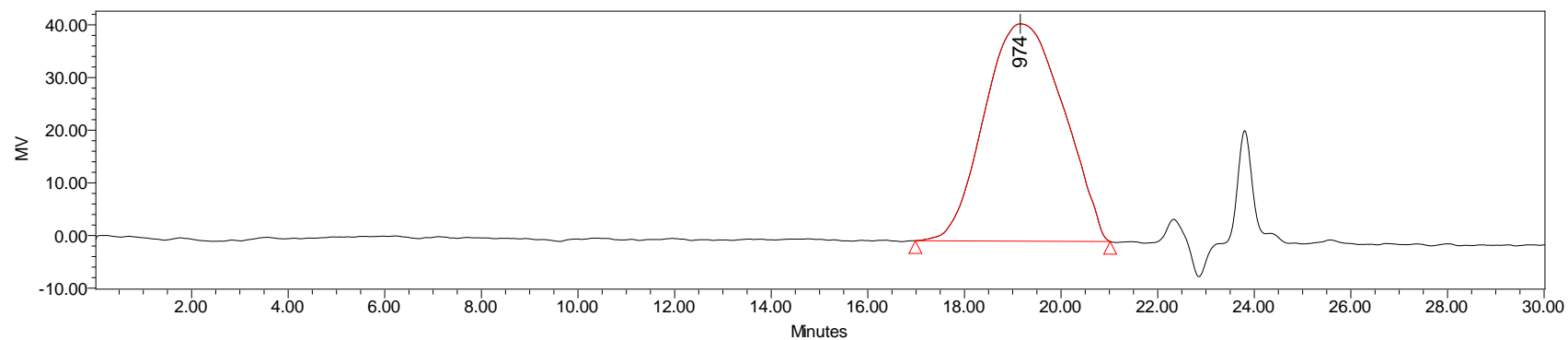


**Figure S63** GPC/SEC chromatogram of the PE obtained with catalyst **1\*** (**1**/[Ni(COD)<sub>2</sub>]), at 9 bar and 25 °C.

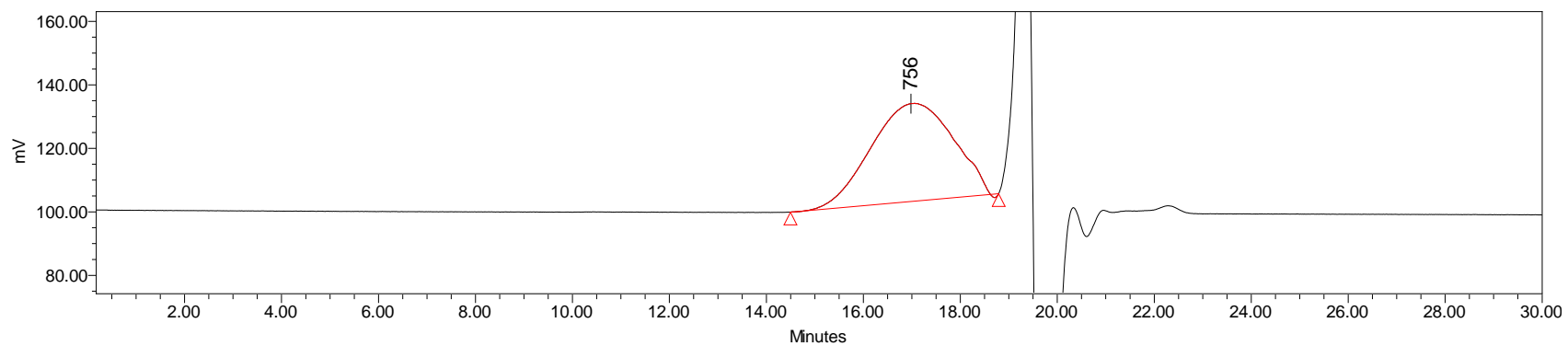


**Figure S64** GPC/SEC chromatogram of the PE obtained with catalyst **1\*** ( $1/[\text{Ni}(\text{COD})_2]$ ), at 9 bar and 50 °C.

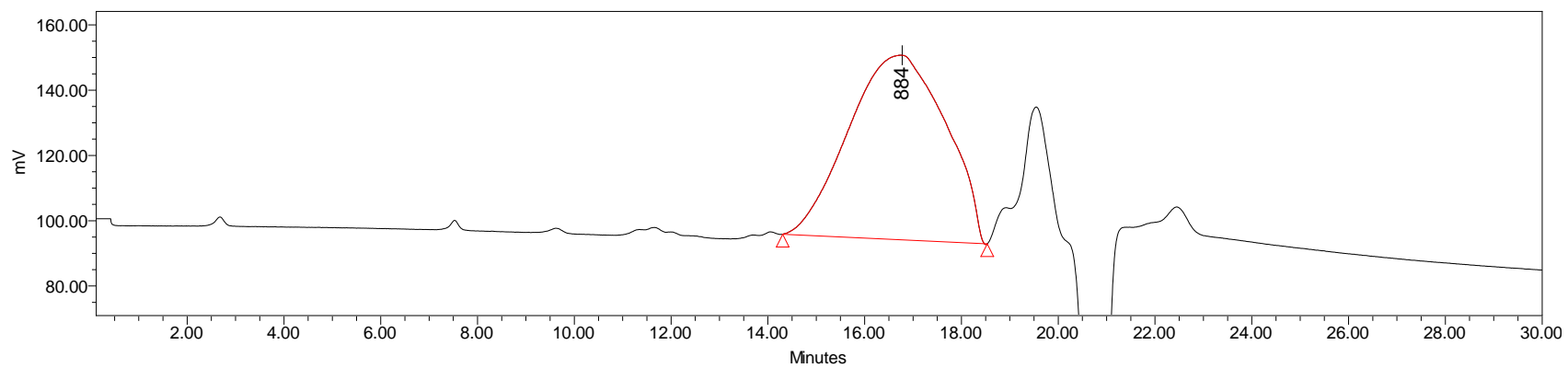


**Figure S65** GPC/SEC chromatogram of the PE obtained with catalyst **2\*** ( $2/[\text{Ni}(\text{COD})_2]$ ), at 9 bar and 50 °C.

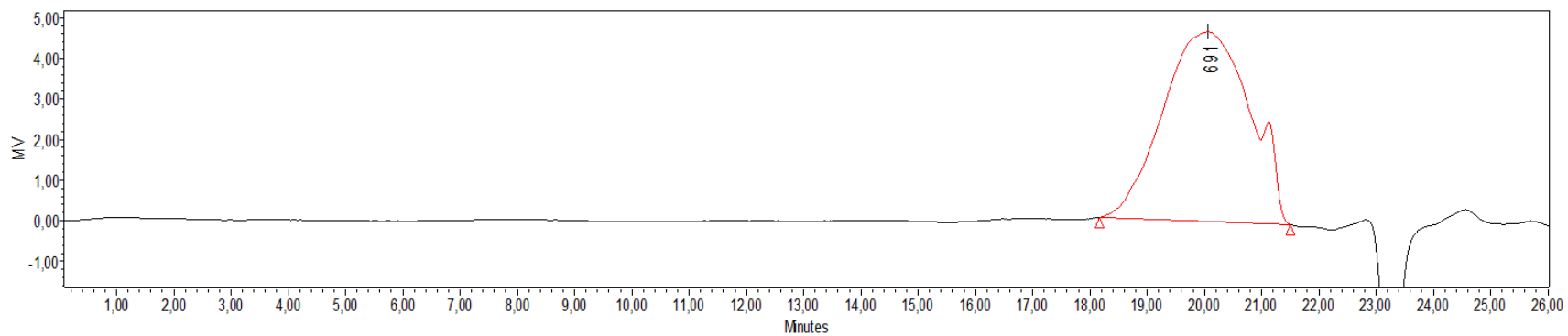


**Figure S66** GPC/SEC chromatogram of the PE obtained with catalyst **4**, at 9 bar and 50 °C.

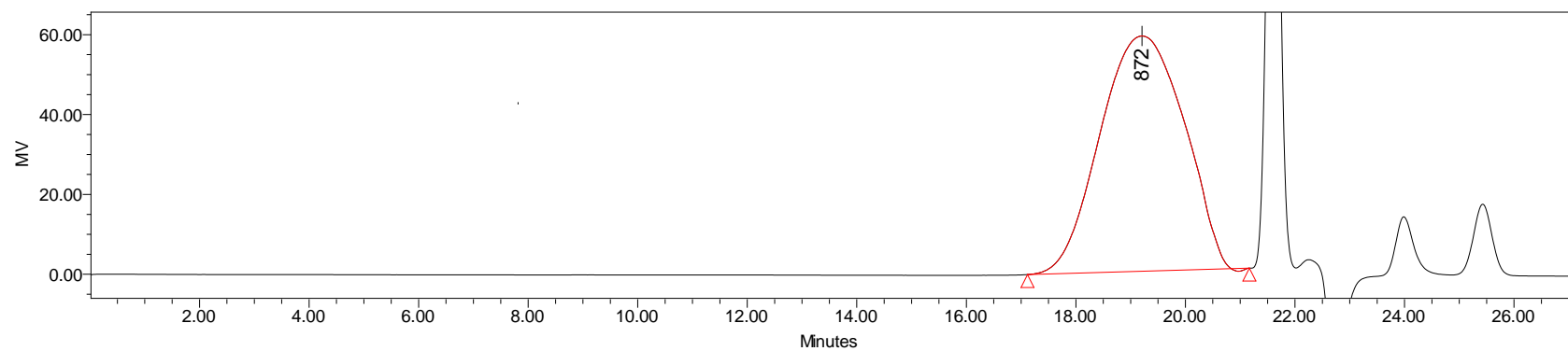


**Figure S67** GPC/SEC chromatogram of the PE obtained with catalyst **4\*** ( $4/[\text{Ni}(\text{COD})_2]$ ), at 9 bar and 25 °C.

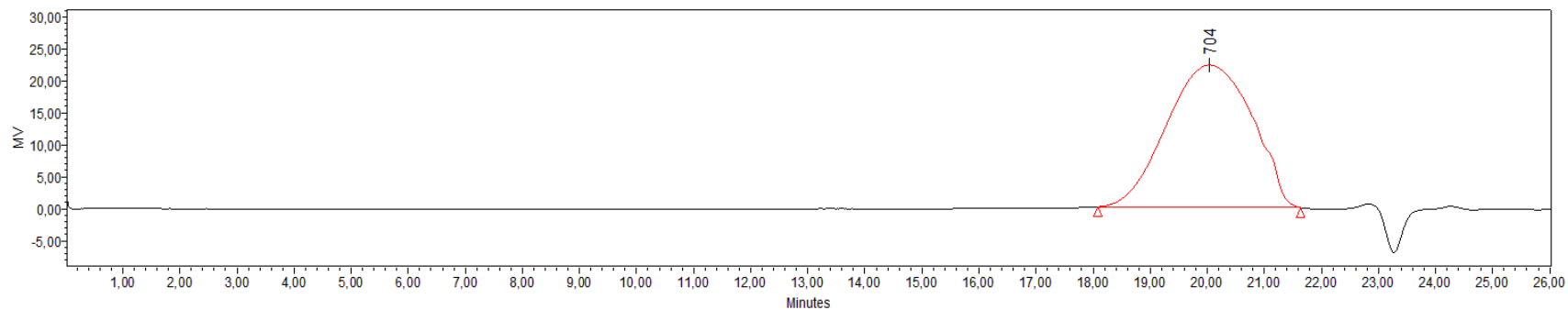


**Figure S68** GPC/SEC chromatogram of the PE obtained with catalyst **4\*** ( $4/[\text{Ni}(\text{COD})_2]$ ), at 9 bar and 50 °C.

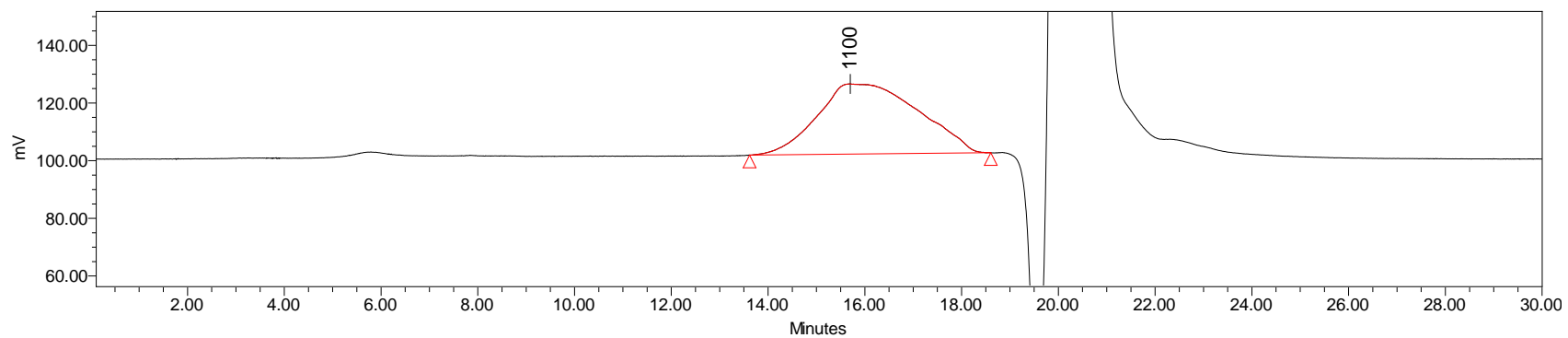


**Figure S69** GPC/SEC chromatogram of the PE obtained with catalyst **5\*** ( $5/[\text{Ni}(\text{COD})_2]$ ), at 3 bar and 25 °C.

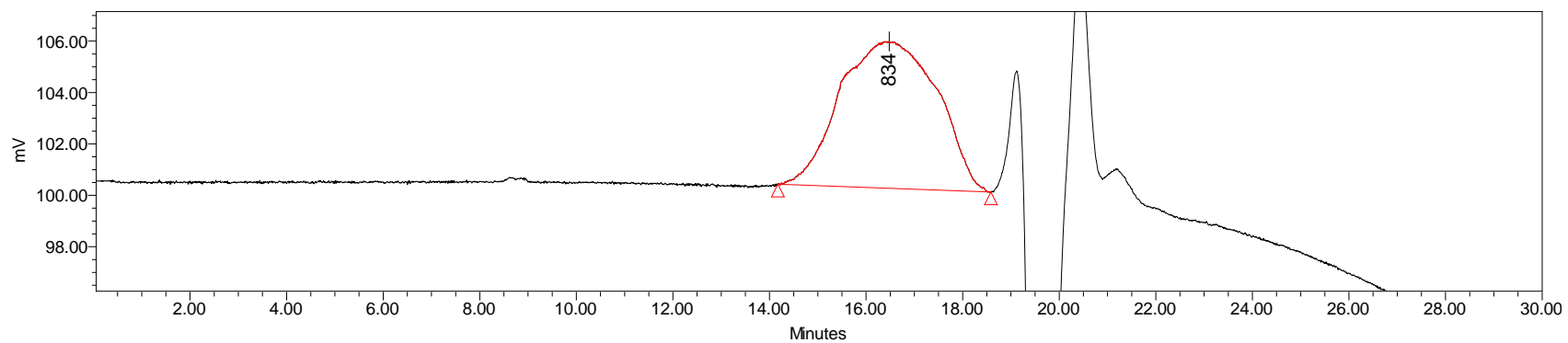


**Figure S70** GPC/SEC chromatogram of the PE obtained with catalyst **5\*** ( $5/[\text{Ni}(\text{COD})_2]$ ), at 3 bar and 50 °C.

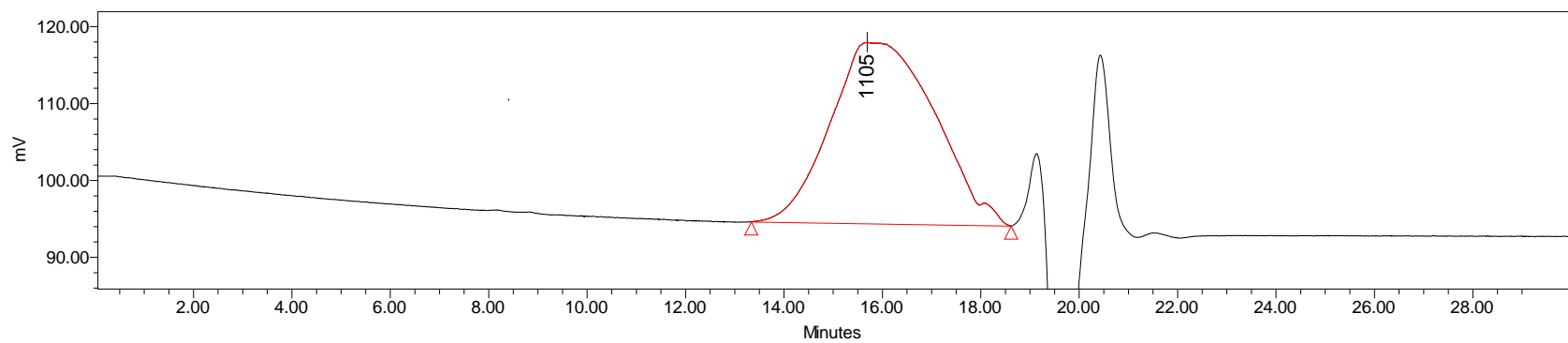


**Figure S71** GPC/SEC chromatogram of the PE obtained with catalyst **5\*** ( $5/[\text{Ni}(\text{COD})_2]$ ), at 9 bar and 25 °C.

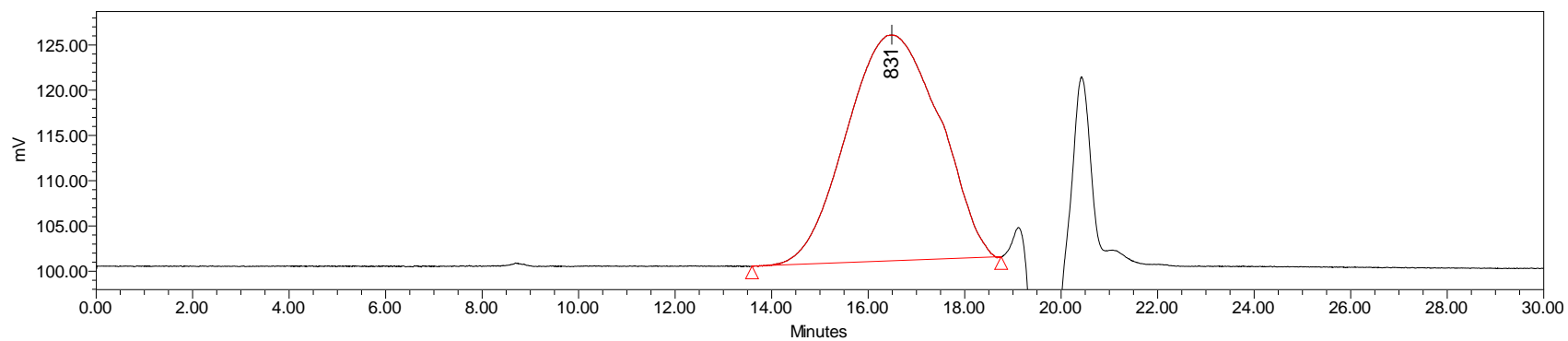


**Figure S72** GPC/SEC chromatogram of the PE obtained with catalyst **5\*** ( $5/[Ni(COD)_2]$ ), at 9 bar and 50 °C.

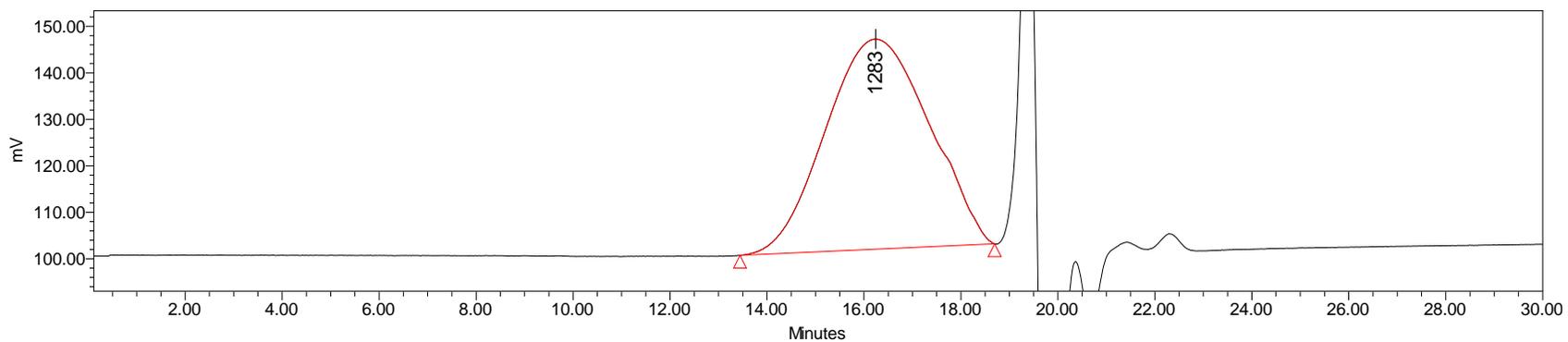


**Figure S73** GPC/SEC chromatogram of the PE obtained with catalyst **5\*** ( $5/[Ni(COD)_2]$ ), at 15 bar and 25 °C.

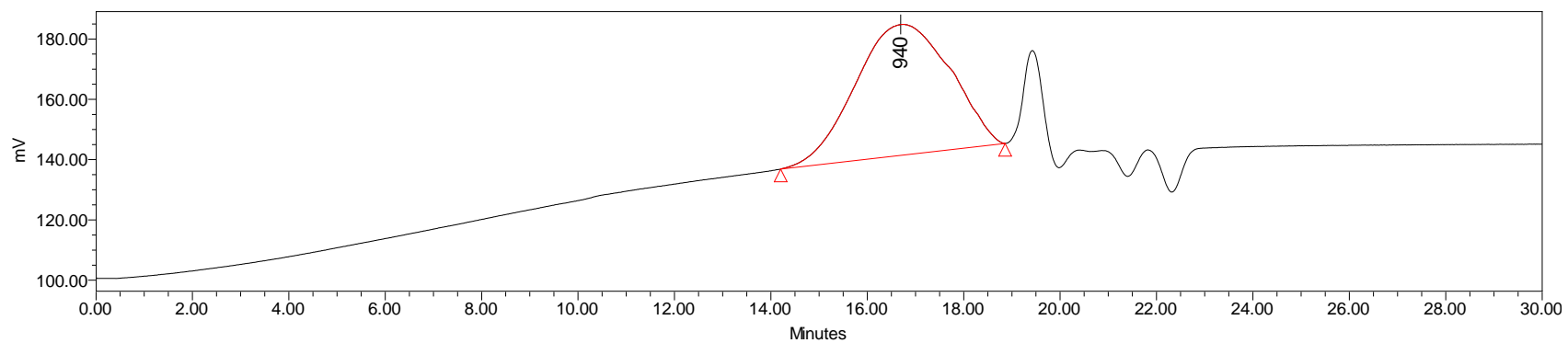


**Figure S74** GPC/SEC chromatogram of the PE obtained with catalyst **5\*** ( $5/[\text{Ni}(\text{COD})_2]$ ), at 15 bar and 50 °C.

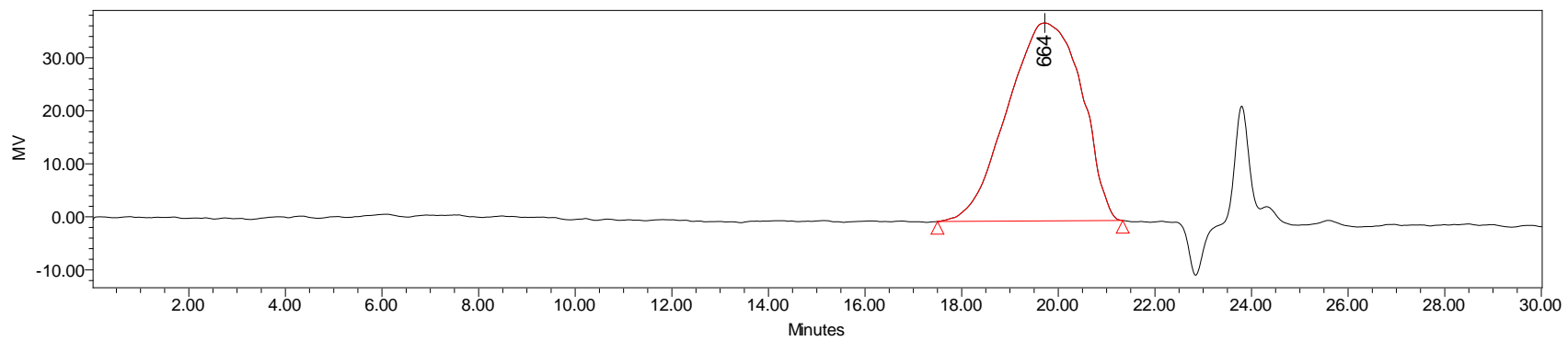


**Figure S75** GPC/SEC chromatogram of the PE obtained with catalyst **6**, at 9 bar and 25 °C.

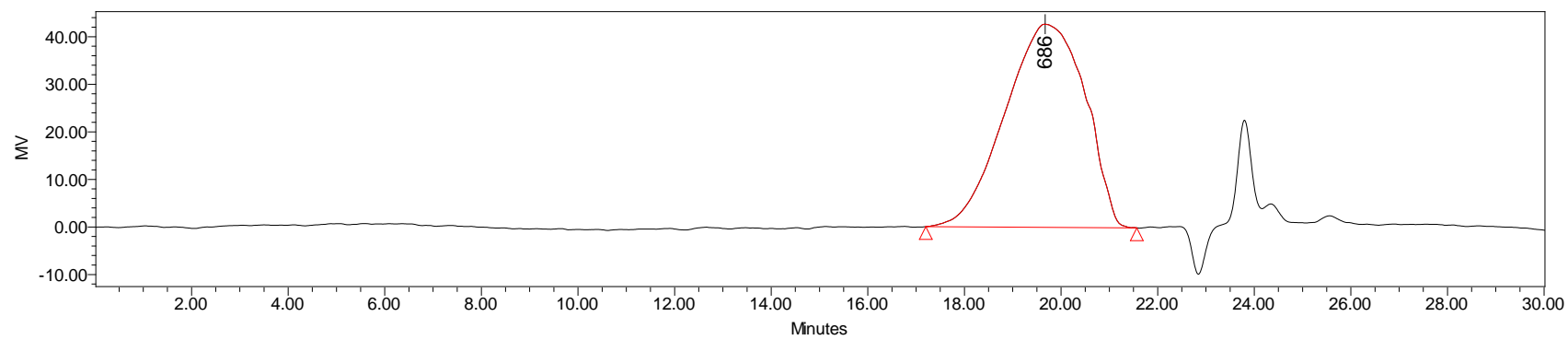


**Figure S76** GPC/SEC chromatogram of the PE obtained with catalyst **6**, at 9 bar and 50 °C.

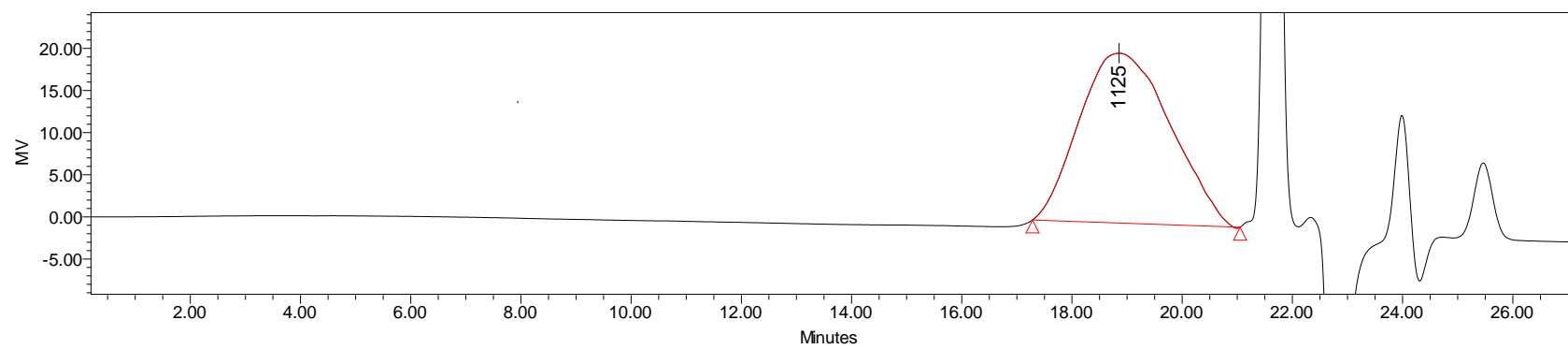


**Figure S77** GPC/SEC chromatogram of the PE obtained with catalyst **6\*** (**6**/[Ni(COD)<sub>2</sub>]), at 9 bar and 25 °C.

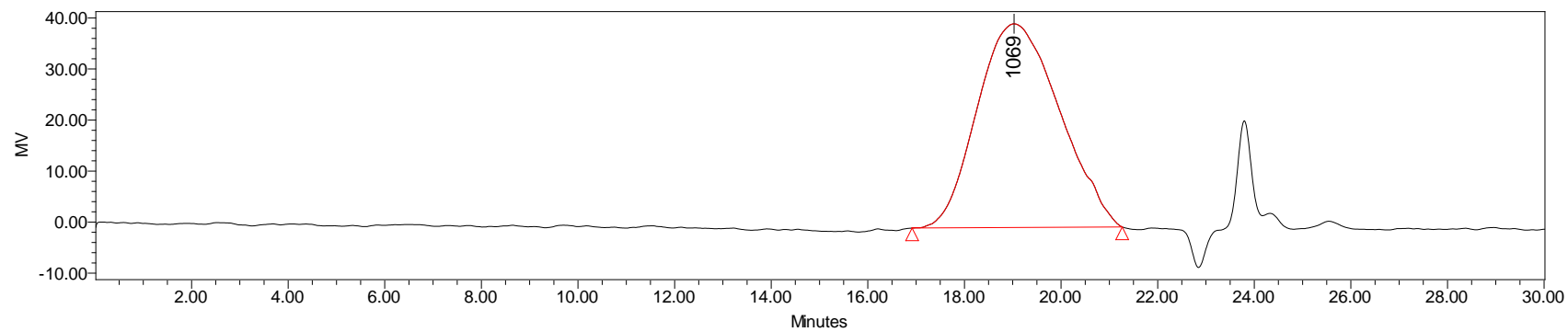


**Figure S78** GPC/SEC chromatogram of the PE obtained with catalyst **6\*** ( $6/[Ni(COD)_2]$ ), at 9 bar and 50 °C.

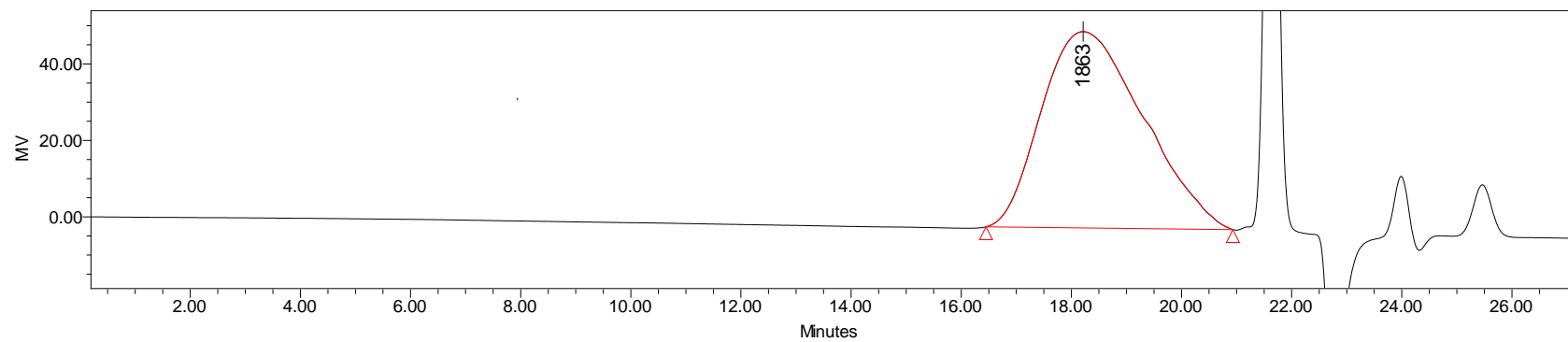


**Figure S79** GPC/SEC chromatogram of the PE obtained with catalyst **6\*** ( $6/[Ni(COD)_2]$ ), at 15 bar and 25 °C.

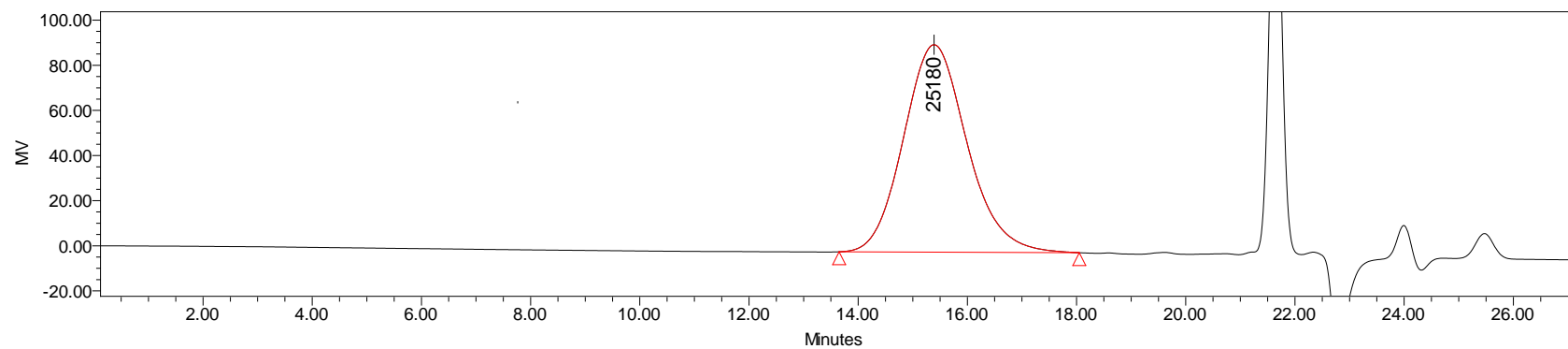


**Figure S80** GPC/SEC chromatogram of the PE obtained with catalyst **7**, at 9 bar and 25 °C.

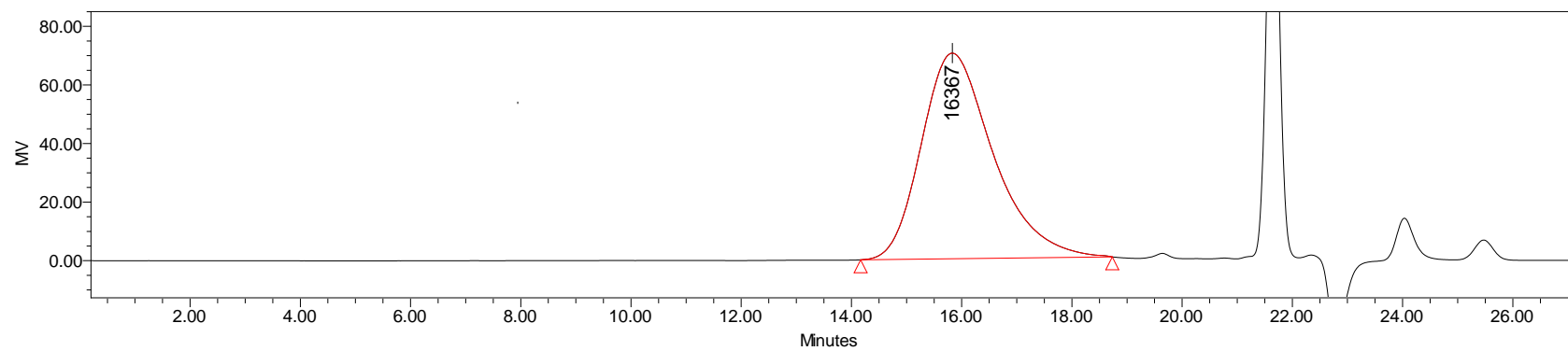


**Figure S81** GPC/SEC chromatogram of the PE obtained with catalyst **7**, at 9 bar and 50 °C.

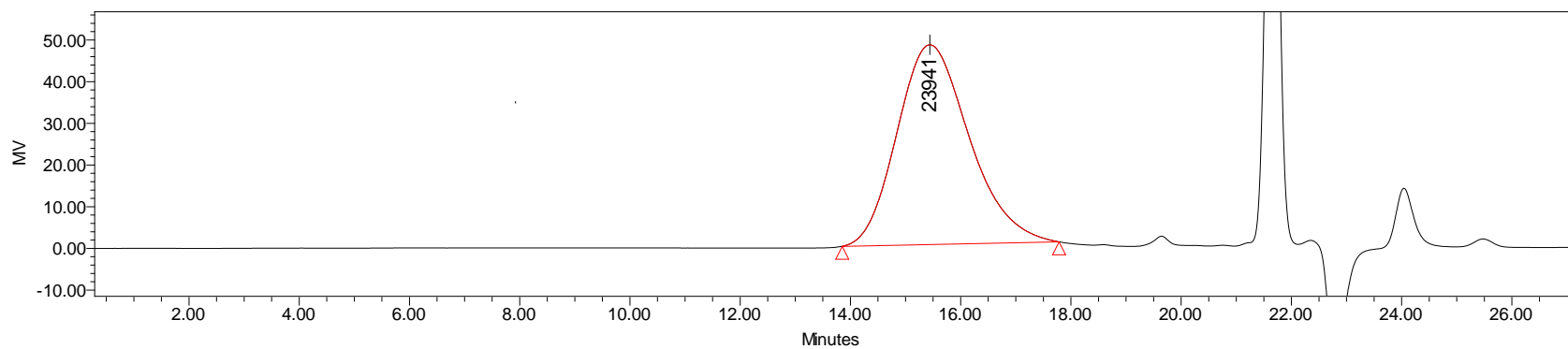


**Figure S82** GPC/SEC chromatogram of the PE obtained with catalyst **7\*** ( $7/[\text{Ni}(\text{COD})_2]$ ), at 9 bar and 25 °C.

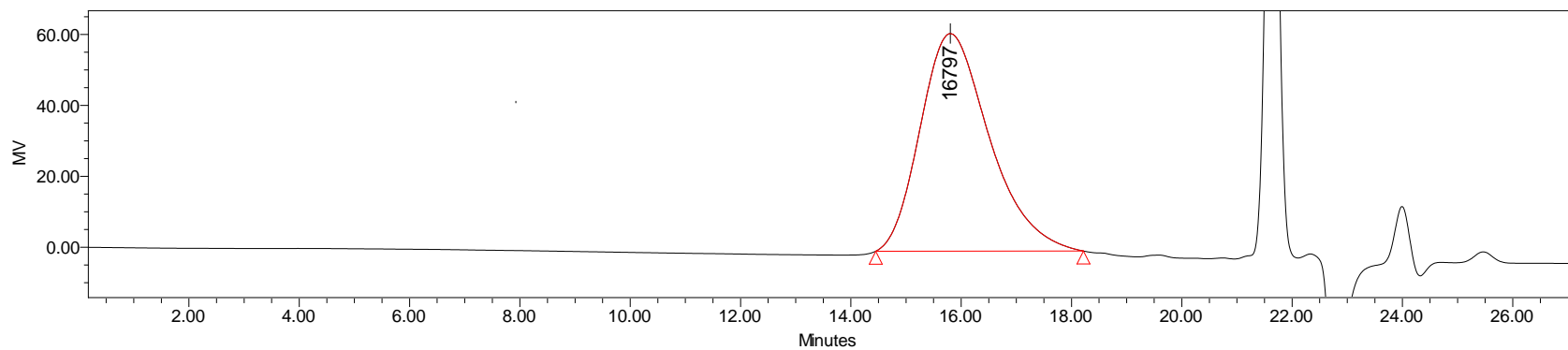


**Figure S83** GPC/SEC chromatogram of the PE obtained with catalyst **7\*** ( $7/[\text{Ni}(\text{COD})_2]$ ), at 9 bar and 50 °C.

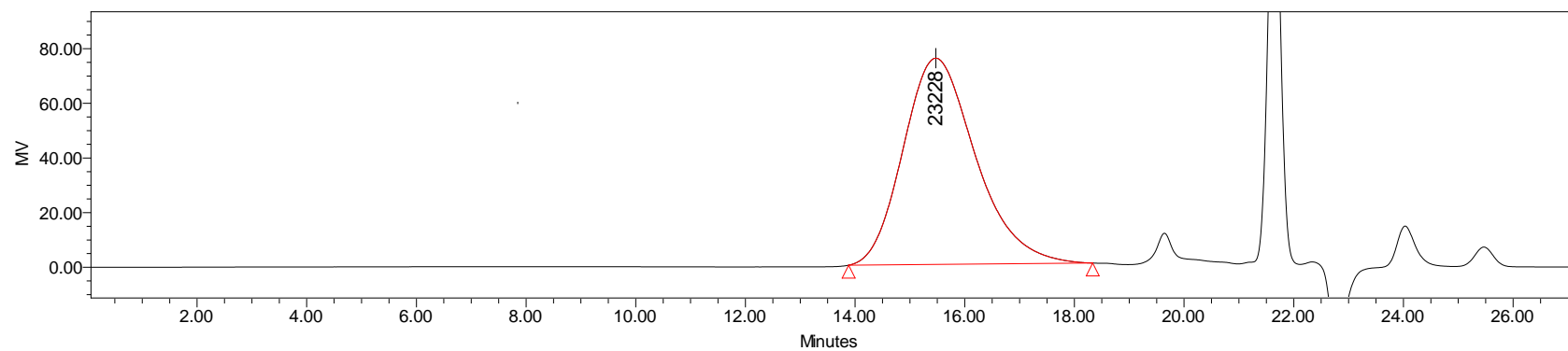


**Figure S84** GPC/SEC chromatogram of the PE obtained with catalyst **7\*** ( $7/[\text{Ni}(\text{COD})_2]$ ), at 15 bar and 25 °C.